Norwegian University of Life Sciences

Master's Thesis 2023 60 ECTS

Faculty of Chemistry, Biotechnology and Food Science

Significance of bacteriocin associated ABC transporter genes in oral streptococci biofilm

Mats Rune Strand Pettersen

M.Sc. Biotechnology

Norwegian University of Life Sciences (NMBU)

Faculty of Chemistry, Biotechnology and Food Science

Significance of bacteriocin associated ABC transporter genes in oral streptococci biofilm

Mats Rune Strand Pettersen

Master's thesis

Norway

May 2023

Supervisors:

Assoc. Prof. Morten Kjos

Dr. Sara Arbulu

Abstract

Biofilms are aggregated communities of microorganisms, that are involved with up to 80% of all human infections including oral diseases, chronic tissue infections, chronic inflammatory diseases, and acute infections. The biofilm microorganisms are embedded within a matrix consisting of extracellular polymeric substances, where the community interacts through secretion and detection of metabolites. One type of these secreted metabolites called bacteriocins are antimicrobial peptides synthesized on the ribosome, exported through ABC transporters and that inhibit a specific group of microorganisms, often species closely related to the bacteriocin producer. Self-immunity against the bacteriocin is acquired through bacteriocin-immunity proteins, which can act through different mechanisms. The aim of this study was to set up assays to assess the impact of putative bacteriocin-immunity proteins in forming and shaping of biofilms.

By *in silico* analysis of *Streptococcus mutans* and *Streptococcus sobrinus* genomes, a total of nine putative bacteriocin-immunity genes were identified through the bioinformatic tool Bagel4. The suggested genes were mostly bacteriocin-associated ABC transporter genes. A Janus cassette system to generate markerless mutations in *S. mutans* was set up. Markerless deletion of two putative bacteriocin-immunity genes were achieved. The effects of inactivating the genes were tested through growth curves, crystal violet biofilm staining, and pairwise strain competitions in different biofilm models. The assays demonstrated that deletion of *immB* [SMU.413] caused reduction in biofilm-formation, in addition individual deletion of either *immA* [SMU.431] or *immB* [SMU.413] caused reduction in fitness in the context of either mono-strain cultures or biofilm competitions.

The study demonstrated the use of the Janus cassette system for markerless gene deletions in *S. mutans*. A biofilm model was set up, which can be used to study bacteriocin interactions of *Streptococcus* in oral biofilms. A link has been established between SMU.413 and biofilm formation, but the function of the proteins studied here is still unknown. Follow-up studies are needed to test whether they are involved in bacteriocin immunity or other functions as suggested in the discussion.

Sammendrag

Biofilmer er aggregerte samfunn av mikroorganismer, som er involvert i opptil 80% av alle menneskelige infeksjoner inkludert orale sykdommer, kroniske vevsinfeksjoner, kroniske inflammatoriske sykdommer og akutte infeksjoner. Mikroorganismene i biofilmer er integrerte i en matrise som består av ekstracellulære polymere stoffer der samfunnet av mikroorganismer interagerer gjennom sekresjon og deteksjon av metabolitter. En type av disse utskilte metabolittene kalt bakteriosiner er antimikrobielle peptider syntetisert på ribosomet, eksportert gjennom ABC-transportører og som hemmer en spesifikk gruppe mikroorganismer, ofte arter nært beslektet med bakteriosinprodusenten. Selvimmunitet mot bakteriosinet blir tilegnet gjennom bakteriosinimmunitetsproteiner, som kan virke gjennom ulike mekanismer. Målet med dette studiet var å sette opp analyser for å vurdere virkningen av påståtte bakteriosinimmunitetsproteiner på biofilmdannelse og biofilmform.

Ved *in silico* analyse av *Streptococcus mutans* og *Streptococcus sobrinus* ble totalt ni påståtte bakteriosinimmunitetsgener identifisert gjennom det bioinformatiske verktøyet Bagel4. De forslåtte genene var stort sett bakteriosinassosierte ABC-transportørgener. Et Janus-kassettsystem ble satt opp for å genere mutasjoner i *S. mutans* uten å etterlate markørgener. Delesjon av to påståtte bakteriosinimmunitetsgener var oppnådd gjennom Janus-kassettsystemet. Påvirkningene av å inaktivere genene ble analysert gjennom vekstkurver, krystallfiolettfarging av biofilm og parvise stammekonkurranser i forskjellige biofilmmodeller. Analysene demonstrerte at delesjon av *immB* [SMU.413] forårsaket reduksjon i biofilmdannelse, i tillegg så førte individuell delesjon av enten *immA* [SMU.431] eller *immB* [SMU.413] til reduksjon i fitness i sammenheng av både monostamme kulturer og biofilm konkurranser.

Studien demonstrerte bruken av Janus-kassettsystemet for delesjon av gener i *S. mutans* uten å etterlate markørgener. En biofilmmodell var satt opp, som kan bli brukt til å studere bakteriosininteraksjoner av *Streptococcus* i orale biofilmer. En sammenheng mellom SMU.413 og biofilmdannelse var etablert, men funksjonen til proteinene studert er fortsatt ikke kjent. Oppfølgingsstudier er krevd for å teste om disse proteinene er involvert i bakteriosinimmunitet eller andre funksjoner som de forslått i diskusjonen.

Acknowledgements

This master thesis was conducted in the Molecular Microbiology research group at the Faculty of Chemistry, Biotechnology and Food Science (KBM) between August 2022 and May 2023. The thesis concludes a two-year Master of Science degree in Biotechnology at the Norwegian University of Life Sciences (NMBU).

The Molecular Microbiology research group provided an excellent environment for academic development that taught me a great deal of microbiology theory together with practical usage of a biotechnology laboratory. I want to express my gratitude to my supervisor, Sara Arbulu, for her immense support and guidance throughout my master project. I appreciate your expertise in the laboratory and all the help you have provided me with. I would also thank my main supervisor, Morten Kjos, for providing me with assistance in planning the experiments and discussions of how to proceed with the thesis. The writing process of my thesis were greatly improved by the both of you. I would also like to thank Zhian Salehian for his insightfulness and support during experiments. Thank to everyone at the Molecular Microbiology research group for the good times!

I want to thank my fellow master's students and friends for the encouragement, feedback, and friendship. I especially want to thank Luis Ramirez for being a good friend and always dropping by the laboratory. Lastly, I want to give a special thanks to my family for their support.

Mats Rune Strand Pettersen

Ås, May 2023

Contents

1 Introduction

Biofilms are widespread in nature as part of the microbial life cycle. While many biofilms are harmless or beneficial, they are also responsible for biofilm-associated infections such as dental caries and periodontitis, and additionally they can also form on the surface of medical devices making infections more difficult to treat. Within biofilms, microbes interact with each other and compete for nutrients, space, survival; one of these competition mechanisms is the production of antimicrobial peptides called bacteriocins. The quorum-sensing regulatory systems induce biofilm formation and additionally regulate production of bacteriocins in tandem with the corresponding bacteriocin-immunity proteins (Li & Tian, 2012; Pérez-Ramos et al., 2021). The aim of this thesis is to set up assays to enable the investigation of the hypothesis that bacteriocin genes and bacteriocin associated genes have important roles in formation and shaping of biofilms. More precisely, bacteriocin-immunity genes will be investigated. Oral streptococci including *Streptococcus mutans* and *Streptococcus sobrinus* is to be used as a model due to their biofilm-forming and bacteriocin-producing capabilities.

1.1 Biofilms

Biofilms are aggregated communities of microorganisms that may adhere to a surface, interface or exist as a unadhered aggregate (Sauer et al., 2022). The formation and adherence of biofilms are facilitated by its extracellular matrix (ECM) consisting of extracellular polymeric substances (EPS) that is produced by microorganisms in the biofilm (Donlan & Costerton, 2002). The EPS can be polysaccharides, proteins or nucleic acids and there are different processes of EPS production: secretion from cells, polymerization of environmental substances by secreted enzymes, cell lysis, and shedding of cellular surface material (Wingender et al., 1999). The EPS are responsible for the molecular interaction between surface and biofilm that allows for adhesion, as well as the cohesion of the ECM (Flemming & Wingender, 2010). The majority of biofilm biomass is usually the ECM rather than the microorganisms with the biofilm, constituting over 90% biomass for most biofilms (Flemming & Wingender, 2010).

Within a biofilm, the microorganisms are stationary and inside cell clusters where they are in a close proximity, allowing cell-cell communication and exchange of metabolites (Flemming & Wingender, 2010). Oxygen and nutrients diffuse from the surrounding liquid into the biofilm perpendicularly to the liquid-biofilm interface (de Beer et al., 1994). The diffusion forms a gradient of oxygen and nutrients, with the highest concentration at the biofilms surface and decreasing the further distance from a liquid-biofilm interface (Siegrist & Gujer, 1985). The

heterogeneity of nutrient, oxygen and waste product concentrations facilitates different niches within the biofilm (Costerton et al., 1978; Sauer et al., 2022). Biofilms have several characteristics that may cause it to be considered pseudo multicellular or a pseudo tissue: cell-cell communication, programmed cell death, and some species have cell differentiation such as sporulation or differences in EPS-production based on proximity to the biofilm surface (Claessen et al., 2014). Extracellular enzymes are found within ECMs that are able to degrade polymers such as polysaccharides, proteins, nucleic acids into smaller molecules (Flemming & Wingender, 2010). The microorganisms can then absorb and catabolize the smaller molecules for carbon and energy (Flemming & Wingender, 2010). These polymers may be or not be EPS.

The ECM structure created by the EPS forms the framework for the three-dimensional architecture of a biofilm (Flemming & Wingender, 2010). The presence or absence of a particular EPS may influence the architecture significantly (Flemming & Wingender, 2010). Nutrient accessibility, intercellular communication, motility of the microorganisms, and the waterflow of the environment may also influence the architecture (Flemming & Wingender, 2010). The three-dimensional biofilm shape has been hypothesized to be optimal for nutrient and oxygen uptake (de Beer et al., 1994). Other variation in biofilm morphology include smoothness, and thickness (Flemming & Wingender, 2010). The microorganisms residing within the biofilm may be single or multiple species, and the cells exhibit a range of phenotypes with respect to growth rate and gene transcription (Donlan & Costerton, 2002).

1.1.1 Biofilm relevance for society

Biofilm control is important for safety of implants, improved antibiotics use, the food and feed industry, and biofilm associated conditions such as dental caries and periodontal diseases (Mah & O'Toole, 2001; Socransky & Haffajee, 2002; Stephan, 1944). Biofilms are involved with up to 80% of all human infections (Römling & Balsalobre, 2012). The microorganisms can gain 10-1000 times higher resistance against antimicrobial agents when residing within a biofilm, causing treatment to become a challenge (Mah & O'Toole, 2001).

Microorganisms may adhere and form biofilms at the surface of medical implants such as catheters, prosthetic joints, prosthetic cardiac valves, pacemakers, tissue fillers, contact lenses, as well as cosmetic implants which may cause unwanted complications (Høiby et al., 2015; Mah & O'Toole, 2001). The biofilm can disperse cells or portions of the biofilm into the surrounding tissue and cause chronic infection (Mah & O'Toole, 2001). The biofilm can also lead to failure of the medical implant (Veerachamy et al., 2014). In cases where the biofilms

are difficult to remove by antibiotics treatment, the only way to cure the infection may be to excise the implant (Mah & O'Toole, 2001). Oral implants such as artificial voice prostheses and dental implants can be colonized by oral microorganisms (Veerachamy et al., 2014).

Biofilms may enhance the pathogenicity of bacterial and fungal infections (Høiby et al., 2015). These biofilm infections have been demonstrated in lung infections, chronic wounds, otitis media, chronic osteomyelitis, and chronic rhinosinusitis, as well as infections associated with soft tissue fillers, implants, catheter, shunt, and contact lenses (Høiby et al., 2015). Biofilms are important for the food and feed industry for a variety of reasons such as biofilm infections of crop, biofertilizer and biocontrol in agriculture, biofilm colonization of food processing surfaces in food safety, and colonization of drinking water distribution systems in water safety (Muhammad et al., 2020). Important foodborne pathogens that are able to form biofilms include *Listeria monocytogenes*, *Pseudomonas* spp., *Bacillus cereus*, *Salmonella* spp., *Escherichia coli*, *Clostridium* spp., *Cronobacter* spp., *Staphylococcus* spp. (Muhammad et al., 2020). Food processing surfaces often include stainless steel that can be colonized by the biofilm producers *L. monocytogenes*, *B. cereus*, *Salmonella* spp., *E. coli*, and *Staphylococcus* spp. (Muhammad et al., 2020). Drinking water distribution systems can be colonized by the biofilm producers *Campylobacter jejuni*, *Legionella pneumophila*, *Mycobacteria* spp., *Aeromonas hydrophila*, and *Klebsiella pneumoniae* (Muhammad et al., 2020). On the other hand, plant roots can be colonized by *Bacillus subtilis* that can produce a biofilm and confer protection to the plant from pathogens (Muhammad et al., 2020).

Periodontal diseases are infections facilitated by supragingival and subgingival biofilms (Socransky & Haffajee, 2002). The most supported etiological model for dental caries is that microorganisms within dental plaque biofilm, and not microorganisms suspended in the saliva, produce acids through fermentation of sugars and thereby cause decalcification of the enamel (Stephan, 1944). Research on biofilms is therefore needed to control biofilm related infections. Treatments that combine antibiotics with biofilm-matrix-degrading enzymes may facilitate better success than antibiotics exclusively (Kaplan, 2010). As an example, it has been reported that the use of ECM-degrading dispersin B produced by the oral bacteria *Aggregatibacter actinomycetemcomitans* together with the antibiotic teicoplanin completely eliminated *Staphylococcus aureus* blood stream infections in sheep (Kaplan, 2010). Research on implant surface modification and coating through nanotechnology may lead to preventative measures against colonization of medical implants (Veerachamy et al., 2014).

1.1.2 Dental plaques

Dental plaque is a type of biofilm that form on the dental surface of animals and is inhabited by a diverse group of microorganisms (Marsh & Bradshaw, 1995; Welch et al., 2016). Within the supragingival plaques there are 13 abundant and prevalent genera: *Corynebacterium*, *Leptotrichia*, *Neisseria*, *Rothia*, *Prevotella*, *Capnocytophaga*, *Actinomyces*, *Haemophilus*, *Lautropia*, *Fusobacterium*, *Streptococcus*, *Porphyromonas*, and *Veillonella* (Welch et al., 2016). Teeth can be coated by a layer of *Streptococcus* spp. and *Actinomyces* spp. that function as primary colonizers (Welch et al., 2016). These bacteria adhere to the glycoproteins of the salivary pellicle through the antigen I/II family of adhesins (Holmes et al., 1998; Ma et al., 1990). Dental plaque extending from the gingival margin have been reported to feature a 'hedgehog structure' where *Corynebacterium* form long filaments that adhere to the margin and the tips of the filaments are bound by the majority of bacteria within the dental plaque as seen in **Figure 1.1** (Welch et al., 2016). At the tips there are 'corncob structures' where *Streptococcus* are bound in a layer around the *Corynebacterium* and around the *Streptococcus* there is a layer of *Haemophilus* (Welch et al., 2016). Instead of *Streptococcus* the tips of the filaments may also be bound in a layer of *Leptotrichia* or *Neisseria* (Welch et al., 2016). Further away from the biofilm-liquid interface there are anoxic conditions where *Capnocytophaga*, *Fusobacterium*, and *Leptotrichia* proliferate (Welch et al., 2016). The base of the biofilm that is close to the gingival margin is largely colonized by *Actinomyces* and *Corynebacterium* (Welch et al., 2016).

The largest portion of the dental plaque ECM consists of glucans and fructans (Bowen & Koo, 2011). *S. mutans* synthesize glucosyltransferases and fructosyltransferases that polymerizes sucrose and starch hydrolysates into polysaccharides (Bowen & Koo, 2011; Kuramitsu et al., 1995). The glucosyltransferases enzymes may adhere to the salivary pellicle (Bowen & Koo, 2011; Vacca-Smith et al., 1996). The fructosyltransferase that synthesizes fructans is encoded by *S. mutans* as well as the salivary pellicle primary colonizers *Streptococcus gordonii* and *Actinomyces viscosus* (Bowen & Koo, 2011; Rozen et al., 2001). In total the soluble and insoluble glucans constitute 10-20% of the dental plaque biomass whereas fructans constitute 1-2% of the biomass (Bowen & Koo, 2011; Marsh & Bradshaw, 1995). These polysaccharides confer structural integrity to the ECM and cause the dental plaque to become larger (Marsh & Bradshaw, 1995). Attachment of cells to the ECM is facilitated by the insoluble glucan and fructans (Jakubovics et al., 2021). Proteins constitutes approximately 40% of the dental plaque biomass (Bowen & Koo, 2011). A portion of the protein component includes fimbriae produced

by the plaque bacteria *A. actinomycetemcomitans* and *Porphyromonas gingivalis* (Kaplan, 2010). Extracellular double-stranded DNA (eDNA) has also been found to interact with the EPS in dental plaque (Castillo Pedraza et al., 2017; Kaplan, 2010). The eDNA could either be secreted or released during lysis by the bacteria *A. actinomycetemcomitans*, *S. mutans*, and *Streptococcus intermedius* (Castillo Pedraza et al., 2017). Extracellular lipoteichoic acids have been found in *S. mutans* cultures, and to be interacting with the EPS in *S. mutans* biofilms (Castillo Pedraza et al., 2017; Markham et al., 1975). Interestingly, glucosyltransferases are inhibited by lipoteichoic acids and biofilm formation by *S. mutans* has been shown to be inhibited by *Lactobacillus plantarum* lipoteichoic acids, indicating that glucosyltransferases are essential for the biofilm formation of *S. mutans* (Ahn et al., 2018; Markham et al., 1975).

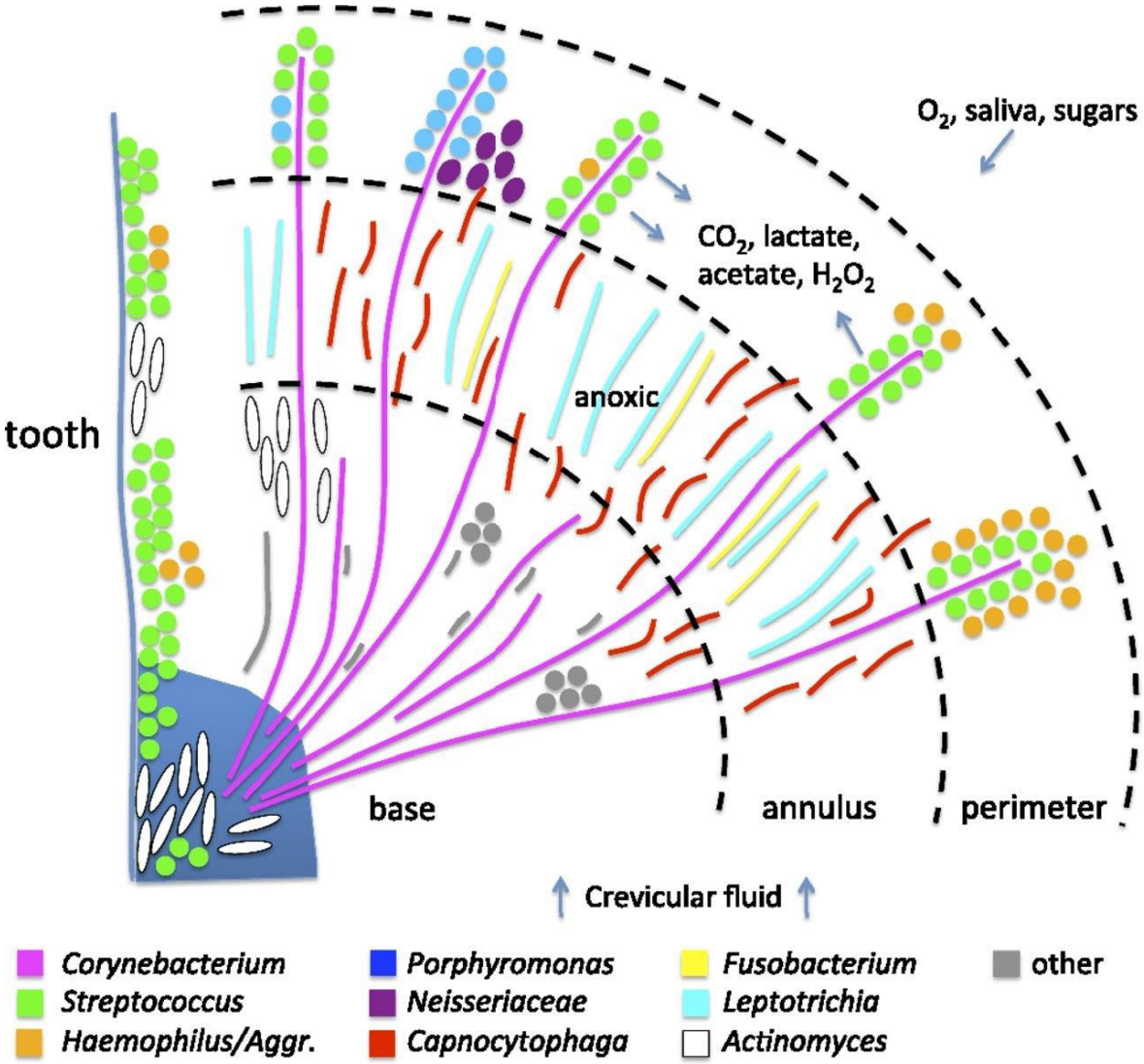

Figure 1.1: Dental plaque extending from the gingival margin. Illustration of the reported 'hedgehog structure' formed by dental plaque microorganisms. The figure is reused from (Welch et al., 2016).

1.1.3 Dental plaque formation model

Biofilm-formation as a generalized concept could be explained by three main events: adherence, proliferation, and dispersal (Sauer et al., 2022). The adherence event includes both aggregation of cells to each other and attachment of cells to a surface (Sauer et al., 2022). The proliferation event includes growth of cells within a biofilm, as well as accumulation of additional cells onto the surface of a biofilm (Sauer et al., 2022). The dispersal event includes both disaggregation of a portion of biofilm leading to single cells being dispersed and detachment of a portion of biofilm leading to new daughter biofilm (Sauer et al., 2022). The daughter biofilm could either disaggregate into single cells, colonize a new surface, or proliferate as a free-floating biofilm (Sauer et al., 2022).

Dental plaque-formation has additional important events compared to the generalized concept of biofilm-formation. There five main events in dental plaque-formation are pre-conditioning of the dental surface, initial colonization, coadhesion, proliferation, and dispersal (Chawhuaveang et al., 2021; Kaplan, 2010; Kolenbrander & London, 1993).

Dental surfaces are pre-conditioned by proteins found in saliva that adhere to the dental surface and over time proteins, carbohydrates, and lipids adhere to form the acquired dental pellicle (**Figure 1.2**) (Chawhuaveang et al., 2021). The acquired dental pellicle has a variety of functions for the host organism that include acid resistance, immune response, antimicrobial, antifungal, lubrication, maintenance of mineral homeostasis, and prevention of microbial colonization (Chawhuaveang et al., 2021). Acid resistance is provided through causing lactic acid to diffuse slower towards the dental surface (Chawhuaveang et al., 2021). Important salivary gland-secreted pellicle proteins for initial colonization include acidic proline-rich proteins, statherin, histatins, and α-amylase, as well as bacterial cell fragments adhered to the pellicle (Chawhuaveang et al., 2021; Kolenbrander & London, 1993).

Initial colonization of the salivary pellicle is carried out predominantly by *Streptococcus* spp., as well as *Actinomyces* spp. (Kolenbrander & London, 1993; Welch et al., 2016). The species *Actinomyces naeslundii*, *Capnocytophaga ochracea*, *Fusobacterium nucleatum*, *Streptococcus crista*, *S. gordonii*, *S. intermedius*, *Streptococcus mitis*, *S. mutans*, *Streptococcus oralis*, *Streptococcus parasanguis*, *Streptococcus sanguis*, and *S. sobrinus* are primary colonizers that are known to have membrane-bound adhesins that can directly bind to proteins in the salivary pellicle (Kolenbrander & London, 1993; Rosan & Lamont, 2000).

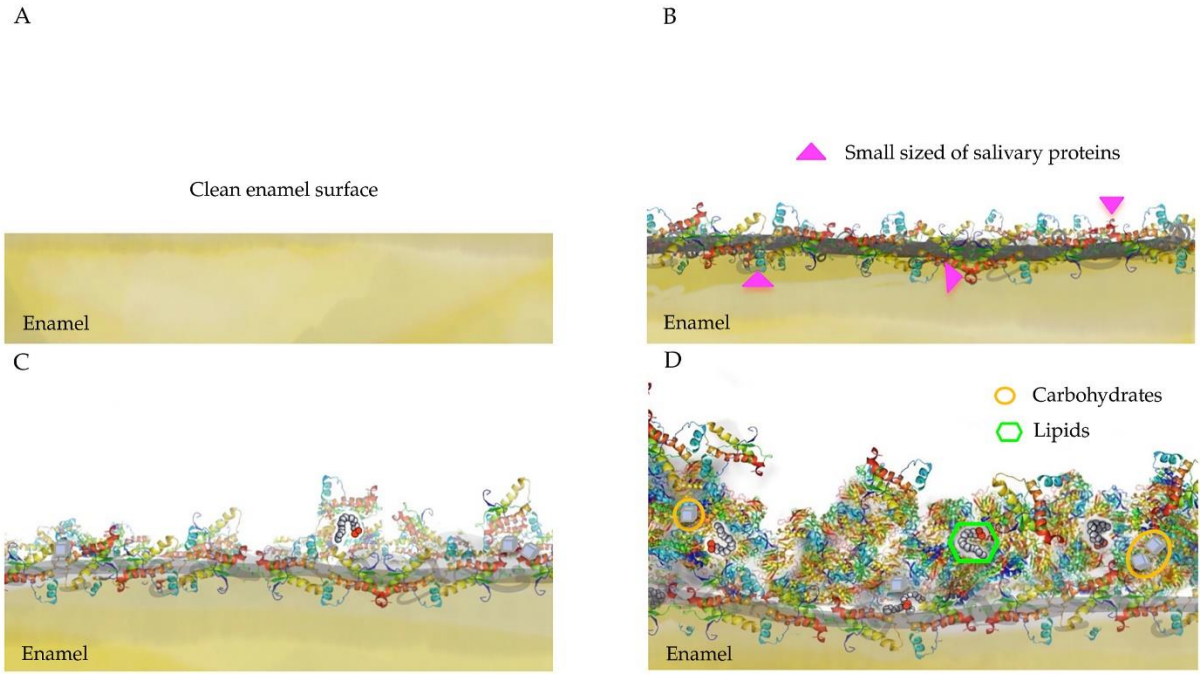

Figure 1.2: Development of the acquired salivary pellicle. Illustration of the acquired salivary pellicle 0 minutes (A), a few minutes (B), 45 minutes (C), and 120 minutes (D) after cleaning the dental surface. The figure is reused from (Chawhuaveang et al., 2021).

Coadhesion between species partner pairs occurs when one species has an adhesin corresponding to a membrane-bound receptor of another species (Rosan & Lamont, 2000). Thus, secondary colonizers can bind to the pellicle through coadhesion with primary colonizers (Kolenbrander & London, 1993). Coadhesion between *A. naeslundii* and *Streptococcus* spp. is facilitated through *A. naeslundii* adhesin type 2 fimbriae-associated protein that can bind cell wall polysaccharides with specific glycosidic linkages (Kolenbrander & London, 1993; Rosan & Lamont, 2000). Early secondary colonizers include the gram-positive species *Actinomyces israelii* and *Propionibacterium acnes*, and the gram-negative species *Capnocytophaga gingivalis*, *Haemophilus parainfluenzae*, *Prevotella denticola*, *Prevotella loescheii* and *Veillonella atypica* (Kolenbrander & London, 1993). Primary colonizers may also bind indirectly to the dental surface through coadhesion with other primary colonizers rather than direct binding to the pellicle components (Kolenbrander & London, 1993). Late colonizers bind to the pellicle almost exclusively through coadhesion with *F. nucleatum*, a primary colonizer with a diverse set of coadhesion partners. Colonization of *S. mutans* to dental plaque is largely independent of coadhesion and is rather dependent on the presence of sucrose and the expression of glycosyltransferase genes that produce adhesive glucans (Gibbons & Van Houte, 1973; Rosan & Lamont, 2000).

Proliferation of the dental plaque constitutes an increase in the number of bacteria within the biofilm and synthesis of EPS (Kaplan, 2010). The percentage-wise composition of species within the biofilm change over the course of the proliferation phase (Elias & Banin, 2012). Different niches exist throughout the dental plaque, and the percentage of biofilm-volume that is anoxic increases as the volume of the biofilm increases (Welch et al., 2016). As the dental plaque develops the proportion of *Actinomyces*, *Corynebacterium*, *Fusobacterium* and *Veillonella* increases while the proportion of *Streptococcus* and *Neisseriaceae* decreases (Kolenbrander & London, 1993; Ritz, 1967).

Dispersal of the dental plaque includes both the disaggregation of a biofilm portion leading to single cells being dispersed and the detachment of a biofilm portion leading to dispersal of a new daughter biofilm (Sauer et al., 2022). The dental plaque bacteria *Aggregatibacter aphrophilus*, *A. actinomycetemcomitans*, *Neisseria subflava*, *S. mutans*, and *S. mitis* disperse cells by forming internal cavities within the biofilm that moves the cells into the surrounding liquid (Kaplan, 2010). *S. mutans* secrete surface-protein-releasing enzyme (SPRE) that degrades adhesin P1 of the antigen I/II family and thus disrupt adhesion to acidic proline-rich proteins, parotid salivary agglutinin, and salivary glycoproteins, as well as coadhesion to *S. gordonii*, *S. mitis*, *S. oralis* (Kaplan, 2010; Rosan & Lamont, 2000). A homologous system to the Cid/Lrg system in *S. aureus* and *P. aeruginosa* can be found in *S. mutans* (Bayles, 2007; Kaplan, 2010). Inhibition of the Cid/Lrg system in *P. aeruginosa* inhibits formation of biofilm cavities (Kaplan, 2010). The Cid/Lrg system in *S. aureus* has also been linked to the production of eDNA that stabilizes the ECM structure (Bayles, 2007). The expression of *lrgAB* in *S. mutans* is solely dependent on activation by the LytST two-component system (Ahn et al., 2010). LytST has been shown to be regulated by signal molecules of the glucose metabolism as well as oxygen (Ahn et al., 2012).

1.1.4 Bacterial interaction in biofilms through two-component systems

Bacteria are able to sense the extracellular environment through two-component systems (TCSs) that consist of a transmembrane histidine kinase and a response regulator (Casino et al., 2010). The extracellular sensor domain of the histidine kinase can be bound by a signal molecule that activates the intercellular catalytic domain that can phosphorylate the response regulator, which can impact the expression of target genes (Casino et al., 2010). Gram-positive bacteria use TCSs to be able to sense cell-density through quorum sensing (Miller & Bassler, 2001). Quorum sensing bacteria secret a peptide signal that can bind a histidine kinase and

thereby cause transcription of certain genes (Miller & Bassler, 2001). The signal only becomes significant at high cell densities, causing a change in phenotype (Miller & Bassler, 2001).

Quorum sensing in *S. mutans* is used to regulate competence through the two-component systems ComRS and ComCDE (Junges et al., 2019; Ricomini Filho et al., 2019). The starting point of the ComCDE system is export and cleaving of the leader sequence of ComC by the ComAB ABC transporter thought to be encoded by *cslA* (SMU.1897 and SMU.1898) and *cslB* (SMU.1900) (Hale et al., 2005; Petersen & Scheie, 2000). Competence stimulating peptide (CSP), processed ComC, is further proteolytically cleaved by SepM producing a more active form of CSP (Petersen et al., 2006). CSP associating with the histidine kinase ComD activates its kinase domain, thereby allowing the phosphorylation of ComE (Junges et al., 2019). Phosphorylated ComE activates many genes including the *comABCDE* operon, bacteriocin genes, and bacteriocin associated genes (Junges et al., 2019). The starting point of the ComRS system is export of ComS possibly by PptAB and some other transporter (Chang & Federle, 2016) and ComS is likely proteolytically cleaved by the exporter or extracellularly into sigX-inducing peptide (XIP) (Tian et al., 2013). Extracellular XIP is internalized by Opp that enables XIP to bind ComR (Junges et al., 2019). The XIP-ComR complex activates transcription of *sigX* (also known as *comX*) and *comS* causing a positive feedback loop (Junges et al., 2019). Competence is activated by the ComRS system through the alternative sigma factor σ^X encoded by *comX* that activates transcription of competence genes and other competence-associated genes (Junges et al., 2019). The involvement of these two different regulatory systems in regulation of competence seems to be dependent on the environmental conditions and whether the strains is grown in chemically-defined or rich medium. The two systems are also interlinked, ComCDE seems to be able to stimulate *comX* via unknown mechanisms and expression of *comE* is controlled by ComRS via σ^X (Junges et al., 2019; Son et al., 2015).

Out of the 15 sets of TCSs identified in *S. mutans* UA159, four have been demonstrated to be associated with bacteriocins (Kawada-Matsuo & Komatsuzawa, 2017). In addition to the systems mentioned above, the VicRK two-component system is a positive regulator of the fructosyltransferase gene, the glucosyltransferase (D) gene, and the glucan-binding protein A gene (Senadheera et al., 2005). These EPS-associated genes are important in the formation of *S. mutans* ECM and biofilm (Senadheera et al., 2005). VicRK has also been shown to influence the *atlA* gene that causes repression of *S. mutans* biofilm formation in the oxic conditions near the biofilm surface (Ahn & Burne, 2007). CiaRH mutants have been shown to have decreased biofilm biomass and cell growth (Lévesque et al., 2007). LcrRS induces *S. mutans* immunity

to the bacteriocin nukacin ISK-1 produced by *Staphylococcus warneri* (Kawada-Matsuo & Komatsuzawa, 2017). The immunity is thought to be induced through the transcription of the LctFEG ABC transporter that actively pumps the bacteriocin out of the cell (Kawada-Matsuo & Komatsuzawa, 2017). NsrRS induces *S. mutans* immunity to the bacteriocin nisin by the transcription of *nsrX* that binds the cell membrane and traps nisin by binding (Kawada-Matsuo & Komatsuzawa, 2017).

1.2 Bacteriocins

Bacteriocins are ribosomally synthesized microbial peptides that are secreted and function as antimicrobial agents against a specific group of microorganisms (Nes et al., 2001; Yang et al., 2014). Research of bacteriocins is important for food preservation, bio-nanomaterial development, biomedical applications, and veterinary applications (López-Cuellar et al., 2016). These peptides also show potential as therapeutic antimicrobial agents against infections (Simons et al., 2020). Bacteriocins generally target a smaller group of microorganisms compared to most antibiotics (Nes et al., 2001). Narrow spectrum bacteriocins only kill closely related microorganisms, whereas broad spectrum bacteriocins kill a wide range of microorganisms (O'Connor et al., 2020). Bacteriocins are produced by gram-positive bacteria, gram-negative bacteria, and archaea (Zimina et al., 2020).

The most studied bacteriocins produced by gram-positive bacteria are the lactic acid bacteria (LAB) bacteriocins. Lactic acid bacteria include *Lactobacillus*, *Leuconostoc*, *Pediococcus*, *Lactococcus*, and *Streptococcus* (Carr et al., 2002). The LAB bacteriocins are divided into four classes that often are used to refer to gram-positive bacteriocin classes in general (Klaenhammer, 1993; Simons et al., 2020).

Lanthipeptide bacteriocins (< 5 kDa) known as lantibiotics are post-translationally modified peptides and constitute class I bacteriocins (Nes et al., 2007). Lanthipeptides contain lanthionine residues which are two crosslinked alanine residues by thioether linkage of their β-carbons (Arnison et al., 2013). Nisin is a class I bacteriocin discovered in 1928 that was reported to inhibit the proliferation of *Lactobacillus delbrueckii* subsp. *bulgaricus* (Rogers, 1928). Nisin was the first bacteriocin used commercially in food preservation due to its non-toxic nature, heat stability, and inhibition of pathogenic *Clostridium* spp. (Klaenhammer, 1993). Nisin inhibits cell wall synthesis and induces pore formation by binding to intermediate lipid II of peptidoglycan biosynthesis (Arnison et al., 2013). The inhibition of peptidoglycan biosynthesis through intermediate lipid II has been found as the target for many class I

bacteriocins (Arnison et al., 2013). This mode of action gives class I bacteriocins a wide spectrum of antimicrobial activity, in contrast to the three other bacteriocin classes that have a much narrower spectrum of antimicrobial activity (Merritt & Qi, 2012).

Class II bacteriocins are peptides characterized by being small (< 10 kDa), non-modified, heat stable, non-lanthionine containing, and membrane active (Klaenhammer, 1993). The class is further divided into four subclasses denoted IIa, IIb, IIc, and IId (Cotter et al., 2005). IIa bacteriocins have antimicrobial activity against *Listeria*, are characterized by having a linear structure and a specific N-terminal sequence (Klaenhammer, 1993; Simons et al., 2020). IIb bacteriocins are heterodimers that require both subunits to form a membrane pore and induce permeabilization of the target membrane (Klaenhammer, 1993; Simons et al., 2020). IIc bacteriocins are thiol-activated peptides that disrupt the membrane potential, causing a collapse of the proton motive force (Klaenhammer, 1993; Venema et al., 1993). IId bacteriocins include all other class II bacteriocins that do not belong in the first three subclasses (Simons et al., 2020). Class III bacteriocins are proteins characterized by being large (> 30 kDa), heat-labile and cell-wall degrading enzymes (Klaenhammer, 1993; Nes et al., 2007). Class IV bacteriocins are complex proteins characterized by being bound to other chemical moieties, such lipid or carbohydrate (Klaenhammer, 1993).

Bacteriocins produced by gram-negative bacteria can also be subdivided into four classes: colicins, colicin-like, microcins, and phage tail-like (Simons et al., 2020). The gram-negative bacteriocins are mostly isolated from *E. coli*, *Pseudomonas*, and *Klebsiella* (Simons et al., 2020).

1.2.1 Bacteriocin biosynthetic gene clusters and ABC transporters

Biosynthetic gene clusters (BGCs) encode for biosynthetic pathways that produce a specialized metabolite (Medema et al., 2015). BGCs encoding class I bacteriocins usually contain the genes for a precursor peptide, modification enzymes, exporter proteins, bacteriocin-immunity proteins, and sometimes regulatory genes (Heilbronner et al., 2021). The other classes of gram-positive bacteriocins are unmodified and thereby do not require modification enzymes for activation (Nes et al., 2001). The genes in a BGC do not require being part of the same operon, however the bacteriocin and bacteriocin-immunity gene often are in the same operon (Håvarstein et al., 1995; Medema et al., 2015).

The bacteriocin precursor peptides contain a core peptide and a leader sequence (Nes et al., 2001). In the case of class I LAB bacteriocins the leader sequence can be important for

molecule recognition by modification enzymes that modifies the core peptide (Arnison et al., 2013; Oman & van der Donk, 2010). The leader sequences target the precursor peptide to the cytoplasmic membrane, where the peptide is exported and the leader sequence is cleaved off (Nes et al., 2001). The proteolytic cleaving of the leader sequence at a double glycine motif could either be carried out by the exporter molecule or by an extracellular enzyme (Nes et al., 2001). There is also a small subset of bacteriocins that are without leader sequences, such as aureocin A53 in *S. aureus* and enterocin Q in *Enterococcus faecium* (Nes et al., 2007). Many of the bacteriocin exporter proteins have been found to belong to the ABC transporter superfamily (Håvarstein et al., 1995). ABC transporters require one domain for ATP-binding located at the C-terminal and one domain for membrane integration located at the N-terminal. The bacteriocin ABC transporters forms a pore in the cytoplasmic membrane through its transmembrane domain that enable secretion of the bacteriocin (Håvarstein et al., 1995).

Bacteriocin-immunity proteins are produced to avoid self-targeting of the bacteriocin-producer. The bacteriocin-immunity genes are often part of a biosynthetic gene cluster where the bacteriocin gene is transcribed in tandem with the bacteriocin-immunity genes to acquire self-immunity (Medema et al., 2015). Diverse mechanisms of immunity have been observed for bacteriocin-immunity proteins (Pérez-Ramos et al., 2021). The nisin producer *Lactococcus lactis* contains two different nisin self-immunity systems (Pérez-Ramos et al., 2021). The first immunity system includes the bacteriocin-immunity protein NisI that can bind nisin and thereby prevent nisin from reaching its molecular target (Pérez-Ramos et al., 2021). NisI can either be anchored to the cytoplasmic membrane or secreted extracellularly (Pérez-Ramos et al., 2021). The second immunity system includes three bacteriocin-immunity proteins that form the ABC transporter NisFEG which actively pumps nisin out of the cell (Pérez-Ramos et al., 2021). The NisFEG ABC transporter differ from the NisT ABC transporter that secrets inactive nisin with the leader sequence still attached (Lagedroste et al., 2020). Bacteriocin-immunity proteins for class IIa bacteriocins have been reported to be majority cytosolic proteins (Drider et al., 2006). It has been suggested that self-immunity for the class IIa bacteriocin enterocin CRL35 is induced by a cytosolic bacteriocin-immunity protein that binds and block the pore formed by the bacteriocin and thereby prevents permeabilization of the membrane (Barraza et al., 2017). Other class II bacteriocin-immunity proteins are membrane-bound and are able to block the bacteriocin pore similarly (Diep et al., 2007).

1.2.2 Mutacins

Mutacins are bacteriocins produced by *S. mutans*, a species predominantly thought of as the causative agent of human dental caries (Merritt & Qi, 2012). The class I mutacins include mutacin I, mutacin II, mutacin III, mutacin B-Ny266, mutacin Smb, and mutacin K8 (Merritt & Qi, 2012; Nes et al., 2007). All class I mutacins have a linear structure as characterized by the class I type A bacteriocins (Jung, 1991; Merritt & Qi, 2012). Production of mutacin I/II/III and likely mutacin K8 are regulated by the protein MutR whereas mutacin Smb is regulated by the phosphorylated ComE that is activated by CSP (**Section 1.1.4**) (Merritt & Qi, 2012). The class II mutacins are more frequently found in *S. mutans* strains compared to class I mutacins (Merritt & Qi, 2012). There are four identified class II mutacins including mutacin IV, mutacin V, mutacin VI, mutacin N (Merritt & Qi, 2012). These class II mutacins have a more narrow spectrum of activity compared to class I mutacins (Merritt & Qi, 2012). Mutacin IV, V, and VI are upregulated by the response regulators ComE, BrsR and HdrR (Perry, Jones, et al., 2009). The regulator BrsR (SMU.2080) is part of a LytTR-type regulatory system (LRS) with BrsM (SMU.2081), a membrane bound BrsR-inhibitor (Xie et al., 2010).

The well-characterized strain *S. mutans* UA159 (ATCC 700610) produces the three class II bacteriocins mutacin IV, mutacin V, and mutacin VI (Hossain & Biswas, 2011). All of which are exported by the NlmTE ABC transporter encoded by *nlmT* (SMU.286) and *nlmE* (SMU.287) (Hale et al., 2005). Mutacin IV is composed of two peptides encoded by *nlmA* (SMU.150) and *nlmB* (SMU.151), characteristic of a class IIb bacteriocin (Hossain & Biswas, 2011). Class IIb bacteriocins have been reported to form pores that induce permeabilization of the target membrane (Klaenhammer, 1993). Mutacin IV inhibits growth of all *Streptococcus* species except that of *S. mutans* and *S. pneumoniae* (Hossain & Biswas, 2011). The bacteriocin-immunity protein for mutacin IV is most likely encoded by SMU.152 (Hossain & Biswas, 2012). Mutacin V is a class II bacteriocin composed of one peptide encoded by *cipB* (SMU.1914, also called *nlmC*) (Perry, Cvitkovitch, et al., 2009). Mutacin V inhibits growth of the five *Streptococcus* species *S. anginosus*, *S. bovis*, *S. gordonii*, *S. iniae*, and *S. pyogenes*, in addition the mutacin also inhibits *Lactococcus lactis* (Hossain & Biswas, 2011). The bacteriocin-immunity protein for mutacin V is encoded by *cipI* (SMU.925) (Perry, Cvitkovitch, et al., 2009). Both *cipB* and *cipI* are upregulated by ComE (Perry, Jones, et al., 2009). Mutacin VI is a class II bacteriocin composed of one peptide encoded by *nlmD* (SMU.423) that inhibit at least *L. lactis*, vancomycin-resistant *Enterococcus faecium* and penicillin-resistant *S. pneumoniae* (Merritt & Qi, 2012; Xie et al., 2010). It has also been reported activity against

non-mutans streptococci in general (Avilés-Reyes et al., 2018). No immunity protein is known for Mutacin VI. The *S. mutans* strains N and K8 encodes the known class II bacteriocin mutacin N encoded by *mutN* (Robson et al., 2007). No immunity protein is known for mutacin N.

An important thing to note is that even though the immunity genes are known for mutacin IV and mutacin V, their mechanism of immunity is not well understood. ABC transporters seem to contribute to immunity, likely through exporting the mature peptide out of the cell.

1.3 *Streptococcus* as a model to study bacteriocin-biofilm interactions

The genus *Streptococcus* belong to the domain bacteria, the phylum Firmicutes, the class Bacilli, the order Lactobacillales (Willey et al., 2011). Streptococci are characterized by fermenting sugars into lactate. ATP generation in *Lactobacillales* only occurs through substrate-level phosphorylation, as they lack electron transport chains and cytochromes. Their limited biosynthetic capabilities cause them to be dependent on import of many vitamins, amino acids, and purines, and pyrimidines (Willey et al., 2011). *Streptococcus* is distinguished from the other *Lactobacillales* genera *Lactobacillus, Leuconostoc, Pediococcus,* and *Lactococcus* by having either incomplete (α-hemolysis) or complete (β-hemolysis) lysis of red blood cells (Willey et al., 2011). Streptococcal species were classically identified by biochemical and serological testing with the Lancefield grouping system (Gillespie, 1994).

S. mutans was discovered in an aetiological study on dental caries conducted by J. Kilian Clarke in 1924 at St. Mary's Hospital, London. He was able to frequently isolate a *Streptococcus* with very distinctive characteristics from early cases of dental caries (Clarke, 1924). The bacterium appeared to change cell morphology from a non-capsulated coccus with a diameter of 0.75 μm in neutral medium to a bacillus with a length from 1.5 μm to more than 3 μm in acidic medium. Clarke chose to name the bacterium *Streptococcus mutans* from the existing genus name *Streptococcus,* derived from the ancient Greek words στρεπτός and κόκκος meaning "chain/twisted" and "seed/berry" respectively, along with mutans derived from the Latin word mutans meaning "changing" (Billroth, 1874). The discovery also indicated that *Streptococcus mutans* was present in early development of dental caries (Clarke, 1924). The hypothesis that a few bacterial species such as *S. mutans, S. sobrinus, Lactobacillus* spp. cause dental caries has been discarded in recent times due to the caries developing in the absence of these species (Pitts et al., 2017). Dental caries is a multifactor disease where many species and environmental factors impact the outcome (Pitts et al., 2017).

1.4 Aim of study

Biofilms play a crucial role in many natural environments, infectious diseases, and industrial processes. Understanding biofilms is important to control microbial growth and to design novel therapeutic agents. Despite many advances in our understanding of biofilm biology, there are significant gaps in our knowledge of their structure and function. In this study, biofilms are studied from a bacteriocin production perspective. Bacteriocins are known as antimicrobial peptides which kill other, often closely related, bacteria. Their production is assumed to confer a competitive advantage in nature due to their killing effect. Production of bacteriocins requires a set of genes involved in biosynthesis, regulation, and immunity. However, the role of bacteriocins, bacteriocin-associated proteins and bacteriocin immunity proteins in shaping of biofilms is poorly understood. The main hypothesis is that bacteriocin-immunity genes might have an important role in formation and shaping of biofilms.

The objective of this study was to gain insights into the function of putative bacteriocin-immunity genes in biofilm formation. To achieve this, biofilm forming and bacteriocin producing oral streptococci were used as a model. The partial objectives of this work were the following:

1. Identification of potential bacteriocin-immunity genes in *S. mutans* ATCC 25175, *S. mutans* ATCC 700610, *S. mutans* ATCC 700611, and *S. sobrinus* ATCC 27352 by bioinformatic tools.
2. Set up a gene deletion system in relevant streptococcal strains.
3. Establish a biofilm model to study bacteriocin-biofilm interactions in *Streptococcus*.
4. Evaluate the role of putative bacteriocin-immunity proteins in shaping of a mono-strain streptococcal biofilm.

2 Materials

2.1 Strains

Table 2.1 Table of strains used in this study along with description and reference.

Species	Strain	Genotype	Reference
S. mutans	ATCC 25175	Wild type	American Type Culture Collection
S. mutans	ATCC 700611	Wild type	American Type Culture Collection
S. mutans	ATCC 700610	Wild type	American Type Culture Collection
S. sobrinus	ATCC 27352	Wild type	American Type Culture Collection
S. pneumoniae	MH108	Janus cassette	Maria Heggenhougen
S. mutans	ATCC 25175 (SA1)	P_{veg}::GFP::spec	Dr. Sara Arbulu
S. mutans	ATCC 25175 (SA2)	P_{veg}::mCherry::cam	Dr. Sara Arbulu

2.2 Kits

Table 2.2 Table of commercial kits used in this study along with supplier and product number.

Commercial kit	Product number	Supplier
Anaerobic atmosphere generation pack	AN0035A	Thermo Fisher
Centrifuge tube, 15 mL	188271	Greiner bio one
Centrifuge tube, 50 mL	227261	Greiner bio one
Chambered coverglass, 8 wells	155411	Thermo Fisher
Dish, 24 mm	GWST-3512	WillCo Wells
Dish, 35 mm	83.3900	Sarstedt
Hydroxyapatite discs	HA48-3	3D Biotek
Inoculation loop, 1 µL	86.1567.010	Sarstedt
Inoculation loop, 10 µL	86.1562.010	Sarstedt
InstaGene Matrix	732-6030	Bio-Rad
LIGHTrun sequencing	3glb-000lrt	Eurofins Genomics
Micro tube, 1.5 mL	MCT-150-C	Corning
Micro tube, 2 mL	72.694.106	Sarstedt
Micro tube, 5 mL	0030119401	Eppendorf
NucleoSpin Gel and PCR Clean-up	740609	Macherey-Nagel
PCR strips, 8-tubes	732-1517	VWR
PCR tubes, 200 µL	PCR-02-C	Corning
Petridish, 90 mm	1065	Heger
Pipette tips, 1250 µL/100 µL/1 µL	4646385	VWR
Pipette tips, 5 mL	9402030	Thermo Fisher
Polystyrene plates, 48-well	353078	Corning
Polystyrene plates, 96-well	82.1581	Sarstedt
Syringe, 50 mL	300866	Becton Dickinson
Syringe filter, 0.2 µm	83.1826.001	Sarstedt
Toothpicks	1202740	Flyingtiger

2.3 Chemicals

Table 2.3 Table of chemicals used in this study along with supplier and product number.

Compound	Product number	Supplier
Acetic acid (HAc)	100063	Supelco
Agar, powder for bacteriology	20767.298	VWR Chemicals
Agarose, UltraPure	16500500	Invitrogen
Agarose, Certified Molecular Biology	1613100	Bio-Rad
Ammonium sulfate ($(NH_4)2SO_4$)	A3678	SIGMA
Bacto Brain Heart Infusion	237500	BD
Bacto Todd Hewitt Broth	249240	BD
Bacto Yeast extract	212750	BD
Crystal violet	C0775	Merck
Cysteine hydrochloride	C7880	SIGMA
Dithiothreitol	D0632	SIGMA
DNA ladder, 1 kb	NO468	New England labs
DNA polymerase, Phusion	F-530L	Thermo Scientific
DNA polymerase, Red Taq	733-1320	VWR
dATP	4026	Takara
dCTP	4028	Takara
dGTP	4027	Takara
dTTP	4029	Takara
Ethanol	20824	VWR
Glucose (D+ isomer)	101176K	VWR
Glycerol	49781	SIGMA
Hemin	H5533	SIGMA
Arginine (L isomer)	W381918	SIGMA
Magnesium Chloride (MgCl)	b9021	New England labs
Magnesium sulfate heptahydrate ($MgSO4 \cdot 7H_2O$)	M2643	Merck
Menadione	M5625	SIGMA
Methanol (MeOH)	20864	VWR
Mucin from porcine stomach Type II	M2378	SIGMA
Proteose peptone	LP0085B	OXOID
peqGREEN	732-3196	VWR
Disodium hydrogen phosphate ($Na_2HPO_4 \cdot 7H_2O$)	0348	VWR
Potassium chloride (KCl)	104936	Merck
Potassium dihydrogen phosphate (KH_2PO_4)	105099	Merck
Potassium nitrate (KNO_3)	83549	VWR
Sodium carbonate (Na_2CO_3)	106392	Supelco
Sodium chloride (NaCl)	26869	VWR
Sucrose	84100	SIGMA
Tryptone	LP0042	OXOID
Urea	U5378	SIGMA

2.4 Primers

Table 2.4 Table of primers used in this study along with sequence and reference if not derived from this study.

Name	Sequence (5' to 3'), reference
Primers for 16S taxonomic identification	
11F_16s_f	TAACACATGCAAGTCGAACG, Laboratory primer
5R_16s_r	GGTTACCTTGTTACGACTT, Laboratory primer
Primers for *rpsL* sequencing	
MRP73_mut_12s_f	ACCATACTCAGTTGCTTGACG
MRP74_mut_12s_r1	ATGAAATTGCGACGTAGCGAACG
MRP81_mut_12s_r2	GCTCAGGAAAAACGTGAGG
MRP75_sob_12s_r1	AGGTCAAAAAGTTGATGCCGTC
MRP76_sob_12s_f	TGATAGTGATTCCACGTTCTTGC
MRP82_sob_12s_r2	CTAATCAGATGGCCCTAGTTGC
Primers for Janus Cassette	
DS_janus_f	GTTTGATTTTTAATGGATAATGTGATATAA, Dr. Daniel Straume
DS_janus_r	CTTTCCTTATGCTTTTGGACG, Dr. Daniel Straume
Primers for *S. mutans* ATCC 25175 immunity gene knock-out	
MRP1_im1_f1	CATCTGATAGTTGCTGATATAATCC
MRP2_im1_r1	TTATCCATTAAAAATCAAACTAAATGTTGGCTTTGGTTAAACG
MRP5_im1_f3	GTCCAAAAGCATAAGGAAAGAAATATCCTTTCTTAAATATTCTGACCA
MRP6_im1_r3	TGATGATGCTGGTGTTGCTC
MRP7_im1_r4	AATATTTAAGAAAGGATATTTTAAATGTTGGCTTTGGTTAAACGT
MRP8_im1_f4	TTAACCAAAGCCAACATTTAAAATATCCTTTCTTAAATATTCTGACCA
MRP9_im2_f1	TCATTGAGACAAAGCATTGC
MRP10_im2_r1	ACATTATCCATTAAAAATCAAACTGATTATGAAGGCAATTTTTACAAA
MRP13_im2_f3	GTCCAAAAGCATAAGGAAAGGACGTTTCTTTCTAACTTTGATATAC
MRP14_im2_r3	AGTTATAATCAAGGAAATTACCAACA
MRP15_im2_r4	CAAAGTTAGAAAGAAACGTCTGATTATGAAGGCAATTTTTACAAA
MRP16_im2_f4	AAAAATTGCCTTCATAATCAGACGTTTCTTTCTAACTTTGATATAC
Primers for *S. mutans* ATCC 25175 verification of knock-out transformants	
MRP83_im1seq_f	GCAAGTAGACTAAGCTGCC
MRP84_im1seq_r	GCCACCCAGTAAAAGATTAGC
MRP85_im2seq_f	CCAAGGGTTTCGACTTATGC
MRP87_im2seq_r	GGAACCAAATGCACATGG
Primers for *S. mutans* ATCC 700610 immunity gene knock-out	
MRP17_im3_f1	AGTTATAATCAAGGAAATTACCAACA
MRP18_im3_r1	TTATCCATTAAAAATCAAACGACGTTTCTTTCTAACTTTGATATACT
MRP21_im3_f3	GTCCAAAAGCATAAGGAAAGTTATGAAGGCAATTTTTACAAAAAGA
MRP22_im3_r3	ACTTCATTGAGACAAAGCATT
MRP23_im4_r4	TGTAAAAATTGCCTTCATAAGACGTTTCTTTCTAACTTTGATATAC
MRP24_im4_f4	CAAAGTTAGAAAGAAACGTCTTATGAAGGCAATTTTTACAAAAAGA
MRP25_im5_f1	GATGATGCTGGTGTTGCTCA
MRP26_im5_r1	ACATTATCCATTAAAAATCAAACAAATATCCTTTCTTAAATATTCTGACCA

MRP29_im5_f3	GTCCAAAAGCATAAGGAAAGTAAATGTTGGCTTTGGTTAAACG
MRP30_im5_r3	CATCTGATAGTTGCTGATATAATCC
MRP31_im5_r4	TTAACCAAAGCCAACATTTAAAATATCCTTTCTTAAATATTCTGACCA
MRP32_im5_f4	AATATTTAAGAAAGGATATTTTAAATGTTGGCTTTGGTTAAACGT
MRP33_im6_f1	TTGGACAAATCTTTCAAACTCC
MRP34_im6_r1	CATTATCCATTAAAAATCAAACGCCTTTCTATTTGTTAAATAAGTGA
MRP37_im6_f3	GTCCAAAAGCATAAGGAAAGTAAAAAAACTAGGTTTTTAGCCTTTAC
MRP38_im6_r3	GTTATACAGCAATAGCAATTATAAAGA
MRP39_im6_r4	GGCTAAAAACCTAGTTTTTTTAGCCTTTCTATTTGTTAAATAAGTGA
MRP40_im6_f4	TATTTAACAAATAGAAAGGCTAAAAAAACTAGGTTTTTAGCCTTTACC
Primers for *S. sobrinus* ATCC 27352 immunity gene knock-out	
MRP57_im7_f1	GATACCAGATGTCGCATCTG
MRP58_im7_r1	TCACATTATCCATTAAAAATCAAACTAGTTTACTACATTACTATTTTAACGATATTC
MRP61_im7_f3	GTCCAAAAGCATAAGGAAAGTCTAATTTTTAAGGACCCTTAAAATTAAT
MRP62_im7_r3	CTATCTTGGTCGCAAGATTAAG
MRP63_im7_r4	AAGGGTCCTTAAAAATTAGATAGTTTACTACATTACTATTTTAACGATATTCT
MRP64_im7_f4	AATAGTAATGTAGTAAACTATCTAATTTTTAAGGACCCTTAAAATTAATTATCACCT
MRP65_im8_f1	TATGAGGAGTAAGCATGGGC
MRP66_im8_r1	TTATCCATTAAAAATCAAACTAATTTCAACAGATAGTTCGGCT
MRP69_im8_f3	GTCCAAAAGCATAAGGAAAGGATTGCTCCTCCCTTAGTTAAACA
MRP70_im8_r3	GCCCTGCAGACCTCACTCAA
MRP71_im8_r4	TAACTAAGGGAGGAGCAATCTAATTTCAACAGATAGTTCGGC
MRP72_im8_f4	CGAACTATCTGTTGAAATTAGATTGCTCCTCCCTTAGTTAAACA
Primers for P_{veg}::GFP::spec and P_{veg}::mCherry::cam amplification	
SA17_mut25175_f	CGTTCGTCTAGCAATCTGGGCATGC, Dr. Sara Arbulu
SA18_mut25175_r	TGGCATAAGTCTTTCCCTCTTGTGG, Dr. Sara Arbulu

2.5 Antibiotics

Table 2.5 Table of antibiotics used in this study along with supplier and product number.

Antibiotic	Product number	Supplier
Spectinomycin ($C_{14}H_{24}N_2O_7 \cdot 2HCl \cdot 5H_2O$)	S9007	SIGMA
Chloramphenicol ($C_{11}H_{12}Cl_2N_2O_5$)	C0378	SIGMA
Erythromycin ($C_{37}H_{67}NO_{13}$)	E6376	SIGMA
Kanamycin sulfate ($C_{18}H_{36}N_4O_{11}$)	K4000	SIGMA
Streptomycin sulfate salt ($C_{21}H_{39}N_7O_{12}$)	S6501	SIGMA

2.6 Competence-stimulating peptides

Table 2.6 Table of competence-stimulating peptides used in this study along with sequence and reference.

Competence-stimulating peptide	Sequence (N to C), reference
XIP *S. mutans* (ComS)	SGSLSTFFRLFNRSFTQA, (Petersen et al., 2006)
XIP *S. sobrinus* (ComS)	LMCTIAR, (Li et al., 2020)

2.7 Instruments

Table 2.7 Table of instruments used in this study along with producer and series.

Instrument	Series	Producer
Autoclave	CV-EL 18 L	CertoClav
Bead beating grinder	FastPrep-24	MP biomedicals
Centrifuge, 0.2 mL	Mini Star silverline	VWR
Centrifuge, 1.5 mL	Biofuge Pico	Heraeus
Centrifuge, 15/50 mL	Allegra X-30R	Beckman Coulter
Colony counter	SC6Plus	Stuart
Electrophoresis Gel imager	Gel Doc XR+ system	Bio-Rad
Electrophoresis system	PowerPac 200	Bio-Rad
Freezer, -80°C	I920CV	Isotemp
Incubator, 37°C	TS9430	Termaks
Incubator, anaerobic 37°C	Forma Steri Cycle	Thermo Fisher
Linear Shaker	05526	Edmund Bühler
Magnetic stirrer	MR 3001 K	Heidolph
Microscope, fluorescent light source	HXP120	Zeiss
Microscope, laser scanning confocal	LSM700	Zeiss
Microscope, laser scanning confocal	LSM800	Zeiss
Microscope, Stereo	Leitz Biomed	Leica
PCR machine	ProFlex PCR system	Applied Biosystems
Plate reader	Synergy H1	BioTek
Scale	PM2000 CP124S	Sartorius
Scale	ENTRIS 6202-1S	Sartorius
Sonicator	2510	Branson
Spectrophotometer, cuvette	Pharmacia Novaspec II	Pharmacia Biotech
Spectrophotometer, glass tubes	Genesys 30	Thermo Fisher
Spectrophotometer, protein	NanoDrop 2000	Thermo Fisher
Vortex	Press-to-mix 34524	Snijders
Vortex	Vortex-Genie 2	Scientific Industries
Water bath	T100-ST12	Grant
Water dispenser, ultrapure	Q-pod	Merck

2.8 Buffers and solutions

Table 2.8 Table of buffers and solutions used in this study along with supplier and product number.

Buffer/Solution	Product number	Supplier
Gel loading dye purple, 6x	B7024A	New England Labs
Phusion GC reaction buffer, 5x	B0519S	New England Labs
Phusion HF reaction buffer, 5x	B0518S	New England Labs

TAE buffer (Tris-acetate-EDTA, 50x) was prepared by mixing 424 g tris base with 57.1 mL acetic acid (CH_3COOH) and 100 mL 0.5 EDTA at pH 8.0. The volume was adjusted by adding ddH_2O to a final volume of 1 L.

Agarose gel (electrophoresis, 1%) was prepared by mixing 5 g agarose with 500 mL TAE buffer before heating it in a microwave until complete agarose dissolution. The agarose solution was then cooled down to 55°C before 10 µL peqGREEN was added.

Agarose gel (microscopy, 1.2%) was prepared by mixing 0.5 g agarose with 50 mL 1x PBS before heating it in a microwave until complete agarose dissolution.

PBS (Phosphate-buffered saline, 10x) was prepared by dissolving 80 g sodium chloride (NaCl), 2 g potassium chloride (KCl), 25.6 g disodium hydrogen phosphate heptahydrate ($Na_2HPO_4 \bullet 7H_2O$), and 2 g potassium dihydrogen phosphate (KH_2PO_4) into 1 liter of ddH_2O. The solution was autoclaved.

Synthetic saliva was prepared by dissolving 7.5 g mucin from porcine stomach type II, 15 g proteose peptone, 15 g yeast extract, 7.5 g potassium chloride (KCl), 7.5 mg hemin, 3 mg menadione, 180 mg urea, and 523 mg arginine into 3 liters of ddH_2O. The solution was homogenized by manual shaking and mixing with a magnetic stirrer. The mix was split into six 0.5-liter aliquots and autoclaved (Montelongo-Jauregui et al., 2016).

Fluid medium (FUM) was prepared by dissolving 30 g tryptone, 15 g yeast extract, 9 g glucose, 6 mg hemin, 3 mg menadione, 1.5 g cysteine hydrochloride, 0.3 g dithiothreitol, 5.7 g sodium chloride (NaCl), 1.5 g sodium carbonate (Na_2CO_3), 3 g potassium nitrate (KNO_3), 1.35 g potassium hydrogen phosphate (K_2HPO_4), 1.35 g potassium dihydrogen phosphate (KH_2PO_4) 2.7 g ammonium sulfate ($(NH_4)_2SO_4$), 0.564 g magnesium sulfate heptahydrate ($MgSO_4 \bullet 7H_2O$) into 3 liters of ddH_2O. Hydrochloric acid (HCl) was added until a final pH of 7.1. The solution was homogenized by manual shaking and mixing with a magnetic stirrer. The mix was split into six 0.5-liter aliquots and autoclaved (Gmur & Guggenheim, 1983).

3 Methods

3.1 Experimental overview

The experiments were done in sequence as seen in **Figure 3.1** from step 1 to step 9. The success of each previous step was required to complete the sequential steps. The working strains used in this study were the *S. mutans* strains ATCC 25175, ATCC 700611 (UA130) and ATCC 700610 (UA159) along with the *S. sobrinus* strain ATCC 27352.

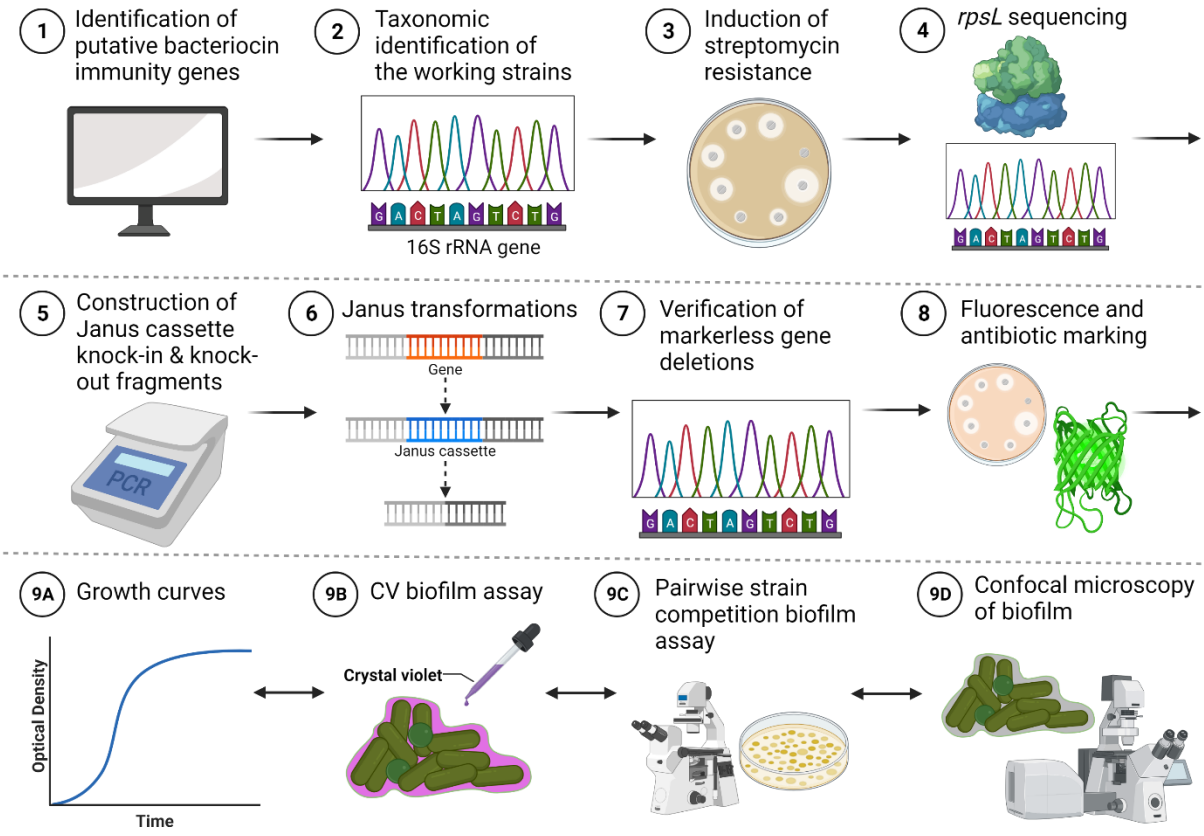

Figure 3.1: Overview of the experimental steps of this study. The steps were completed from 1 to 9. Steps 1-2 were to set up the study. Steps 3-7 were to generate markerless knock-out mutants of the identified putative bacteriocin-immunity genes. Step 8 was to label the knock-out mutants with unique fluorescence and antibiotic resistance. The bioassays of the step 9A, 9B, 9C, 9D were used to characterize the knock-out mutants. Created with BioRender.com

3.2 Identification of putative bacteriocin-immunity genes

The FASTA formatted genome sequences (ATCC Genome Portal: 25175, 27352, 700610, 700611) were uploaded to the bioinformatic tool Bagel4, a bacteriocin mining platform (van Heel et al., 2018). Bagel4 outputs bacteriocin gene clusters based on the inputted sequence. The putative bacteriocin-immunity genes of the genome sequences were annotated in the bioinformatic tool Benchling.

3.3 Growth and storage of *S. mutans* and *S. sobrinus*

The strains were grown in C-medium and on TH-medium plates with 1.5% agar (w/v). Agar plates were supplemented with the following antibiotics for selection during genetic manipulation: streptomycin (200 μg/mL), kanamycin (400 μg/mL), chloramphenicol (4.5 μg/mL), or spectinomycin (100 μg/mL) (Shields et al., 2019; Sung et al., 2001). For long term storage, the strains were cryopreserved with glycerol at a final concentration of 15% and stored in a freezer at -80°C.

3.4 Isolation of genomic DNA

DNA extraction was conducted using the InstaGene Matrix kit according to the instructions provided by the supplier. An isolated bacterial colony was suspended in 1 mL autoclaved water. The microfuge tube was then centrifuged for 1 minute and the supernatant removed. A volume of 200 μL InstaGene Matrix, previously mixed on a magnetic stirrer, was added to the pellet and incubated at 55°C for 25 minutes. The microfuge tube was vortexed for 10 seconds before being placed in a 100°C water bath for 8 minutes. The tube was vortexed again for 10 seconds before being centrifuged for 3 minutes. The supernatant was transferred to a micro tube and used further for polymerase chain reactions. All centrifugation steps were done at 12000 rpm.

3.5 DNA purification

DNA purification was conducted using the NucleoSpin Gel and PCR clean-up kit according to the instructions provided by the supplier. The kit was used for both PCR product clean-up, and DNA extraction from agarose gel. For both protocols, the NE buffer was placed in a 55°C water bath. The following step differs for the two protocols. For the PCR clean-up protocol, the PCR product was mixed with NTI buffer of a volume two times the PCR product volume. For the DNA extraction from agarose gel protocol, DNA bands were excised with a sterile scalpel. The <200 mg gel cutout was mixed with 400 μL NTI buffer. The mixture was incubated for 10 minutes at 55°C. Every 150 seconds the micro tube was vortexed briefly.

The remaining steps are the same for both protocols. The NTI buffer and sample mixture was loaded to a NucleoSpin column with a 2 mL collection tube underneath. The column and tube were centrifuged for 30 seconds and the flow-through was discarded. A volume of 700 μL NT3 buffer was loaded to the NucleoSpin column. The column and tube were centrifuged for 30 seconds and the flow-through was discarded. The column and tube were centrifuged for another 60 seconds. The 2 mL collection tube was discarded, and the column was placed into a 1.5 mL

micro tube. The NE buffer was retrieved from the water bath. A volume of 20 µL warm NE buffer was loaded to the column and left to incubate at room temperature for 60 seconds. The column and tube were centrifuged for 60 seconds, and the column was discarded. The purified DNA product in the 1.5 mL micro tube was stored at -20°C. All centrifugation steps were done at 12000 rpm.

3.6 Polymerase chain reactions

The polymerase chain reaction (PCR) is a laboratory method that amplifies the number of a particular DNA-fragment (Mullis, 1990). The method was invented by Kary Mullis in 1983, however Kjell Kleppe et al. described a similar method of DNA amplification prior to Mullins in a paper published in 1971 (Kleppe et al., 1971). The molecules involved in PCR are DNA polymerase, two short oligonucleotide primers, the template DNA and deoxynucleotide triphosphates (dNTPs) including dGTP, dATP, dTTP and dCTP (Grunberg-Manago et al., 1955).

PCR consists of reaction cycles that repeat twenty-five to thirty times, or more in the case of other DNA polymerases, to exponentially copy more of the target DNA-fragment. Every cycle the number of DNA molecules is approximately doubled. Each reaction cycle consists of three temperature-specific steps. The first step called the denaturation step increases the temperature up to 94-98°C. At this temperature the template double stranded DNA (dsDNA) molecules are melted, and the DNA strands separate. The optimal temperature is determined by the stability of the DNA polymerase used. The second step called the annealing step decreases the temperature down to 40-65°C. In this step the short oligonucleotide primers hybridize with the template DNA and thereafter DNA polymerase initiates extension of the primers. The final step of the reaction cycle is called the elongation step or extension step, where the temperature is increased to the temperature optimum for DNA polymerase activity (Mullis, 1990). In the case of the two DNA polymerases used in this study Taq polymerase and Phusion polymerase, the temperature optimum is 72°C (Chien et al., 1976; Dolgova & Stukolova, 2017). Taq DNA polymerase originates from *Thermus aquaticus*, a bacterium that inhabits hot springs and have evolved towards having thermostable enzymes that remain its activity at high temperatures. Remaining its activity at 94°C (Mullis, 1990). Phusion DNA polymerase is a fusion enzyme of a DNA polymerase from the thermophilic archaea *Pyrococcus furiosus* and a non-specific dsDNA binding protein Sso7d from the thermophilic archaea *Sulfolobus solfataricus* (Lundberg et al., 1991; Wang et al., 2004).

The temperature set for the annealing step is called the annealing temperature. The optimal annealing temperature is impacted by the affinity of the primers to the template strand. The affinity of the primers to the template strand is negatively correlated with the tendency of dsDNA primer melting into single stranded DNA (ssDNA). A higher temperature increases the tendency of dsDNA melting into ssDNA. At a certain temperature, the concentration of dsDNA and ssDNA at equilibrium becomes equal. This temperature is called the melting temperature. The standard for PCR is to set the annealing temperature around or slightly below the melting temperature of the primers. This ensures that the primers have a high rate of annealing to the template DNA. The melting temperature of a primer is positively correlated with the length of the primer and the percentage of guanine and cytosine. A common rule of thumb for the relationship between a primers nucleotide content and melting temperature is called the Wallace rule. The Wallace rule states that adding an adenine or thymine to a primer increases the melting temperature by two degrees Celsius, whereas adding a guanine or cytosine increases the melting temperature by four degrees Celsius. Using the Wallace rule, it is possible to estimate the optimal annealing temperature of a PCR (Wu et al., 1991). Another way of ensuring a high rate of annealing for the primers to the template DNA is by making the primer molecules greatly outnumber the template DNA molecules. This ensures that all molecules of single stranded template DNA are saturated with primer and will not anneal back together.

The primers with overhang used for splicing by overlap extension (SOE) were designed according to the Gibson assembly method (Gibson et al., 2009). This resulted in primers with overhang ranging in length from 47-57 nucleotides. All other primers were designed to have a melting temperature in the range 50-65°C with a length of 18-25 nucleotides, a GC content of 40-60% and with 1-2 G/C pairs in the 3’ end of the sequence.

3.6.1 PCR by Taq DNA polymerase

Red Taq DNA polymerase Master Mix contains 0.2 units/µL Taq DNA polymerase, tris-HCl (pH 8.5), ammonium sulfate ($(NH_4)_2SO_4$), 0.2% Tween 20, 0.4 mM of each deoxynucleotide triphosphate (dNTPs), 4 mM magnesium chloride ($MgCl_2$), an inert red dye and a stabilizer. The thermostable DNA polymerase harvested from *Thermus aquaticus* is what is referred to as Taq DNA polymerase. The buffers tris-HCl and ammonium sulfate stabilize the pH at around the pH-optimum of Taq polymerase activity. Tween 20, also known as Polysorbate 20, is a non-ionic detergent that boost the yield by reducing the number of secondary structures (Seal et al., 1992). Taq DNA polymerase requires a divalent cation as a cofactor to function. Ionic

magnesium (Mg^{2+}) fulfils the cofactor role efficiently, even more so than ionic manganese (Mn^{2+}) (Chien et al., 1976). The inert red dye functions as a loading dye for agarose gel electrophoresis. Preventing the DNA sample from diffusing away from the well and making it possible to track the progress of the electrophoresis (Lee et al., 2012).

PCRs using Red Taq DNA polymerase master mix were performed by adding template DNA, forward primer, reverse primer, and ddH_2O to the master mix on ice according to **Table 3.1**. The Colony PCRs were mixed according to the 10 µL reaction volume, whereas the PCRs for sequencing of the 16S rRNA genes were mixed according to the 50 µL reaction volume. The PCR program used for Taq DNA polymerase were according to the instructions provided by the supplier as listed in **Table 3.2**. Cells used as template DNA were lysed with an additional 10-minute 94°C initial lysing step prior to the used PCR program.

Table 3.1 Table of the used reaction volumes for PCR using Red Taq DNA polymerase master mix.

Component	10 µL reaction	50 µL reaction
Red Taq Pol Master Mix	5 µL	25 µL
Forward primer (10 µm)	1 µL	1 µL
Reverse primer (10 µm)	1 µL	1 µL
Template DNA	1 smear of colony	100 ng DNA/1 µL cells
ddH_2O	3 µL	19-23 µL

Table 3.2 Table of used reaction cycles for PCR using Red Taq DNA polymerase master mix.

	Temperature	Duration	Cycles
Initial denaturation	94°C	2 minutes	1x
Denaturation	94°C	30 seconds	25-30x
Annealing	60°C	30 seconds	
Elongation	72°C	60 seconds/kilobase	
End extension	72°C	5 minutes	1x
Hold	4°C	∞	

3.6.2 PCR by Phusion DNA polymerase

The Phusion DNA polymerase has 50 times higher fidelity than Taq DNA polymerase. The higher fidelity makes Phusion polymerase the superior enzyme for reactions where the PCR product is used for sequencing or transformation (Frey & Suppmann, 1995).

PCRs using Phusion DNA polymerase were performed by adding template DNA, forward primer, reverse primer, ddH_2O, Phusion HF buffer, and deoxynucleotide triphosphates to Phusion DNA polymerase on ice according to **Table 3.3**. The PCRs used for DNA sequencing were mixed according to the 25 µL reaction volume, whereas the PCRs used for synthesizing DNA constructs were mixed according to the 50 µL reaction volume. When needed, half of the final volume was pipetted over to a separate PCR tube and mixed with 1 µL magnesium chloride. The PCR program used for Phusion polymerase were according to the instructions provided by the supplier as listed in **Table 3.4**. Cells used as template DNA were lysed with an additional 10-minute 94°C initial lysing step prior to the used PCR program.

Table 3.3 Table of used reaction volumes for PCR using Phusion DNA polymerase.

Component	25 µL reaction	50 µL reaction
5X Phusion HF buffer	5 µL	10 µL
dNTPs (10 mM)	0.5 µL	1 µL
Forward primer (10 µm)	1.25 µL	2.5 µL
Reverse primer (10 µm)	1.25 µL	2.5 µL
Template DNA	25-125 ng DNA/1 µL cells	50-250 ng DNA/1 µL cells
Phusion DNA polymerase	0.25 µL	0.5 µL
ddH_2O	15 µL	30 µL

Table 3.4 Table of used reaction cycles for PCR using Phusion DNA polymerase.

	Temperature	Duration	Cycles
Initial denaturation	98°C	2 minutes	1x
Denaturation	98°C	10 seconds	25-30x
Annealing	60°C	30 seconds	
Elongation	72°C	30 seconds/kilobase	
End extension	72°C	5 minutes	1x
Hold	4°C	∞	

3.7 Agarose gel electrophoresis

Agarose gel electrophoresis is a laboratory method that separates DNA fragments based on their permeability through agarose gel. Agarose is a polysaccharide with the chemical formula $[C_{12}H_{14}O_5(OH)_4]_n$ and it is one of the two polysaccharide constituents of Agar-agar (Choji, 1956). The gel framework that is created by solidified agarose consists of double helices that assemble side-by-side and form pores (Arnott et al., 1974). The size of the pores is negatively correlated with the concentration of the agarose (Lee et al., 2012). The permeability of DNA fragments is negatively correlated with the length of the DNA fragments. An electric current is applied through the agarose gel for a duration of time. The DNA fragments form a gradient in the agarose gel from longest to shortest. The relationship between the logarithm of the DNA fragment molecular weight and the distance travelled is approximately linear (Helling et al., 1974). The concept of electrophoresis was invented by Arne Tiselius who was awarded the Nobel prize in chemistry 1948.

For each agarose gel electrophoresis in this study, approximately 50 mL agarose solution was poured into a gel tray and two combs were attached to the top of the trays. After solidification, the gels and the corresponding tray were moved into an electrophoresis chamber filled with TAE buffer. Additional TAE buffer was added until the top of the gels was submerged. DNA samples require a loading dye that makes the DNA sink to the bottom of the wells and makes it possible to observe how far into the gel the sample has travelled (Lee et al., 2012). The Red Taq DNA polymerase master mix contains an inert dye whereas the Phusion polymerase kit does not contain a pre-mixed dye. For PCR products generated by Phusion polymerase, loading buffer (6x) was added to a final concentration of 1x per DNA sample. To each well in the agarose gel 10-50 µL DNA sample was added. A volume of 5 µL 1 kb DNA ladder was added to an outer well.

3.8 Taxonomic identification of the working strains

To verify the homogeneity of the strains used in this study, they were grown on TH agar plates. The colony morphology was observed by direct observation and the cell morphology was observed by stereo microscopy.

To taxonomically identify the working strains, one colony from each strain was sampled. The sampled colonies were used for PCR and sequencing of the 16S rRNA genes. This sequencing is based on the gene encoding 16S ribosomal RNA found within the smaller 30S bacterial ribosome subunit (Kurland, 1960; Woese et al., 1975). The universal presence and conservation

of ribosomal genes in bacteria make them a prime target for taxonomic identification (Fox et al., 1977; Johnson et al., 2019). The DNA of the colonies were extracted with the InstaGene Matrix kit mentioned in **Section 3.4**. The isolated DNA was used as template DNA for PCR by Taq DNA polymerase and a reaction volume of 50 µL according to **Table 3.1** and **Table 3.2** in **Section 3.6.1**. The primers used in the reaction were 11F and 5R. To verify that the PCR amplified DNA fragments of the expected size, 10 µL of the PCR product was used in agarose gel electrophoresis according to **Section 3.7**. The remaining 40 µL PCR product was purified using the NucleoSpin Gel and PCR clean-up kit according to **Section 3.5**. The DNA concentration and quality was measured using a Nanodrop spectrophotometer. In a micro tube, 100-200 ng of the purified DNA was mixed with 2 µL primer (10 µm) and filled up with ddH_2O to a final volume of 10 µL. The micro tube was tagged with a LIGHTrun-sequencing barcode and shipped to Eurofins genomics for Sanger sequencing. The 16S rRNA gene sequencing results were analysed by the nucleotide BLAST bioinformatic tool provided by the NCBI.

3.9 Generation of transformant streptococcal strains using the Janus system

The Janus cassette system can be used to generate markerless deletions of target genes in *S. pneumoniae* and some other streptococcal species. The Janus cassette is a 1.3-kb construct that induces kanamycin resistance and streptomycin sensitivity (Sung et al., 2001). The cassette consists of two genetic elements: the *rpsL* gene encoding the ribosomal protein S12 with a mutation in the 56^{th} amino acid that converts the WT lysine into a threonine and causes dominant streptomycin sensitivity, and the *aphIII* gene that encodes aminoglycoside phosphotransferase that phosphorylates kanamycin and other aminoglycosides and thereby inactivates them (Hachler et al., 1996; Sung et al., 2001). Streptomycin interacts with the bacterial ribosomes and inhibit protein synthesis (Vianna et al., 2019). Mutated alleles of the *rpsL* gene may confer immunity to streptomycin by blocking binding or activity (Timms et al., 1992). The Janus cassette was set up in this study for markerless deletions of the putative bacteriocin-immunity genes in *S. mutans*.

To use this system, the first step was to generate streptomycin resistance in the working strains. This was achieved by growing the strains on TH agar plates with increasing supplemented streptomycin concentration (50, 100, 200, 500 µg/mL). The *rpsL* gene of the generated streptomycin resistant strains and their corresponding wildtype strains were sequenced. A volume of 1 µL frozen stock was used as template DNA for PCR by Phusion DNA polymerase as described in **Section 3.6.2**. The primer pairs (MRP73, MRP74) and (MRP73, MRP81) were

used for *S. mutans*, whereas the primer pairs (MRP75, MRP76) and (MRP76, MRP82) were used for *S. sobrinus*. The additional primers MRP81 and MRP82 were used to acquire proper sequencing quality for the nucleotides in the centre of the *rpsL* gene. A volume of 10 µL PCR product was used in agarose gel electrophoresis according to **Section 3.7** to verify that the PCR amplified a DNA fragment of the expected size. The remaining 40 µL PCR product was purified using the NucleoSpin Gel and PCR clean-up kit according to **Section 3.5**. The DNA concentration and quality of the purified DNA was measured using a Nanodrop spectrophotometer. In a micro tube, 100-200 ng of the purified DNA was mixed with 2 µL primer (10 µm) and filled up with ddH_2O to a final volume of 10 µL. The micro tube was tagged with a LIGHTrun-sequencing barcode and shipped to Eurofins genomics for Sanger sequencing.

3.9.1 Construction of Janus cassette knock-in and knock-out fragments

To achieve a markerless gene deletion using the Janus cassette, construction of two DNA fragments is required (Sung et al., 2001). The Janus knock-in fragments were designed to consist of 1000 bp upstream of the target gene, followed by the Janus cassette, and then 1000 bp downstream of the target gene. The Janus knock-out fragments were designed to consist of 1000 bp upstream of the target gene and 1000 bp downstream of the target gene. The 1000 bp flanking sequences function as a guide for homologous recombination (Capecchi, 1989).

Splicing by overlap extension (SOE) was used to generate the knock-in and knock-out fragments (Horton et al., 1989). Individual fragments were generated and then spliced together in a second PCR (**Figure 3.2**). The individual fragments were designed to contain overhang complementary to the terminal nucleotides of other individual fragments desired to splice together. The complementary overhangs make it possible for the individual fragments to partially anneal together through the overhangs. The annealed overhangs can then be extended by DNA polymerase to synthesize a larger fragment containing both individual fragments.

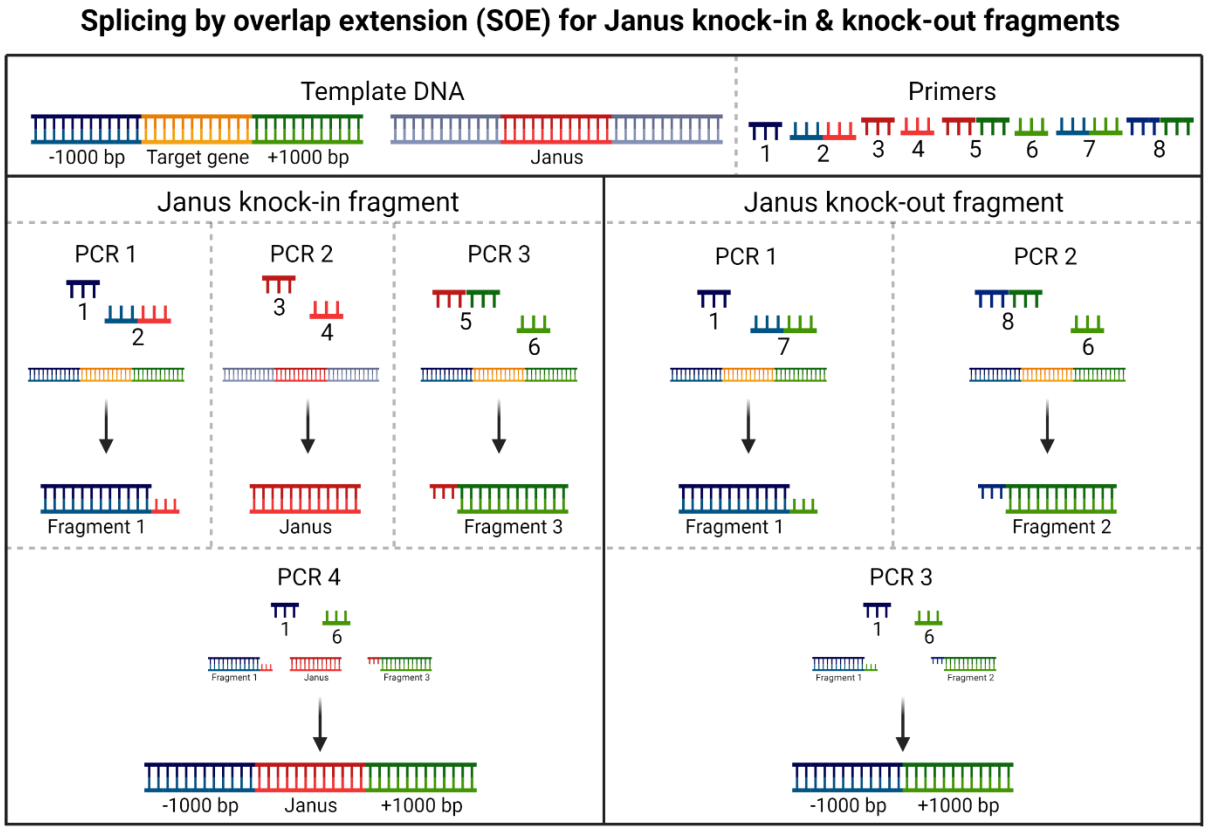

Figure 3.2: Overview illustration of splicing by overlap extension (SOE) to generate Janus knock-in and knock-out fragments. Template DNA and primers used for the PCRs are shown at the top. The PCR reagents and products for Janus knock-in fragments on the left and Janus knock-out fragments on the right. Created with BioRender.com

The three individual fragments for the Janus knock-in fragments: the Janus cassette, one fragment of 1000 bp upstream of the target gene, and one fragment of 1000 bp downstream of the target gene, were generated by PCR according to **Section 3.6.2** with the primers and the template DNA in **Table 3.6**. The Janus cassette was amplified with no overhang to the corresponding flanking regions with the primers in **Table 3.6**. The fragments of 1000 bp downstream/upstream of the gene were generated with an outer primer without overhang 1000 bp away from the target gene and one primer directly flanking the gene with overhang complementary to the terminal nucleotides of the Janus cassette. The overhang of the flank fragments corresponded to opposite sides of the Janus cassette. The 50 µL PCR product was used in agarose gel electrophoresis according to **Section 3.7**. The bands of expected fragment size were excised from the agarose gel and purified according to **Section 3.5**.

The two individual fragments for the Janus knock-out fragments: one fragment of 1000 bp upstream of the gene, and one fragment of 1000 bp downstream of the gene, were generated by PCR according to **Section 3.6.2** with the primers and template DNA in **Table 3.6**. The individual fragments were generated with an outer primer without overhang 1000 bp away from the target gene and one primer directly flanking the gene with overhang complementary to the terminal nucleotides of the other individual fragment. The 50 µL PCR product was used in agarose gel electrophoresis according to **Section 3.7**. The bands of expected fragment size were excised from the agarose gel and purified according to **Section 3.5**.

Splicing by overlap extension (SOE) was used to splice the individual fragments for the Janus knock-in and knock-out fragments. The concentration and quality of the individual fragments was measured with a Nanodrop spectrophotometer. An amount of 100 pmol of each individual fragment was used as template DNA and mixed with the Phusion PCR reagents according to the 50 µL reaction volume of **Table 3.3** in **Section 3.6.2**, however excluding the addition of primers. The mixture was used for twenty reaction cycles according to **Table 3.5**. A volume of 2.5 µL forward primer (10 µm) and 2.5 µL reverse primer (10 µm) was added to the mixture according to **Table 3.6**. A standard PCR program for Phusion polymerase as in **Table 3.4** in **Section 3.6.2** was then used for the mixture. The 50 µL PCR product was used in agarose gel electrophoresis according to **Section 3.7**. The bands of expected fragment size were excised from the agarose gel and purified according to **Section 3.5**. The purified DNA constructs were stored at -20°C and used further for transformations as described in **Section 3.9.3**.

Table 3.5 Table of used reaction cycles for the first PCR for SOE using Phusion DNA polymerase.

	Temperature	Duration	Cycles
Initial denaturation	98°C	2 minutes	1x
Denaturation	98°C	10 seconds	20x
Annealing	60°C	30 seconds	
Elongation	72°C	30 seconds/kilobase	
End extension	72°C	5 minutes	1x
Hold	4°C	∞	

Table 3.6 Overview of primers used for each PCR and SOE to synthesize the Janus knock-in and knock-out fragments. The gene names denoted for the putative bacteriocin-immunity are described in **Section 4.1**.

Product	Template DNA	Primers (fwd, rev)
Constituent Janus cassette		
Janus cassette (Janus)	*S. pneumoniae* MH108 DNA	DS_janus_f, DS_janus_r
Janus knock-in fragment and its individual fragments for immunity gene *immA*		
-1000 bp (A1)	*S. mutans* ATCC 25175 DNA	MRP1, MRP2
+1000 bp (A1)	*S. mutans* ATCC 25175 DNA	MRP5, MRP6
Janus knock-in [A]	-1000 bp (A2), Janus cassette, +1000 bp (A2)	MRP1, MRP6
Janus knock-out fragment and its individual fragments for immunity gene *immA*		
-1000 bp (A2)	*S. mutans* ATCC 25175 DNA	MRP1, MRP7
+1000 bp (A2)	*S. mutans* ATCC 25175 DNA	MRP8, MRP6
Janus knock-out [A]	-1000 bp (A2), Janus cassette, +1000 bp (A2)	MRP1, MRP6
Janus knock-in fragment and its individual fragments for immunity gene *immB*		
-1000 bp (B1)	*S. mutans* ATCC 25175 DNA	MRP9, MRP10
+1000 bp (B1)	*S. mutans* ATCC 25175 DNA	MRP13, MRP14
Janus knock-in [B]	-1000 bp (B1), Janus cassette, +1000 bp (B1)	MRP9, MRP14
Janus knock-out fragment and its individual fragments for immunity gene *immB*		
-1000 bp (B2)	*S. mutans* ATCC 25175 DNA	MRP9, MRP15
+1000 bp (B2)	*S. mutans* ATCC 25175 DNA	MRP16, MRP14
Janus knock-in [B]	-1000 bp (B2), Janus cassette, +1000 bp (B2)	MRP9, MRP14
Janus knock-in fragment and its individual fragments for immunity gene *immE*		
-1000 bp (E1)	*S. mutans* ATCC 700610 DNA	MRP17, MRP18
+1000 bp (E1)	*S. mutans* ATCC 700610 DNA	MRP21, MRP22
Janus knock-in [E]	-1000 bp (E1), Janus cassette, +1000 bp (E1)	MRP17, MRP22
Janus knock-out fragment and its individual fragments for immunity gene *immE*		
-1000 bp (E2)	*S. mutans* ATCC 700610 DNA	MRP17, MRP23
+1000 bp (E2)	*S. mutans* ATCC 700610 DNA	MRP24, MRP22
Janus knock-out [E]	-1000 bp (E2), Janus cassette, +1000 bp (E2)	MRP17, MRP22
Janus knock-in fragment and its individual fragments for immunity gene *immF*		
-1000 bp (F1)	*S. mutans* ATCC 700610 DNA	MRP25, MRP26
+1000 bp (F1)	*S. mutans* ATCC 700610 DNA	MRP29, MRP30
Janus knock-in [F]	-1000 bp (F1), Janus cassette, +1000 bp (F1)	MRP25, MRP30
Janus knock-out fragment and its individual fragments for immunity gene *immF*		
-1000 bp (F2)	*S. mutans* ATCC 700610 DNA	MRP25, MRP31
+1000 bp (F2)	*S. mutans* ATCC 700610 DNA	MRP32, MRP30
Janus knock-out [F]	-1000 bp (F2), Janus cassette, +1000 bp (F2)	MRP25, MRP30
Janus knock-in fragment and its individual fragments for immunity gene *immG*		
-1000 bp (F1)	*S. mutans* ATCC 700610 DNA	MRP33, MRP34
+1000 bp (F1)	*S. mutans* ATCC 700610 DNA	MRP37, MRP38
Janus knock-in [G]	-1000 bp (F1), Janus cassette, +1000 bp (F1)	MRP33, MRP38
Janus knock-out fragment and its individual fragments for immunity gene *immG*		
-1000 bp (F2)	*S. mutans* ATCC 700610 DNA	MRP33, MRP39

+1000 bp (F2)	*S. mutans* ATCC 700610 DNA	MRP40, MRP38
Janus knock-out [G]	-1000 bp (F2), Janus cassette, +1000 bp (F2)	MRP33, MRP38
Janus knock-in fragment and its individual fragments for immunity gene *immH*		
-1000 bp (H1)	*S. sobrinus* ATCC 27352 DNA	MRP57, MRP58
+1000 bp (H1)	*S. sobrinus* ATCC 27352 DNA	MRP61, MRP62
Janus knock-in [H]	-1000 bp (H1), Janus cassette, +1000 bp (H1)	MRP57, MRP62
Janus knock-out fragment and its individual fragments for immunity gene *immH*		
-1000 bp (H2)	*S. sobrinus* ATCC 27352 DNA	MRP57, MRP63
+1000 bp (H2)	*S. sobrinus* ATCC 27352 DNA	MRP64, MRP62
Janus knock-out [H]	-1000 bp (H2), Janus cassette, +1000 bp (H2)	MRP57, MRP62
Janus knock-in fragment and its individual fragments for immunity gene *immI*		
-1000 bp (I1)	*S. sobrinus* ATCC 27352 DNA	MRP65, MRP66
+1000 bp (I1)	*S. sobrinus* ATCC 27352 DNA	MRP69, MRP70
Janus knock-in [I]	-1000 bp (I1), Janus cassette, +1000 bp (I1)	MRP65, MRP70
Janus knock-out fragment and its individual fragments for immunity gene *immI*		
-1000 bp (I2)	*S. sobrinus* ATCC 27352 DNA	MRP65, MRP71
+1000 bp (I2)	*S. sobrinus* ATCC 27352 DNA	MRP72, MRP70
Janus knock-out [I]	-1000 bp (I2), Janus cassette, +1000 bp (I2)	MRP65, MRP70

3.9.2 Labelling of the strains

The strains were labelled with unique fluorescence and antibiotics markers under the expression of the constitutive promoter P_{veg} to enable monitoring of their behavior during biofilm formation and for visualization purposes. The P_{veg}::GFP::spec fragment providing fluorescence through GFP and spectinomycin resistance, and the P_{veg}::mCherry::cam fragment providing fluorescence through mCherry and chloramphenicol resistance.

The reporter DNA fragments P_{veg}::GFP::spec and P_{veg}::mCherry::cam were respectively in the laboratory strains SA1 and SA2. The fragments were amplified by PCRs with Phusion polymerase according to **Section 3.6.2**. The frozen stock of SA1 or SA2 were used as template DNA along with the primer pairs (SA17_mut25175_f, SA18_mut25175_r) for *S. mutans* ATCC 25175 and mixed according to the 50 µL reaction volume of **Table 3.4**. The cells were lysed with an additional 10-minute initial lysing step in the PCR program. The 50 µL PCR product was used in agarose gel electrophoresis according to **Section 3.7**. The bands of expected fragment size were excised from the agarose gel and purified according to **Section 3.5**. The purified DNA constructs were stored at stored at -20°C and used further for transformations as described in **Section 3.9.3**.

3.9.3 Transformations

The transformation protocol for the *S. mutans* strains was adapted from (Salvadori et al., 2017). Streptomycin resistant stocks were plated onto 1.5% (w/v) TH agar plates. Three to ten colonies were transferred by inoculation loop to 5 mL C-medium and incubated at 37°C until ~ 0.5 OD550. The cultures were cryopreserved with glycerol at a final concentration of 15% and stored in a freezer at -80°C. The frozen stocks were diluted by a factor of 10 to a final volume of 5 mL. The competence stimulating peptide XIP *S. mutans* was thawed on ice until the culture reached ~ 0.1 OD550. A volume of 10 µL XIP *S. mutans* (100 µM) was added to 1 mL culture. The culture was incubated at 37°C for 3 hours. A volume of 100 µL culture was transferred to each of two 1.5 mL micro tubes: a sample tube and a negative control tube. Into the sample tube 50-100 ng donor DNA was added. The micro tubes were tapped gently, and the cultures incubated at 37°C for 20 minutes. To each micro tube 200 µL warm C-medium was added. The cultures were incubated at 37°C for 2 hours. A volume of 100 µL sample and 100 µL control was each plated on 1.5% (w/v) TH agar plates supplemented with the respective antibiotic: kanamycin (400 µg/mL) for Janus knock-in, streptomycin (200 µg/mL) for Janus knock-out, spectinomycin (100 µg/mL) for P_{veg}::GFP::spec knock-in and chloramphenicol (4.5 µg/mL) for P_{veg}::mCherry::cam knock-in. The plates were incubated at 37°C, 5% CO_2 for 24 to 48 hours.

Colony PCR screening of the transformants was used to indicate successful insertion of DNA fragments into the bacterial genome. Pipette tips were used to sample 3-6 colonies and smear the cells onto the inside of PCR tubes. The cells were used as template DNA for PCR by Taq DNA polymerase as described in **Section 3.6.1**. Both single and accumulative deletions were made for the putative bacteriocin-immunity genes. The markerless deletions were further verified by DNA sequencing of the gene locus. All deletion combinations generated were sequenced. A volume of 1 µL frozen stock was used as template DNA for PCR by Phusion DNA polymerase as described in **Section 3.6.2**. For the two putative bacteriocin-immunity genes of *S. mutans* ATCC 25175 the primer pairs (MRP83, MRP84) were used for the first gene and (MRP85, MRP87) for the second gene. The PCR was verified to amplify a DNA fragment of the expected size by using 10 µL of the PCR product in agarose gel electrophoresis according to **Section 3.7**. The remaining 40 µL PCR product was purified using the NucleoSpin Gel and PCR clean-up kit according to **Section 3.5**. The DNA concentration was measured by a nanodrop spectrophotometer. In a micro tube 100-200 ng of the purified DNA was mixed with 2 µL primer (10 µm) and filled up with ddH_2O to a final volume of 10 µL. The tube was tagged with a LIGHTrun-sequencing barcode and shipped to Eurofins for Sanger sequencing.

3.10 Growth curves

Growth curves were used to characterize the growth of the deletion mutants with wildtype as a control. Two separate growth curve experiments were conducted. In the first experiment, the optical density at 550 nm was measured every 10 minutes for 20 hours on 96-well plates by a plate reader. In the second experiment, the optical density at 550 nm was measured every hour for 12 hours in glass tubes by a spectrophotometer along with plating a dilution series of the samples every second hour.

To prepare the samples, the working strains were grown to ~ 0.5 OD550 and then cryopreserved with a final concentration of 15% glycerol at -80°C. The frozen stocks were diluted by a factor of 50 in C-medium to a total volume of 5 mL each. The cultures were incubated at 37°C to an OD550 of ~ 0.5. The cultures were again diluted by a factor of 50 in C-medium to an OD550 of ~ 0.01. For both experiments, four technical replicates were used. The 96-well plates were filled with 300 µL per well. The outer wells were filled with ddH_2O to avoid evaporation impacting the optical density. The glass tubes were filled with 5 mL per tube. The optical density measurements were taken of the cultures either by a plate reader or by a spectrophotometer. The samples were shaken/vortexed prior to measurement to avoid cells aggregating.

The cultures grown in glass tubes were single plate-serial dilution spotted in a way adapted from (Thomas et al., 2015). Every 2 hours, a negligible volume of 10 µL from each sample was transferred to a 96-well plate to create a dilution series. The dilution series consisted of diluting the samples 10-fold in 5 steps. A volume of 20 µL from each step of the dilution series was spotted onto a 1.5% (w/v) TH agar plate supplemented with spectinomycin (100 µg/mL) for strains containing P_{veg}::GFP::spec or chloramphenicol (4.5 µg/mL) for strains containing P_{veg}::mCherry::cam. For the spotting, four technical replicates per dilution step was done. At the 12-hour mark, the last timepoint of the experiment, the strains were spotted onto TH agar plates supplemented with the corresponding antibiotic as well as TH agar plates supplemented with the other antibiotic as a control. Spectinomycin (100 µg/mL) for strains containing P_{veg}::mCherry::cam and chloramphenicol (4.5 µg/mL) for strains containing P_{veg}::GFP::spec. The blanks used to blank the optical density measurements were also plated on both antibiotics as a control.

3.11 Biofilm assays

Two different models were used to assess the *S. mutans* biofilms in this study. The standard biofilm model consisted of biofilms forming for 24 hours on the bottom of microtiter wells in BHI medium enriched with 1% sucrose whereas the Guggenheim's oral biofilm model based on (Lopez-Nguyen 2020) consisted of biofilms forming for 72 hours on the top of hydroxyapatite (HA) discs in synthetic saliva and fluid medium (FUM) enriched with 0.15% glucose and 0.15% sucrose (Azeredo et al., 2017; Lopez-Nguyen et al., 2020). The Guggenheim's oral biofilm model simulates the surface of teeth (Lopez-Nguyen et al., 2020). The synthetic saliva and fluid medium (FUM) are described in **Section 2.8** (Gmur & Guggenheim, 1983; Montelongo-Jauregui et al., 2016).

3.11.1 Crystal violet staining of biofilm

Crystal violet (CV) staining was used to stain the biofilms which indicates the presence of a biofilm and demonstrates the biofilm-formation capability of the strains (Christensen et al., 1985). Crystal violet stains both live and dead cells, in addition to some ECM components that could be used to quantify biomass of the biofilm (Azeredo et al., 2017).

To set up the standard biofilm model, a small volume of frozen stock was transferred with an inoculation loop to 5 mL of brain heart infusion (BHI) and the cultures were grown overnight. The overnight cultures were diluted by a factor of 1/100 in BHI supplemented with 1% sucrose. From the diluted cultures, 100 µL was added to wells in a 96-well plate or in the case of the pairwise combinations 50 µL from both overnight cultures. The outer wells were filled with ddH_2O to avoid evaporation impacting the formation of biofilm. The 96-well plate was placed in an incubator at 37°C for 24 hours.

The crystal violet staining was carried out with 8 replicates per strain. After the 24-hour incubation, the medium was removed from each of the wells. The wells were washed twice with 100 µL sterile saline (0.9%). The biofilms were dried for 5 minutes and then fixed with 200 µL methanol for 15 minutes at room temperature. The methanol was removed after the incubation period and the wells were dried for 15 minutes. To each well, 100 µL crystal violet (0.02%) was added and the plate was incubated for 15 minutes at room temperature. The crystal violet was pipetted out, and any residual crystal violet was washed away three consecutive times with 100 µL sterile saline (0.9%). To disassociate the crystal violet from the biofilms, a volume of 200 µL 33% acetic acid was added. The crystal violet suspension was transferred to a new 96-well plate used to measure the optical density at 600 nm with a plate reader.

Statistical analysis of the measurements was done to test for outliers and to test for significant differences between the samples. Grubb's test (alpha=0.05) was used to check for and remove statistical outliers. The Shapiro-Wilk normality test was used to test the normality of the sample distributions. Levene's test (alpha=0.05) was used to test the homogeneity of the variance between the sample distributions. An unpaired parametric t test was used to check for statistically significant difference between samples also between the samples and the blank.

To set up the Guggenheim's oral biofilm model, a small volume of frozen stock was transferred with an inoculation loop to 5 mL brain heart infusion (BHI) and the cultures were grown overnight. Hydroxyapatite (HA) discs were placed in the bottom of a 48-well culture plate (**Figure 3.3**) and coated with 800 µL synthetic saliva. The plate was gently shaken for 4 hours. The synthetic saliva was pipetted out of the wells and replaced with a mix of 329 µL synthetic saliva, 329 µL FUM, and 82 µL bacterial inoculum or 41 µL of both overnight cultures in the case of pairwise combinations. The plate was placed in an incubator at 37°C in anaerobic conditions for 24 hours. The medium was removed and replaced by 740 µL FUM enriched with 0.15% glucose and 0.15% sucrose (FUMe). The plate was incubated at 37°C in anaerobic conditions for 72 hours in total, replacing the medium with fresh FUMe every 24 hours.

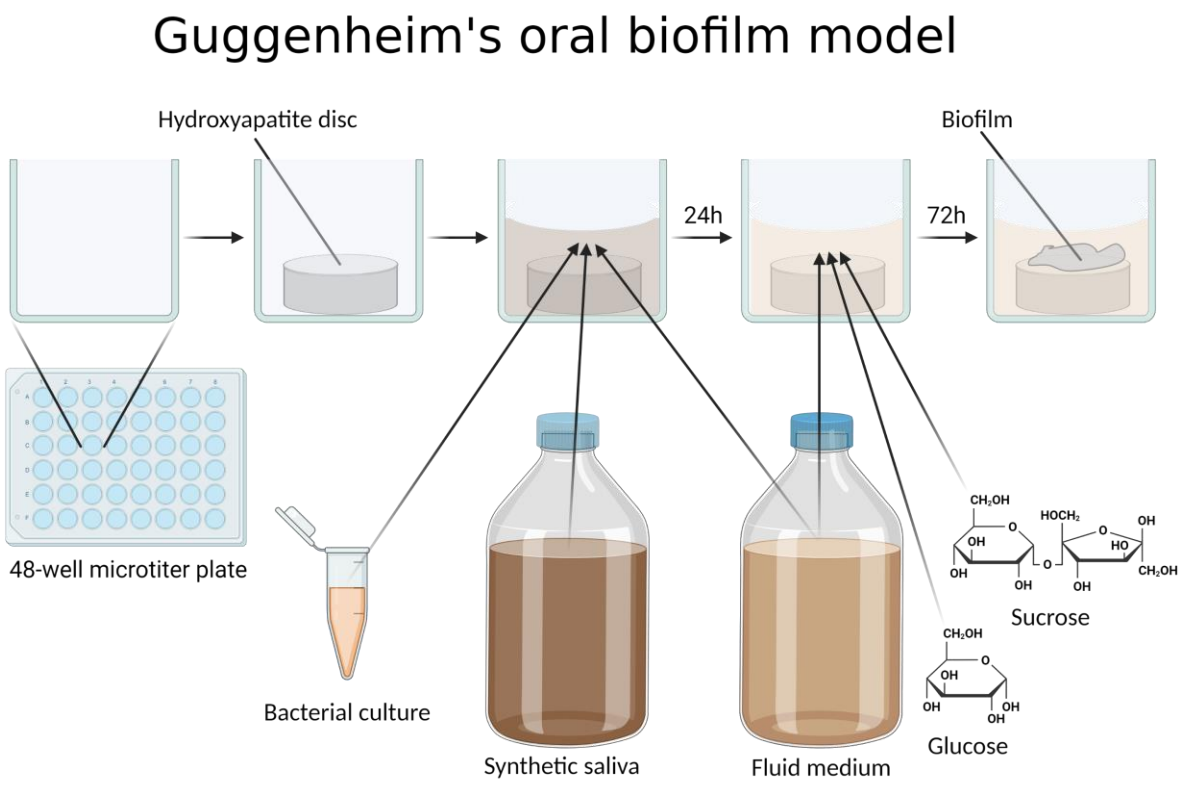

Figure 3.3: Overview illustration of Guggenheim's oral biofilm model. Created with BioRender.com

The crystal violet staining with the Guggenheim's oral biofilm model was carried out with 2 replicates per strain. After the 72-hour incubation, the medium was removed from the wells. The HA discs and wells were washed twice with 200 µL sterile saline (0.9%). The biofilms were dried for 5 minutes and then fixed with 200 µL methanol for 15 minutes at room temperature. The methanol was then removed after the incubation period, and the wells were then dried for 30 minutes. To each well, 200 µL crystal violet (0.02%) was added and the plate was incubated for 15 minutes at room temperature. The crystal violet was removed, and any residual crystal violet was washed away three consecutive times with 100 µL sterile saline (0.9%). The 48-well culture plate was photographed.

3.11.2 CFU count of pairwise strain competition in biofilm

Pairwise strain competitions were used to test for competitive advantage of strains in a biofilm. The strains used in the pairwise competitions had different reporter fragments, one strain with P_{veg}::GFP::spec and one strain with P_{veg}::mCherry::cam. The pairwise combinations used for *S. mutans* ATCC 25175 and its two putative bacteriocin-immunity genes *immA* and *immB* were as following: wild type with wild type, wild type with ΔA strain, wild type with ΔB strain, wildtype with ΔAB strain, and ΔA strain with ΔB strain. The resulting strain compositions within the biofilms were measured by three different techniques: CFU count on plates supplemented with spectinomycin (100 µg/mL) along with plates supplemented with chloramphenicol (4.5 µg/mL), fluorescent microscopy of suspended biofilm, and confocal laser scanning microscopy of the biofilms.

The CFU count and fluorescence microscopy of the standard biofilm model was carried out with 2 replicates per strain combination and 1 replicate per single strain control. The biofilms were set up as in **Section 3.11**. After the 24-hour incubation, the medium was removed from the wells. The wells were washed twice with 200 µL sterile saline (0.9%) and then the wells were filled with 250 µL sterile saline (0.9%). The saline was pipetted up and down for 30 seconds to suspend the biofilm.

For CFU counts of each replicate, the suspended biofilm was used to create a ten-fold dilution series of five steps. From each step in the dilution series, 20 µL cell suspension was spotted onto two TH agar plates supplemented with chloramphenicol (4.5 µg/mL) and two TH agar plates supplemented with spectinomycin (100 µg/mL). The plates were incubated for 24 hours at 37°C in anaerobic conditions and the CFU were counted with a colony counter.

The remaining suspended biofilm was used for fluorescence microscopy. Microscopy slides with wells were prepared by pipetting 600 µL microscope-grade agarose (1.2%) in phosphate-buffered saline (PBS) upon the slide and pressing a secondary slide gently down onto the agarose to distribute it evenly. The top slide was removed carefully after agarose solidification. To each well of the microscopy slides 0.5 µL sample was added. The objective lens of Zeiss LSM700 was immersed in oil and the slides placed upside down on top of the objective lens. Images were taken with light microscopy, GFP fluorescence, and mCherry fluorescence to observe cell morphology and distribution of the strain compositions.

The CFU count and fluorescence microscopy of the Guggenheim's oral biofilm model was carried out with 1 replicate per pairwise composition and 1 replicate per single strain control. The biofilms were set up as in **Section 3.11**. After the 72-hour incubation, the FUMe medium was removed from the wells. The HA discs and wells were washed twice with 200 µL sterile saline (0.9%) and the HA discs were gently transferred to large 5 mL microtubes filled with 1 mL of sterile saline (0.9%). The micro tubes were sonicated for 1 minute at 25 watts and then vortexed for 2 minutes while maintaining the HA discs loose inside the tubes to ensure proper mixing. The suspended biofilm was used for CFU counts and fluorescent microscopy as previously mentioned in this section.

3.11.3 Confocal microscopy of pairwise strain competition in biofilm

The pairwise strain competitions were observed directly with confocal laser scanning microscopy of the biofilms.

To set up the standard biofilm model for confocal microscopy, a small volume of frozen stock was transferred with an inoculation loop to 5 mL of brain heart infusion (BHI) and the cultures were grown overnight. The overnight cultures were diluted by a factor of 1/100 in BHI supplemented with 1% sucrose. From the diluted cultures, 300 µL was added to wells in an 8-well chambered coverglass or in the case of the pairwise combinations 150 µL from both overnight cultures. The chambered coverglass was placed in an incubator at 37°C for 24 hours.

The confocal microscopy was carried out with 2 replicates per pairwise combination and 1 replicate per single strain control. The wells were washed twice with 250 µL sterile saline (0.9%) and then the wells were filled with 300 µL sterile saline (0.9%). The objective lens of Zeiss LSM700 was immersed in oil and the chambered coverglass placed on top of the objective lens. Images were taken as confocal Z-stack of the detected biofilms with the signals produced by GFP and mCherry.

To set up the Guggenheim's oral biofilm model for confocal microscopy, a small volume of frozen stock was transferred with an inoculation loop to 5 mL brain heart infusion (BHI) and the cultures were grown overnight. Hydroxyapatite (HA) discs were placed in the bottom of a 24 mm WillCo dishes and coated with 4 mL synthetic saliva. The plate was gently shaken for 4 hours. The synthetic saliva was pipetted out of the wells and replaced with a mix of 1778 µL synthetic saliva, 1778 µL FUM, and 444 µL bacterial inoculum or 222 µL of both overnight cultures in the case of pairwise combinations. The plate was placed in an incubator at 37°C in anaerobic conditions for 24 hours. The medium was removed and replaced by 4 mL FUM enriched with 0.15% glucose and 0.15% sucrose (FUMe). The plate was incubated at 37°C in anaerobic conditions for 72 hours in total, replacing the medium with fresh FUMe every 24 hours.

The confocal microscopy was carried out with 2 replicates per pairwise combination of strains and 1 replicate per single strain control. After the 72-hour incubation, the FUMe medium was removed from the wells. The wells were washed twice with 4 mL sterile saline (0.9%) and then the wells were filled with 4 mL sterile saline (0.9%). The dipping objective of Zeiss LSM800 was placed into the saline solution of the 24 mm WillCo dishes. Images were taken as confocal Z-stack of the detected biofilms with the signals produced by GFP and mCherry.

4 Results

4.1 Identification of putative bacteriocin-immunity genes

To identify bacteriocin biosynthetic gene clusters and putative bacteriocin-immunity genes, bioinformatic BGC predictor tools can be used. The bioinformatic tool Bagel4 was used to identify bacteriocin gene clusters in the genomes of *S. mutans* ATCC 25175, *S. mutans* ATCC 700611 (UA130), *S. mutans* ATCC 700610 (UA159), and *S. sobrinus* ATCC 27352 (van Heel et al., 2018). The search resulted in a total of 13 bacteriocin areas of interest (AOIs) as seen in **Figure 4.1**.

The strain *S. mutans* ATCC 25175 had three AOIs with a total of nine putative bacteriocin genes. The annotated bacteriocin genes were the class II bacteriocins mutacin IV (named NlmAB in AOI 3) and mutacin VI (AOI 1), in addition to several uncharacterized putative bacteriocin genes denoted as Bacteriocin[1] in AOI 2 and Bacteriocin[2-6] in AOI 3. Dedicated immunity genes are known for *nlmA*/*nlmB* where the contiguous downstream ORF encode an immunity protein, however no dedicated immunity genes are known for mutacin VI. Two putative bacteriocin-immunity genes were found, encoding the ABC-transporter subunits ImmA and ImmB. The two other *S. mutans* strains ATCC 700611 (UA130) had two AOIs with a total of two putative bacteriocin genes and two putative bacteriocin-immunity genes encoding ImmC and ImmD whereas the well-characterized strain ATCC 700610 (UA159) had five AOIs with a total of eight putative bacteriocin genes (including mutacin IV, V, and VI) and three putative bacteriocin-immunity genes encoding ImmE, ImmF and ImmG.

Several bacteriocin loci are shared between the *S. mutans* strains. The first AOI (AOI 1, 4, 6) for the three *S. mutans* strains had conserved synteny and each AOI contained two putative bacteriocin-immunity genes. The pairwise sequence alignments of the protein sequences ImmA, ImmC, and ImmE resulted in a >99.3% sequence identity, in addition the pairwise sequence alignment of protein sequences ImmB, ImmD, and ImmF resulted in a >99.5% sequence identity. This demonstrated that *immA*, *immC*, *immE* (SMU.431) represent the same gene in the three strains and the same is true for *immB*, *immD*, *immF* (SMU.413). The bacteriocin gene encoding mutacin VI is also conserved in these AOIs. Pairwise sequence alignment between the protein encoded by SMU.431 and the protein encoded by SMU.413 resulted in a ~32.6% sequence identity. The protein ImmH had a ~25% sequence identity with either of the proteins encoded by the genes SMU.431 and SMU.413. Lastly, pairwise sequence alignment between ImmG and ImmI resulted in a ~48% sequence identity. The second AOI

(AOI 2, 5, 7) for the three *S. mutans* strains had conserved synteny with a putative bacteriocin gene encoding Bacteriocin [1]. The third AOI (AOI 3, 8) for *S. mutans* ATCC 25175 and *S. mutans* ATCC 700610 (UA159) had a conserved synteny for the first half of the AOI with a putative regulatory gene. The 8th AOI contain *nlmAB* and the putative bacteriocin genes denoted Bacteriocin[7-9] whereas the 3rd AOI contains the gene encoding mutacin IV. Instead, the strain *S. mutans* ATCC 700610 (UA159) has *nlmAB* in AOI 9 in addition to a putative bacteriocin-modification gene in AOI 10 denoted BmbF.

The strain *S. sobrinus* ATCC 27352 had a total of three AOIs with a total of eight putative bacteriocin genes and two putative bacteriocin-immunity genes encoding ImmH and ImmI. The putative bacteriocin genes are denoted BlpM in AOI 11, Bacteriocin[11-15] in AOI 12, and Zoocin A in AOI 13. The putative bacteriocin-immunity genes are in different AOIs where *immH* is in AOI 11 and *immI* is in AOI 12.

All the genes identified as putative immunity genes by Bagel4 encoded either ABC-transporter subunits or homologs to another membrane-located secretion protein known as HlyD, while the known immunity protein of NlmAB was not detected. ABC transporter proteins are known to be involved as bacteriocin exporters and as bacteriocin-immunity proteins (Diep et al., 2007; Pérez-Ramos et al., 2021) however the genetic location of the ABC transporter does not indicate any direct involvement as dedicated exporters. On the other hand, the genes *immB*, *immD*, and *immF* encode a homolog of the ABC transporter EcsAB which has been reported to secrete non-cognate peptides (Heinrich et al., 2008). We do currently not have any evidence that these proteins in fact are involved in the immunity function, but we decided to denote these as putative immunity proteins in the context of this study.

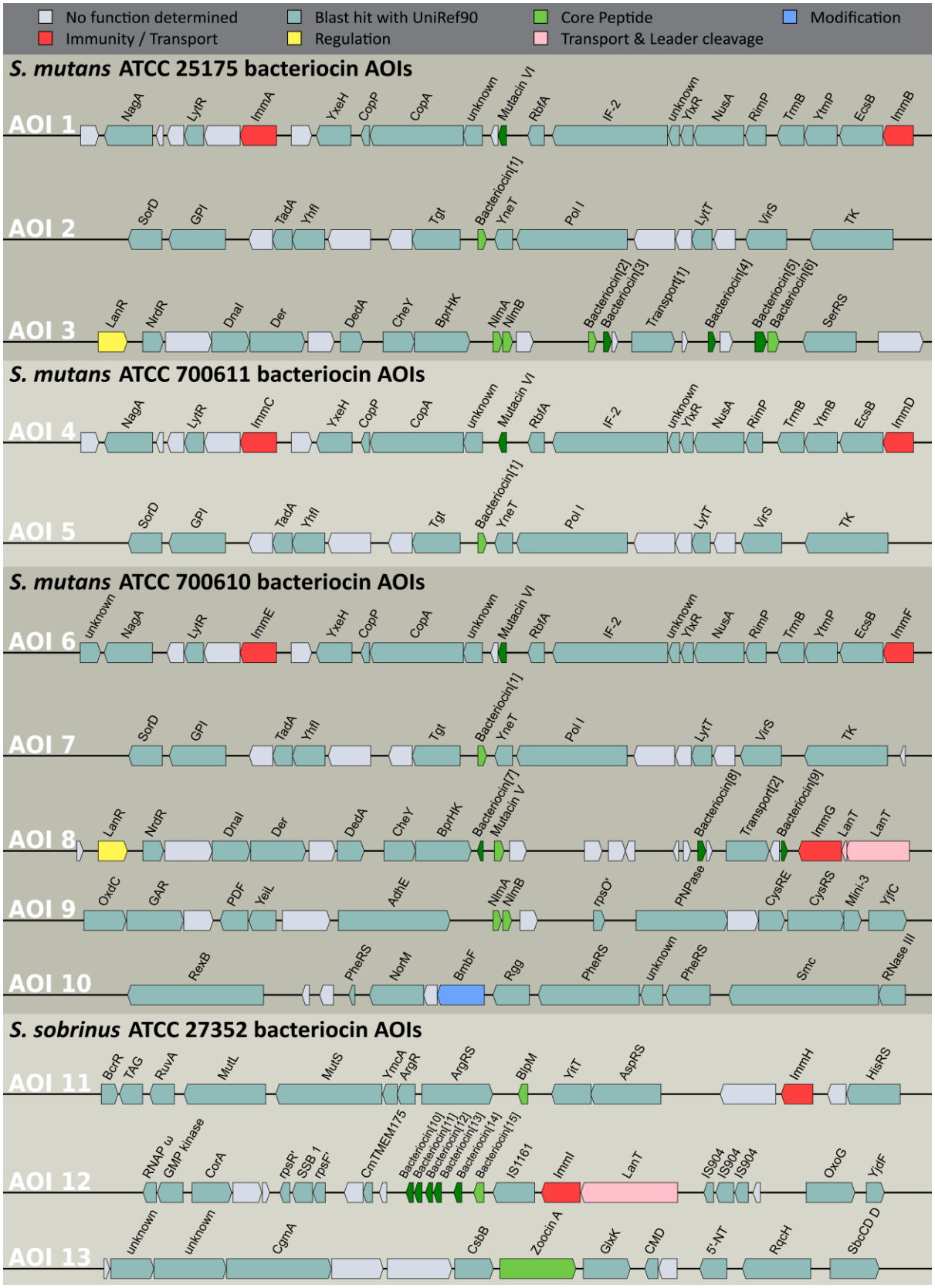

Figure 4.1: Overview of the bacteriocin areas of interest (AOIs) obtained from Bagel4. The grey open reading frames (ORFs) had no query hits of motif/sequence information, the teal ORFs had a query hit with UniRef90, the green ORFs are putative bacteriocin genes, the blue ORFs are putative bacteriocin-modification genes, the red ORFs are putative bacteriocin-immunity/transport genes, the yellow ORFs are putative bacteriocin-regulation genes, and the pink ORFs are putative bacteriocin-transport and leader-cleavage genes.

4.2 Verification of working strains

Before using the provided strains for the succeeding experiments, their identity was checked by 16S rRNA gene sequencing and analysed regarding homogeneity of morphology. The isolates of *S. mutans* ATCC 25175, *S. mutans* ATCC 700610, and *S. sobrinus* ATCC 27352 formed morphologically uniform colonies when grown on TH agar plates and the cells had uniform and expected cell morphology when observed in the microscope. The isolate of *S. mutans* ATCC 700611 showed signs of contamination by forming dissimilar colonies. Attempts to isolate the strain were unsuccessful. The strain was therefore disregarded for further use in this study. Bioinformatic searches of the 16S rRNA gene sequencing results for the three remaining working strains using BLAST (NCBI) resulted in query hits of species matching the expected strains. The isolates of *S. mutans* ATCC 25175, *S. mutans* ATCC 700610, and *S. sobrinus* ATCC 27352 were used further in this study.

4.3 Streptomycin resistance by *rpsL* mutation

The use of the Janus cassette system for counterselection and generation of successive gene deletions relies on the strains being streptomycin resistant due to mutations in the *rpsL* gene (Sung et al., 2001). The strains *S. mutans* ATCC 25175, *S. mutans* ATCC 700610, and *S. sobrinus* ATCC 27352 were successfully induced to streptomycin resistance by exposure to increasing streptomycin concentrations on TH agar plates (**Section 3.9**). The resistance was verified by the growth of the strains on TH agar plates supplemented with 500 µg/mL streptomycin. The *rpsL* gene of the streptomycin-resistant strains and the corresponding wildtype strains were sequenced. *S. mutans* ATCC 25175 had a single missense mutation of nucleotide 168 in the *rpsL* gene exchanging a guanine to a thymine and causing the 56^{th} amino acid of the 12S protein to change from a lysine to an asparagine. *S. mutans* ATCC 700610 had a single missense mutation of nucleotide 310 in the *rpsL* gene exchanging a cytosine to an adenine and causing the 104^{th} amino acid of the 12S protein to change from a proline to a threonine. *S. sobrinus* ATCC 27352 had no mutations in the *rpsL* gene, therefore the Janus cassette system could not be used for this strain. The strain was disregarded from further use in this study.

4.4 Using the Janus cassette system to genetically modify streptococci

To generate markerless deletion mutants using the Janus cassette system two fragments must be synthesized for each gene, a Janus knock-in fragment and a Janus knock-out fragment (**Section 3.9.1**). The strains can then be transformed using the Janus fragments. To verify the markerless deletions of the putative bacteriocin-immunity genes, the target gene loci must be sequenced.

The Janus knock-in and Janus knock-out fragments for *immA*, *immB*, *immE*, *immF*, *immG*, *immH*, and *immG* were successfully generated by overlap extension (SOE). This required two PCRs and two agarose gel electrophoreses per fragment, as mentioned in **Section 3.9.1**. The first PCRs amplified fragments of the 1000 bp flanking regions or the 1319 bp fragment of the Janus cassette, which both were verified by agarose gel electrophoresis, as seen in **Figure 4.2A** for the 1000 bp flanking regions. The second PCRs amplified fragments of either 3319 bp corresponding to the Janus cassette with both flanking regions of the target gene or 2000 bp corresponding to the fused flanking regions of the target gene, both fragments were verified by agarose gel electrophoresis as seen in **Figure 4.2B**.

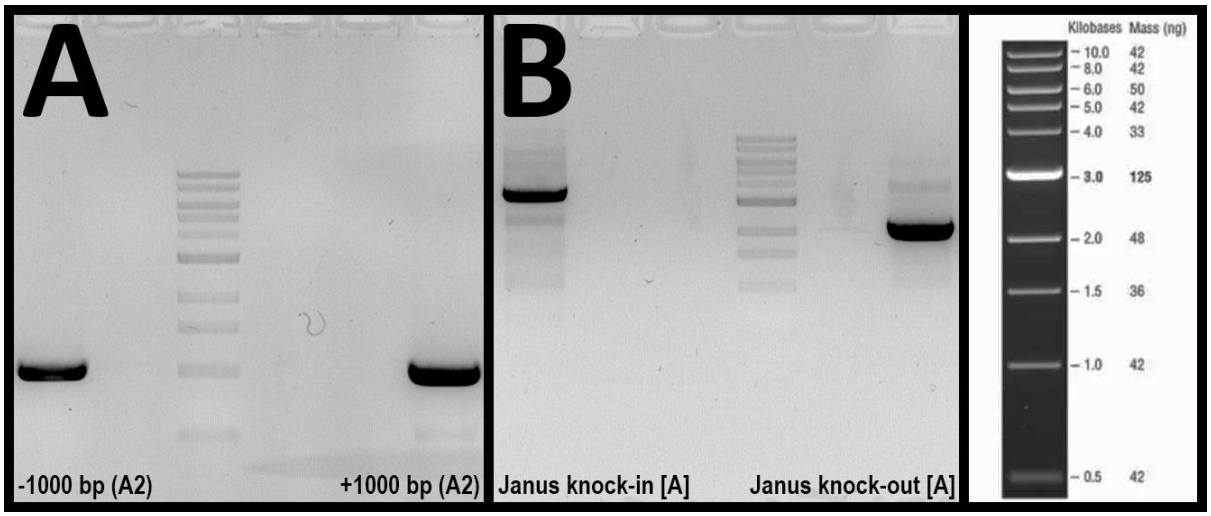

Figure 4.2: Agar gel electrophoreses verifying successful PCR amplification of DNA fragments for the Janus system. A: electrophoresis image of the amplified 1000 bp fragments: '-1000 bp (A2)', and '+1000 bp (A2)'. B: electrophoresis image of the amplified 3319 bp fragment 'Janus knock-in [A]', and 2000 bp fragment 'Janus knock-out [A]'. The fragment names are according to **Table 3.6**. The 1 kb ladder was used in both electrophoreses.

Janus knock-in and Janus knock-out transformations were successful to generate single and double markerless deletion mutants of *immA* and *immB* in *S. mutans* ATCC 25175. The deletion combinations generated for the strain were: 'ΔA' with *immA* deleted, 'ΔB' with *immB* deleted, and 'ΔAB' with both *immA* and *immB* deleted. For transformations with *S. mutans*

ATCC 700610 the Janus knock-in at bacteriocin-immunity gene loci was successful, however the following Janus knock-out transformations were unsuccessful. The strain was therefore disregarded for further use in this study.

The loci of *immA* and *immB* were sequenced for the four following *S. mutans* ATCC 25175 strains: wildtype, 'ΔA', 'ΔB', and 'ΔAB'. The strains were as expected: 'ΔA' had a clean deletion of *immA*, 'ΔB' had a clean deletion of *immB*, 'ΔAB' had a clean deletion of both *immA* and *immB*. In addition, the sequencing verified 300 bp downstream of the 1000 bp flanking region involved in homologous recombination, therefore confirming that the insertions occurred at the correct loci.

The four *S. mutans* ATCC 25175 strains wildtype, 'ΔA', 'ΔB', and 'ΔAB' were then labelled with fluorescence and antibiotic markers through insertion of the fragments P_{veg}::GFP::spec or P_{veg}::mCherry::cam. The transformations with the markers were successful. Generating a total of eight transformant strains denoted as seen in **Table 4.1**.

Table 4.1 Table of transformant strains generated in this study along with description and names used to reference the strain. P_{veg}::GFP::spec strains are fluorescent by GFP and spectinomycin resistant. P_{veg}::mCherry::cam strains are fluorescent by mCherry and chloramphenicol resistant.

Strain	Genotype	Reference name
S. mutans ATCC 25175	Wild type with P_{veg}::GFP::spec	'WT GFP-spec'
S. mutans ATCC 25175	Wild type with P_{veg}::mCherry::cam	'WT mCherry-cam'
S. mutans ATCC 25175	Δ*immA* with P_{veg}::GFP::spec	'ΔA GFP-spec'
S. mutans ATCC 25175	Δ*immA* with P_{veg}::mCherry::cam	'ΔA mCherry-cam'
S. mutans ATCC 25175	Δ*immB* with P_{veg}::GFP::spec	'ΔB GFP-spec'
S. mutans ATCC 25175	Δ*immB* with P_{veg}::mCherry::cam	'ΔB mCherry-cam'
S. mutans ATCC 25175	Δ(*immA, immB*) with P_{veg}::GFP::spec	'ΔAB GFP-spec'
S. mutans ATCC 25175	Δ(*immA, immB*) with P_{veg}::mCherry::cam	'ΔAB mCherry-cam'

4.5 Growth of modified *S. mutans* ATCC 25175 strains

The growth of the constructed strains was assayed to check whether the genetic modifications had affected their fitness. Growth curves for the eight transformant strains: 'WT GFP-spec', 'WT mCherry-cam', 'ΔA GFP-spec', 'ΔA mCherry-cam', 'ΔB GFP-spec', 'ΔB mCherry-cam', 'ΔAB GFP-spec', and 'ΔAB mCherry-cam' were evaluated. As expected, the growth curve of the strains with the same deletions of target genes but with differing reporter fragments were nearly identical as seen in **Figure 4.3**, **Figure 4.4**, **Figure 4.5**, and **Figure 4.6**.

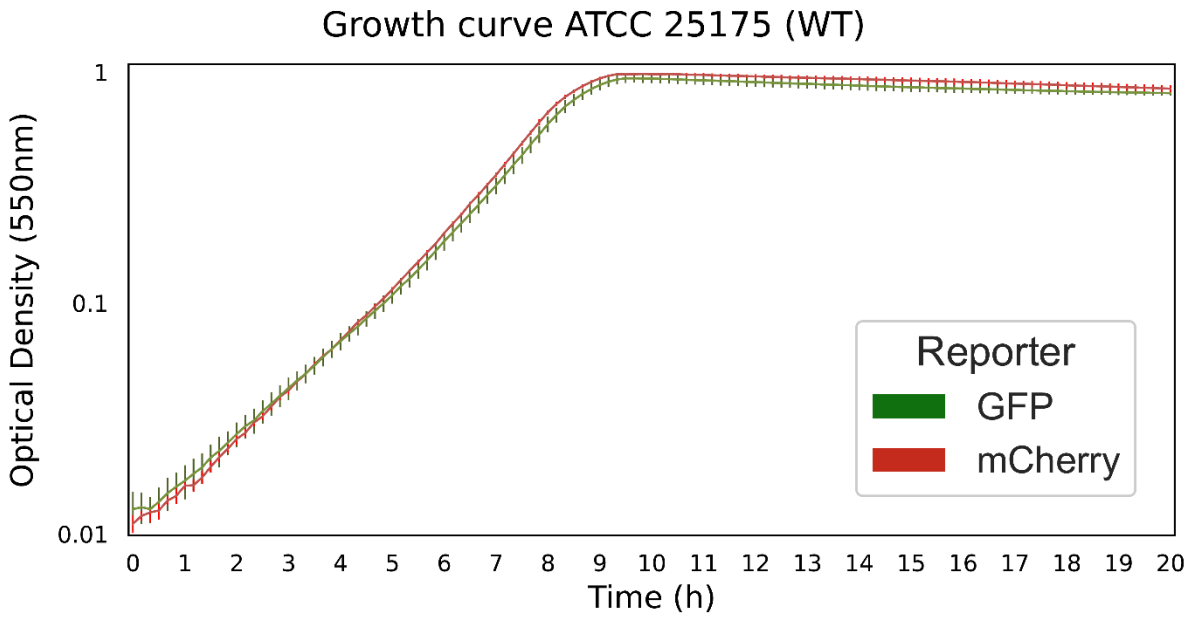

Figure 4.3: Growth curve of *S. mutans* ATCC 25175 strains 'WT GFP-spec' and 'WT mCherry-cam'. The optical density at 550 nm was measured every 10 minutes. The error bars show the standard deviation of the measurements.

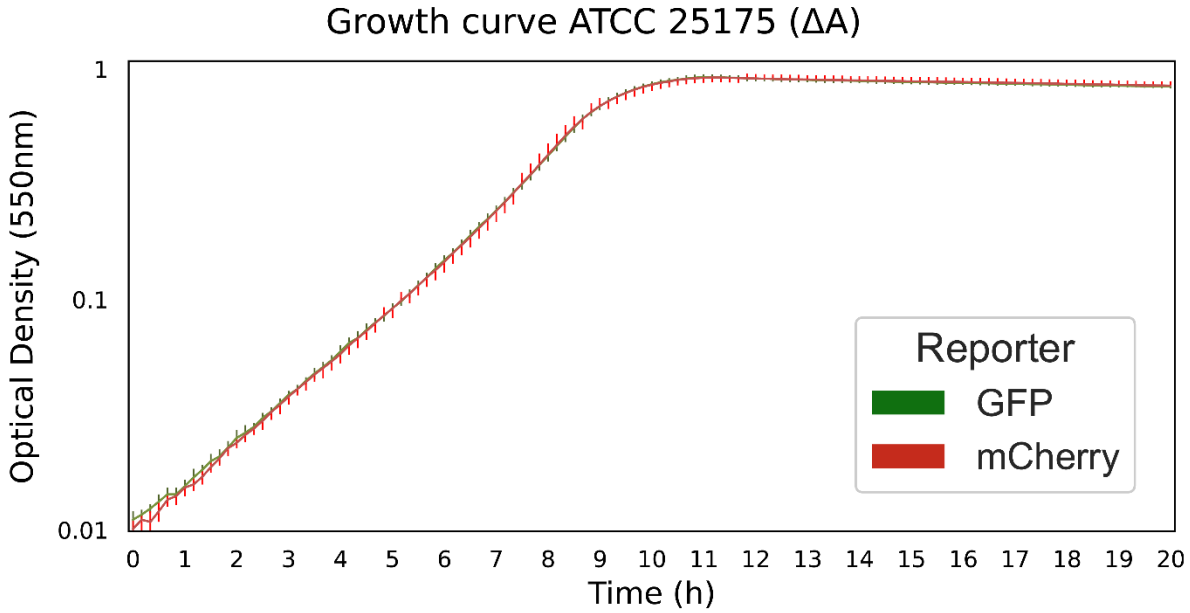

Figure 4.4: Growth curve of *S. mutans* ATCC 25175 strains 'ΔA GFP-spec' and 'ΔA mCherry-cam'. The optical density at 550 nm was measured every 10 minutes. The error bars show the standard deviation of the measurements.

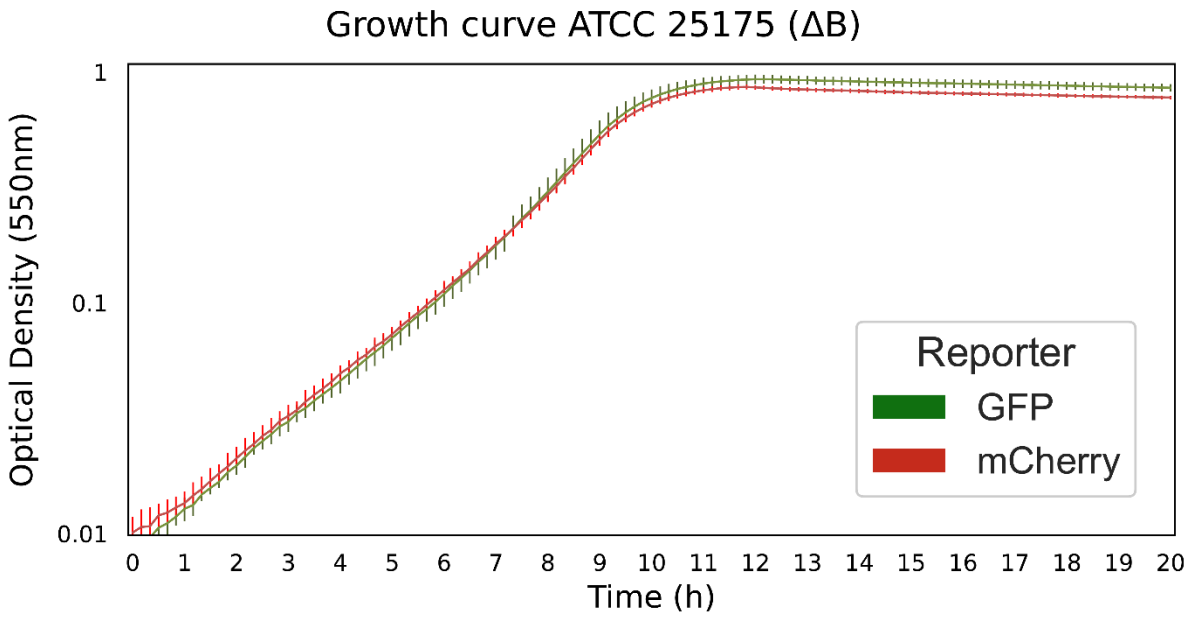

Figure 4.5: Growth curve of *S. mutans* ATCC 25175 strains 'ΔB GFP-spec' and 'ΔB mCherry-cam'. The optical density at 550 nm was measured every 10 minutes. The error bars show the standard deviation of the measurements.

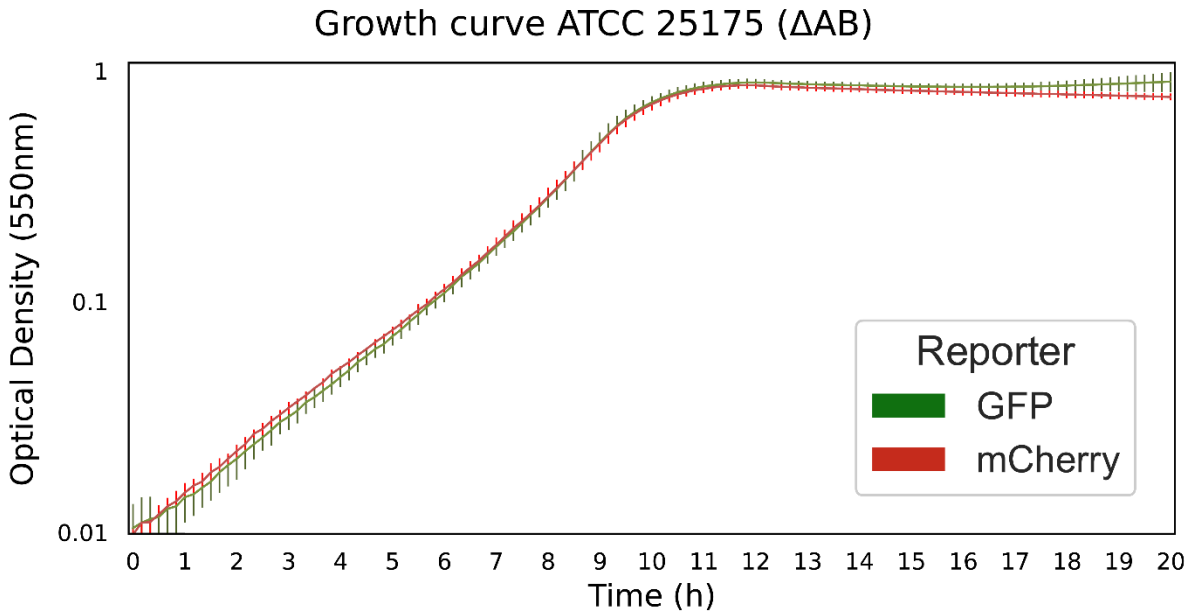

Figure 4.6: Growth curve of *S. mutans* ATCC 25175 strains 'ΔAB GFP-spec' and 'ΔAB mCherry-cam'. The optical density at 550 nm was measured every 10 minutes. The error bars show the standard deviation of the measurements.

As seen in **Figure 4.7** with P_{veg}::GFP::spec strains and **Figure 4.8** with P_{veg}::mCherry::cam strains: the growth rates of the wildtype strains were slightly higher than the knock-out strains, further the growth rates of the 'ΔA' strains were slightly higher than both of the 'ΔB' strain and 'ΔAB' strain, while the growth rates of the 'ΔB' strains and the 'ΔAB' strains were nearly identical.

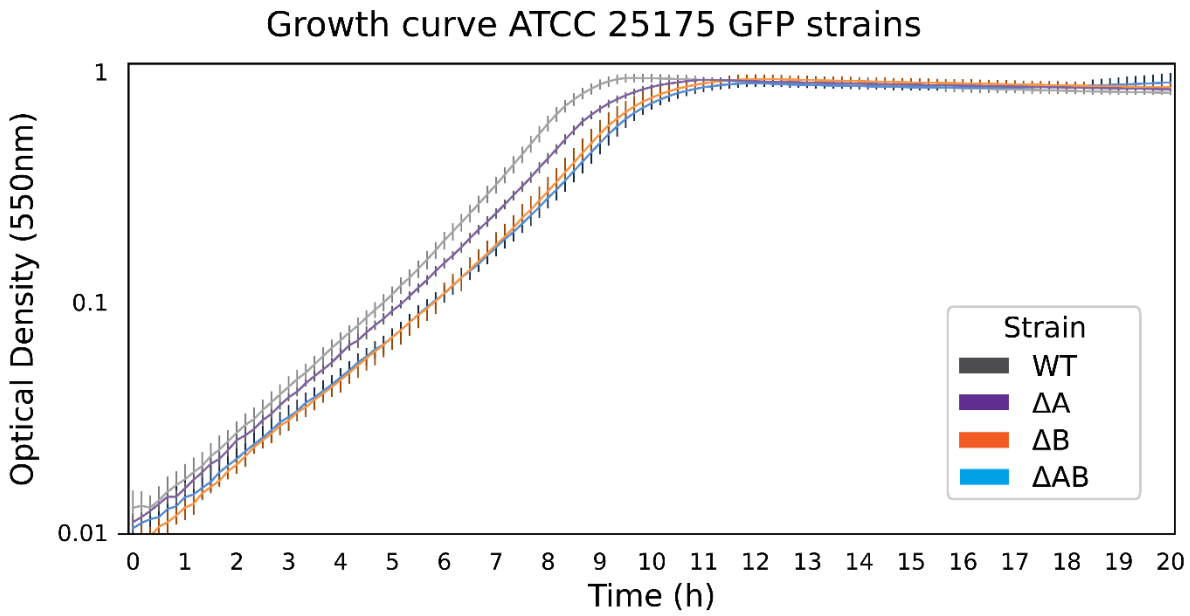

Figure 4.7: Growth curve of *S. mutans* ATCC 25175 knock-out strains labelled with P_{veg}::GFP::spec. The optical density at 550 nm was measured every 10 minutes by a plate reader. The error bars show the standard deviation of the measurements. 'WT GFP-spec' in grey. 'ΔA GFP-spec' in purple. 'ΔB GFP-spec' in orange. 'ΔAB GFP-spec' in cyan.

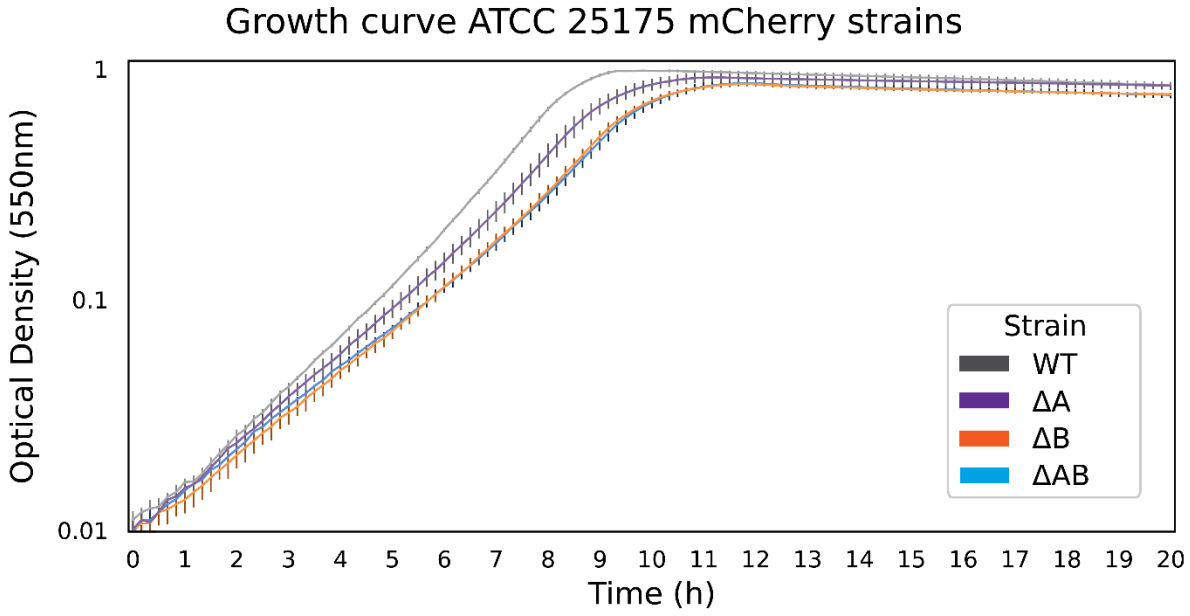

Figure 4.8: Growth curve of *S. mutans* ATCC 25175 knock-out strains labelled with P_{veg}::mCherry::cam. The optical density at 550 nm was measured every 10 minutes. The error bars show the standard deviation of the measurements. 'WT mCherry-cam' in grey. 'ΔA mCherry-cam' in purple. 'ΔB mCherry-cam' in orange. 'ΔAB mCherry-cam' in cyan.

The growth rates above were made using microtiter-plates. In addition, the growth of the strains was also monitored in volumes of 5 ml in glass tubes and CFU/ml was also determined in the same cultures. The growth curves for the optical density (550 nm) measured in glass tubes as mentioned in **Section 3.10** had a trend where wildtype strains had a higher growth rate than the rest of the strains, whereas the other strains had a similar growth rate (**Appendix Figure A.1**, **Figure A.2**). The growth curves based on the CFU/mL measurements, on the other hand, seemed to have no distinguishable trend between the different variants (**Appendix Figure A.3**, **Figure A.4**). Taken together, the growth assays demonstrate that wild type *S. mutans* ATCC 25175 grow slightly better than the *immA* and *immB* knock-out mutants, although this difference is not observed when measuring CFU/mL. This indicates that it may be favourable for the fitness of the strain to carry these two genes.

4.6 Assessing biofilm formation of *S. mutans* strains by standard biofilm model

4.6.1 Crystal violet biofilm staining with the standard biofilm model

The amount of biofilm formed by the constructed strains were assayed through crystal violet staining to check whether the genetic modifications had affected the biofilm-formation capabilities of the strains. The crystal violet staining mentioned in **Section 3.11.1** describes biofilm staining with the standard biofilm model. There was a statistically significant (****, **p< 0.0001**) higher optical density (600 nm) for the crystal violet suspended from the biofilms created by the eight *S. mutans* ATCC 25175 strains: 'WT GFP-spec', 'WT mCherry-cam', 'ΔA GFP-spec', 'ΔA mCherry-cam', 'ΔB GFP-spec', 'ΔB mCherry-cam', 'ΔAB GFP-spec', and 'ΔAB mCherry-cam' compared to the blank, showing that all strains had the capability to form biofilm. There were only minor differences between the strains in terms of biofilm formation, indicating that all the strains form biofilm to a similar extent. It should be noted, however, that there was a statistically significant difference (***, p< 0.05**) difference in the biofilm formed by 'WT GFP-spec' compared to 'ΔB GFP-spec', 'WT GFP-spec' compared to 'ΔAB GFP-spec', and 'ΔA mCherry-cam' compared to 'ΔB mCherry-cam' as seen in **Figure 4.9**.

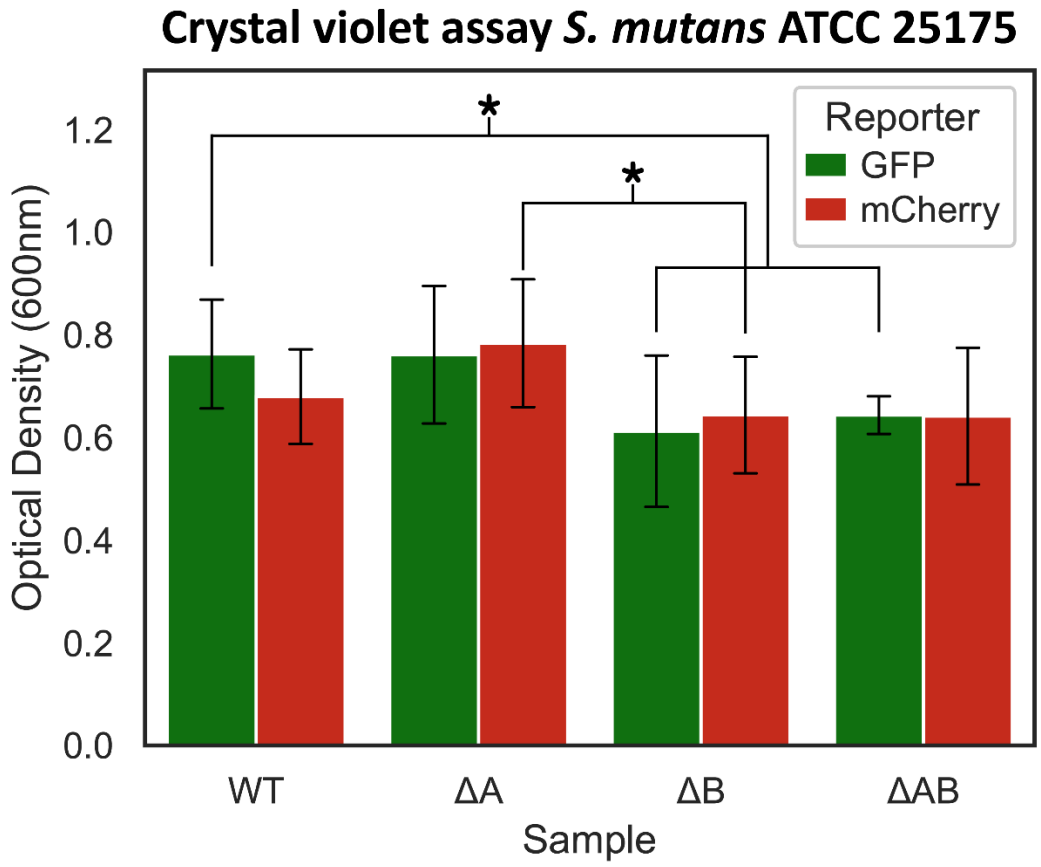

Figure 4.9: Crystal violet assay for the standard biofilm model of *S. mutans* ATCC 25175 strains. The OD values of the samples were subtracted by the average value of the blank technical replicates. The error bars show the standard deviation of the measurements. The average difference between strain pairs with similar putative bacteriocin-immunity gene deletions and strains with similar reporter fragments were analysed with unpaired parametric t tests with Welch's correction. There was a statistically significant difference between 'WT GFP-spec' with 'ΔB GFP-spec', 'WT GFP-spec' with 'ΔAB GFP-spec', and 'ΔA mCherry-cam' with 'ΔB mCherry-cam' by a p-value of below 0.05 (***, p< 0.05**).

4.6.2 Pairwise strain competition with the standard biofilm model

The competitive advantage of having the putative bacteriocin-immunity genes *immA* and *immB* when aggregated in a biofilm was analysed through pairwise strain competitions. The predominance of a strain within a two-strain may indicate the competitive advantage of the strain. The pairwise strain competitions were carried out in the standard biofilm model, using CFU-counts for quantification, as mentioned in **Section 3.11.2**.

The mono-strain biofilm controls of the strains 'WT GFP-spec', 'WT mCherry-cam', 'ΔA GFP-spec', 'ΔB mCherry-cam', and 'ΔAB mCherry-cam' had a similar CFU/mL (**Figure 4.10A**) showing that the strains form biofilm to a similar degree. The pairwise competitions were carried out with the pairs (WT GFP-spec', 'WT mCherry-cam'), ('WT mCherry-cam', 'ΔA GFP-spec'), ('WT GFP-spec', 'ΔB mCherry-cam'), ('WT GFP-spec', 'ΔAB mCherry-

cam'), and ('ΔA GFP-spec', 'ΔB mCherry-cam') and the percentage-wise compositions were estimated by dividing the CFU/mL measured on TH agar plates supplemented with either spectinomycin or chloramphenicol to the total CFU/mL measured on both the plates (**Figure 4.10B**). The dataset met the criteria for a nonparametric Kolmogorov-Smirnov t test. There was a statistically significant difference in percentage-wise strain composition with a p-value of below 0.05 (*) for only the first, second, and forth pair. Dissolved cells from the biofilms were observed by fluorescence microscopy (**Appendix Figure A.5**).

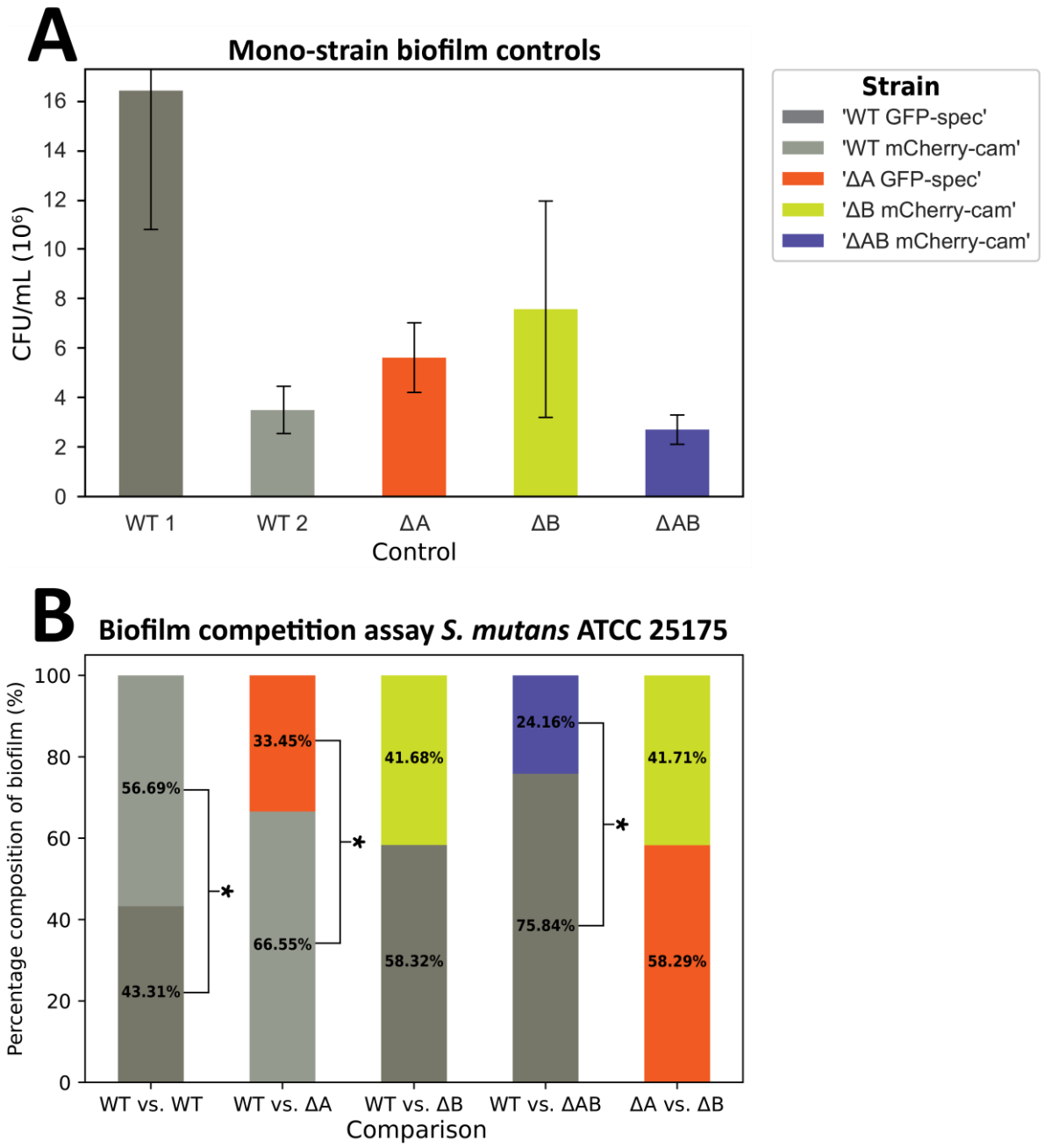

Figure 4.10: Percentage-wise composition of strains in the first standard biofilm model experiment. The CFU/mL of antibiotic resistant strains were measured on TH agar plates supplemented with either spectinomycin or chloramphenicol. The percentages were calculated by dividing CFU/mL on one antibiotic to the total CFU/mL.

The experiment was repeated with combinations of opposite selective markers as the first experiment. The mono-strain biofilm controls of the strains ‘WT mCherry-cam’, ‘WT GFP-spec’, ‘ΔA mCherry-cam’, ‘ΔB GFP-spec’, and ‘ΔAB GFP-spec’ had a similar CFU/mL (**Figure 4.11A**). The pairwise competitions were carried out with the pairs (‘WT mCherry-cam’, ‘WT GFP-spec’), (‘WT GFP-spec’, ‘ΔA mCherry-cam’), (‘WT mCherry-cam’, ‘ΔB GFP-spec’), (‘WT mCherry-cam’, ‘ΔAB GFP-spec’), and (‘ΔA mCherry-cam’, ‘ΔB GFP-spec’) that resulted in a significant difference in the percentage-wise composition with a p-value of below 0.05 (*) for only the third and fourth pairs (**Figure 4.11B**). Taken together, this suggests that the deletion mutants of the putative bacteriocin-immunity genes lose competitive advantage in a biofilm when compared to the wildtype strains.

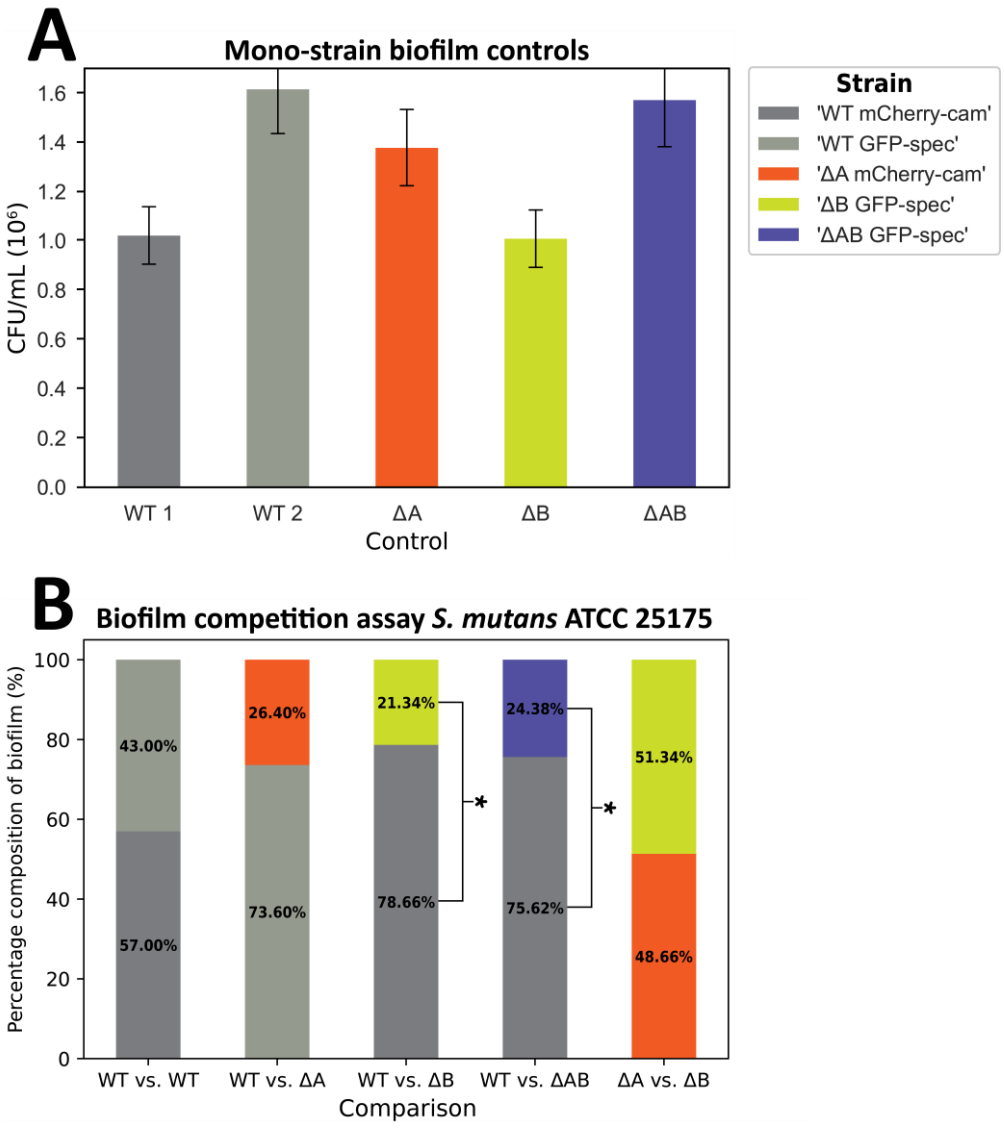

Figure 4.11: Percentage-wise composition of strains in the second standard biofilm model experiment. The CFU/mL of antibiotic resistant strains were measured on TH agar plates supplemented with either spectinomycin or chloramphenicol. The percentages were calculated by dividing CFU/mL on one antibiotic to the total CFU/mL.

4.6.3 Confocal Laser Scanning microscopy of the standard biofilm model

The biofilms were also observed through confocal laser scanning microscopy to check if similar strain compositions as estimated by the CFU/mL measurements in the previous section could be observed within the biofilms. Microscopy of the biofilms formed by individual strains as well as pairwise combinations in the standard biofilm model was carried out as mentioned in **Section 3.11.3**. The depth of the biofilms ranged from 15 to >40 μm (**Figure 4.12**). In the twenty confocal images taken, there was a clear tendency of predominantly signal from mCherry signal regardless of the combinations, suggesting that the setup of the microscopy was not optimal for the assay (**Appendix Figure A.6A-D**). However, in **Appendix Figure A.6E** there was roughly equal signal between GFP and mCherry.

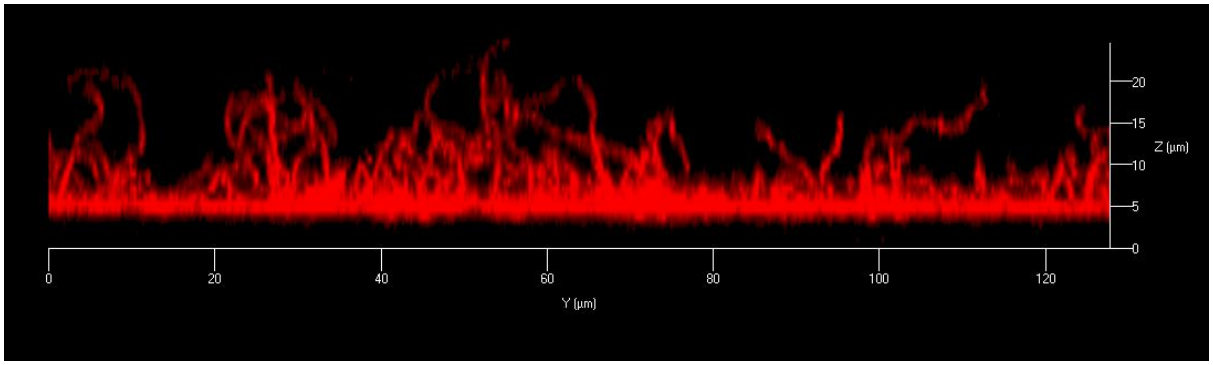

Figure 4.12: Confocal z-stack of biofilm viewed from side, 15 μm depth. Image of 'ΔA mCherry-cam' control.

4.7 The Guggenheim's oral biofilm model

4.7.1 Crystal violet biofilm staining with the Guggenheim's oral biofilm model

To mimic the conditions during biofilm formation on the dental surfaces of the oral cavity, the in vitro Guggenheim oral biofilm model (Lopez-Nguyen et al., 2020) with hydroxyapatite discs was used. The crystal violet staining of the Guggenheim's oral biofilm model (**Section 3.11.1**) was done to test whether the individual *S. mutans* strains could form biofilms under these conditions. The HA discs without biofilm stained with a pale purple, whereas biofilm displayed a dark purple color in this experimental setup (**Figure 4.14**). The fact that sample replicates stained partially dark purple, indicates successful biofilm formation for the individual strains.

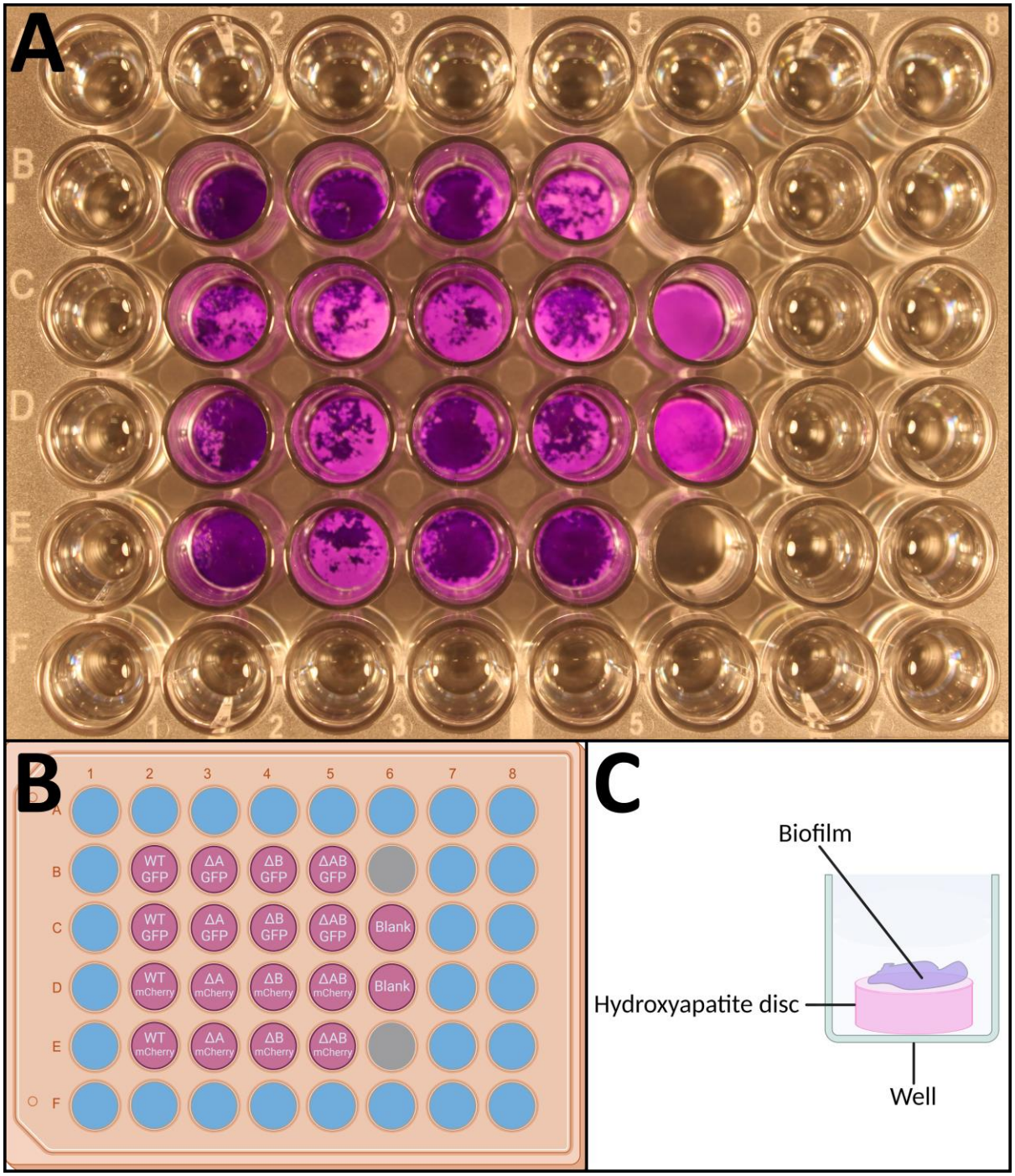

Figure 4.14: Crystal violet assay for the Guggenheim's oral biofilm model of *S. mutans* ATCC 25175 strains. A: photograph of the 48-well microtiter plate containing the stained HA discs. B: illustration demonstrating the location of the samples for each well in the image. Strains are indicated by gene deletions and fluorescent marker. C: Illustration demonstrating a well with stained biofilm on top of a hydroxyapatite disc. Created with BioRender.com

4.7.2 Pairwise strain competition with the Guggenheim's oral biofilm model

The competitive advantage of having the genes *immA* and *immB* when aggregated in a biofilm was analysed through pairwise strain competitions with the Guggenheim's oral biofilm model (**Section 3.11.2**) that mimics conditions in the oral cavity. In contrast to the previous twenty-four hours pairwise strain competitions with the standard biofilm model, the pairwise strain competitions with the Guggenheim's oral biofilm model were conducted for ninety-six hours. The predominance of a strain within a pairwise biofilm should therefore be clearer, in addition the mimicking of the oral cavity should indicate to a better degree the conditions found during dental plaque formation.

Pairwise competition of *S. mutans* ATCC 25175 strains was carried out in the Guggenheim's oral biofilm model as mentioned in **Section 3.11.2**. The suspended biofilms of pairwise strain combinations were plated out on TH agar plates supplemented with spectinomycin or chloramphenicol. The mono-strain biofilm controls of the strains 'WT GFP-spec', 'WT mCherry-cam', 'ΔA GFP-spec', 'ΔB mCherry-cam', and 'ΔAB mCherry-cam' had a similar CFU/mL (**Figure 4.15A**) showing that the strains form biofilm to a similar degree. The pairwise competitions were carried out with the pairs (WT GFP-spec', 'WT mCherry-cam'), ('WT mCherry-cam', 'ΔA GFP-spec'), ('WT GFP-spec', 'ΔB mCherry-cam'), ('WT GFP-spec', 'ΔAB mCherry-cam'), and ('ΔA GFP-spec', 'ΔB mCherry-cam') and the percentage-wise compositions were estimated by dividing the CFU/mL measured on TH agar plates supplemented with either spectinomycin or chloramphenicol to the total CFU/mL measured on both the plates (**Figure 4.15B**). The dataset clearly shows that the wildtype strains outcompete the competitor strains 'ΔA GFP-spec', 'ΔB mCherry-cam', and 'ΔAB mCherry-cam' whereas the wildtype versus wildtype competition show more similar ratios. In addition, the competition between 'ΔA GFP-spec' and 'ΔB mCherry-cam' also less significant differences in the ratios. The suspended biofilms were also observed by fluorescence microscopy, which indicated similar distribution of the strains in the pairwise strain combinations as determined by the CFU/mL measurements (Data not shown). No statistical comparisons were made due to the low number of replicates.

Together, this indicates that the deletion mutants of the putative bacteriocin-immunity genes *immA* and *immB* are outcompeted by the wildtype strain. The genes therefore give increased fitness to *S. mutans* in single strain biofilms.

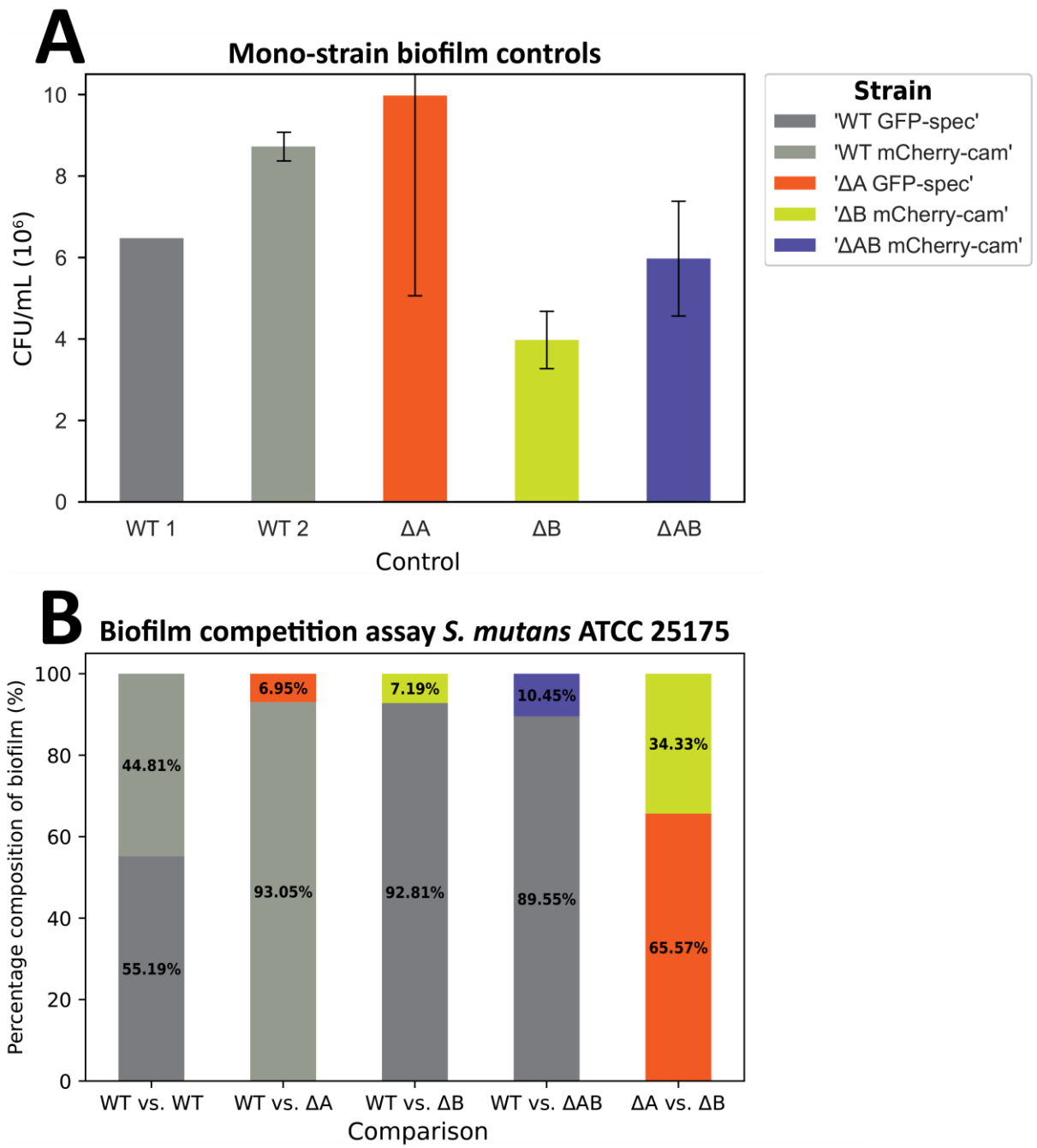

Figure 4.15: Percentage-wise composition of strains in the Guggenheim's oral biofilm model. The CFU/mL of antibiotic resistant strains were measured on TH agar plates supplemented with either spectinomycin or chloramphenicol. The percentages were calculated by dividing CFU/mL on one antibiotic to the total CFU/mL.

4.7.3 Confocal Laser Scanning microscopy of Guggenheim's oral biofilm model

The biofilms were observed through confocal laser scanning microscopy with a dipping objective to check if similar percentage-wise strain compositions as estimated by the CFU/mL measurements in the previous section could be observed within the biofilms.

Microscopy of the biofilms formed by the pairwise combinations in the Guggenheim's oral biofilm model was carried out as mentioned in **Section 3.11.3**. By visual inspection of the microscopy images, the competition between the strains 'WT GFP-spec' and 'WT mCherry-cam' seemed to result in roughly equal ratios (**Figure 4.16A**). In the competition between 'ΔA GFP-spec' and 'WT mCherry-cam' the wildtype strain seemed to be significantly more prevalent (**Figure 4.16B**). No confocal images were taken of the other combinations of interest. The images further support the conclusion of **Section 4.7.1** that biofilms can form on the HA discs of the Guggenheim's oral biofilm model. The perceived percentage-wise compositions observed of the combinations ('WT GFP-spec', 'WT mCherry-GFP') and ('ΔA GFP-spec', 'WT mCherry-cam') seems to match those found in **Section 4.7.2**.

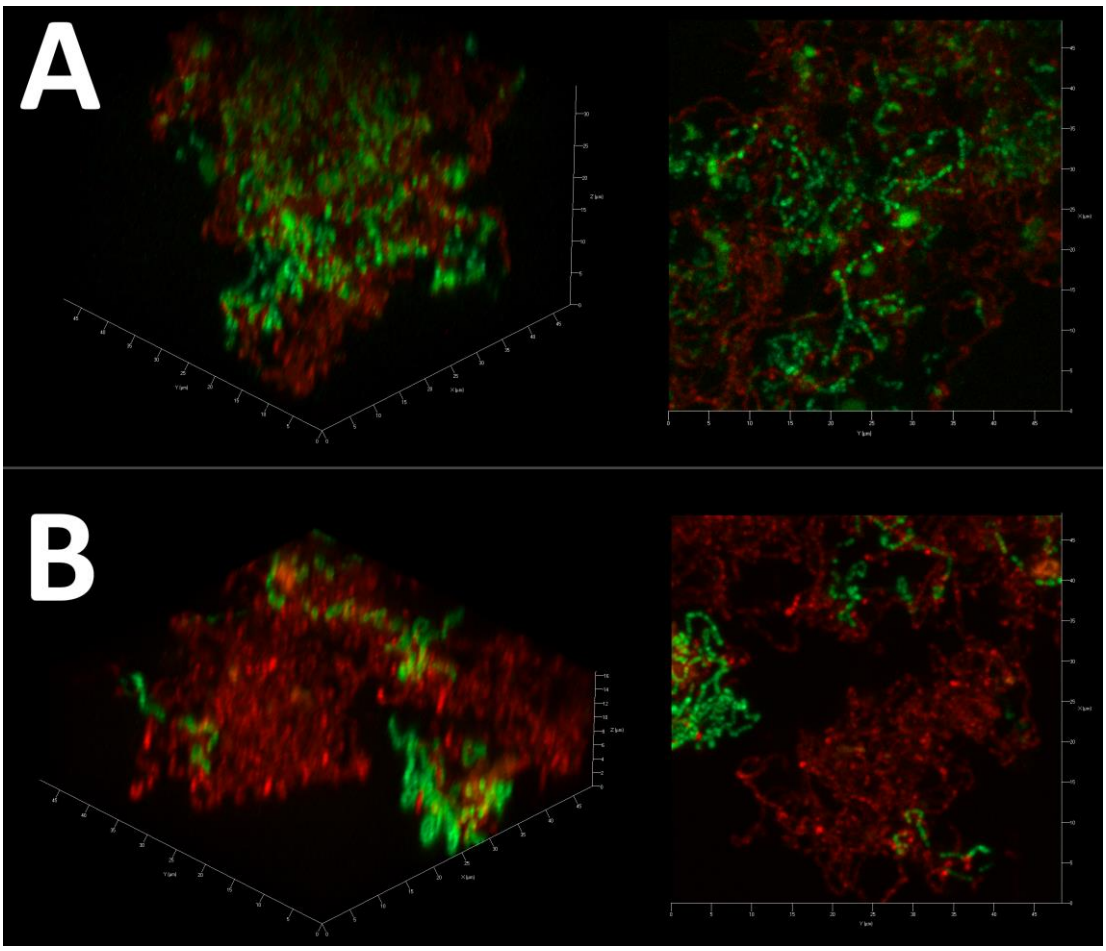

Figure 4.16: Confocal microscopy images of pairwise strain combinations in the Guggenheim's oral biofilm model. A: 'WT GFP-spec' and 'WT mCherry-cam'. B: 'ΔA GFP-spec' and 'WT mCherry-cam'.

5 Discussion

The objective of the thesis was to gain insights into the function of putative bacteriocin-immunity genes in biofilm formation. Genes of interest were identified through *in silico* analysis of the working strain genomes with the bioinformatic tool Bagel4. Also, the Janus cassette system (Sung et al., 2001) was set up for markerless gene deletions in *S. mutans*. The effects of deleting the genes *immA* [SMU.431] and *immB* [SMU.413] in *S. mutans* ATCC 25175 were tested through growth curves, crystal violet biofilm staining, and pairwise strain competitions in different biofilm models. These biofilm models were established to study bacteriocin-biofilm interactions in *Streptococcus*. The role of the proteins ImmA and ImmB in shaping of a single strain streptococcal biofilm were evaluated through the assays, which demonstrated that deletion of *immB* [SMU.413] caused reduction in biofilm-formation. in addition, individual deletion of both *immA* [SMU.431] and *immB* [SMU.413] caused reduction in fitness in the context of either mono-strain cultures or biofilm competitions.

5.1 Setting up the Janus cassette system for markerless deletions in *S. mutans*

Systems for deletion of genes in bacteria could either replace the gene with a selective marker or remove the gene without incorporating a selective marker into the genome. In *S. mutans* gene deletions with selective markers have previously been carried out with an erythromycin resistance gene spliced with the flanking region of a gene (Hazlett et al., 1998). Also markerless deletions have been carried out previously with a system based on Cre recombinase and *loxP* sites (Banerjee & Biswas, 2008). Although the system is markerless, the gene is replaced with a *loxP* site and having multiple identical *loxP* sites could severely impair the genome, meaning that this system requires n unique non-interacting mutant *loxP* sites to delete n genes (Banerjee & Biswas, 2008; Sternberg & Hamilton, 1981). Cre-*lox* recombination homologs such as Flp-*frt* could also be implemented similarly (Hoang et al., 1998). It has also been shown that transformation using extensive flanking homology regions with markerless amplicons can be used to make changes in the genome (Junges et al., 2017). The Janus cassette system used for markerless gene deletions in *S. pneumoniae* does not incorporate any genetic elements into the genome, making it possible to do accumulative gene deletions (Sung et al., 2001). In *S. mutans* the Janus system has previously been tested unsuccessfully by (Atlagic et al., 2006) however in this study the system was successfully implemented with a high rate of transformation.

The use of the Janus cassette system for counterselection and to generate markerless gene deletions relies on the strains being streptomycin resistant due to mutations in the *rpsL* gene (Sung et al., 2001). As mentioned in **Section 4.3** two distinct missense mutations were found in the *rpsL* gene that caused streptomycin resistance for *S. mutans*. These missense mutations caused amino acid replacement of the 56th and 104th residues of the 12S protein. Streptomycin resistant and streptomycin dependent amino acid replacements occur at two known regions within the amino acid sequence of the 12S protein (Timms et al., 1992). Pairwise sequence alignment of the amino acid sequence of the 12S protein used by (Timms et al.) with the amino acid sequence encoded by *S. mutans* show that the two regions correspond to amino acids 53 to 70 and amino acids 97 to 110 in the 12S protein of *S. mutans* (**Figure 5.1**). Both amino acid replacements found in this study were in either of these two regions. Additionally, the predicted protein structure of *S. mutans* 12S by AlphaFold (Jumper et al., 2021) show that the two amino acid replacements are in spatial proximity (**Figure 5.2A**). The experimentally measured structure of streptomycin bound to the *Thermus thermophilus* 30S ribosomal subunit (Demirci et al., 2013) show that the 56th residue in *S. mutans* directly interacts with streptomycin, furthermore the 104th residue in *S. mutans* directly interacts with the 56th amino acid (**Figure 5.2B, C, D, E**). It has been hypothesized by (Demirci et al.) that the 56th residue form hydrogen bonds with streptomycin, however it could not be concluded due to a lack of electron density for the protein side chain. In conclusion, to use the Janus cassette system in *S. mutans* there must be amino acid replacements in the amino acids 53 to 70 or 97 to 110 of the 12S protein to cause streptomycin resistance (**Figure 5.1**).

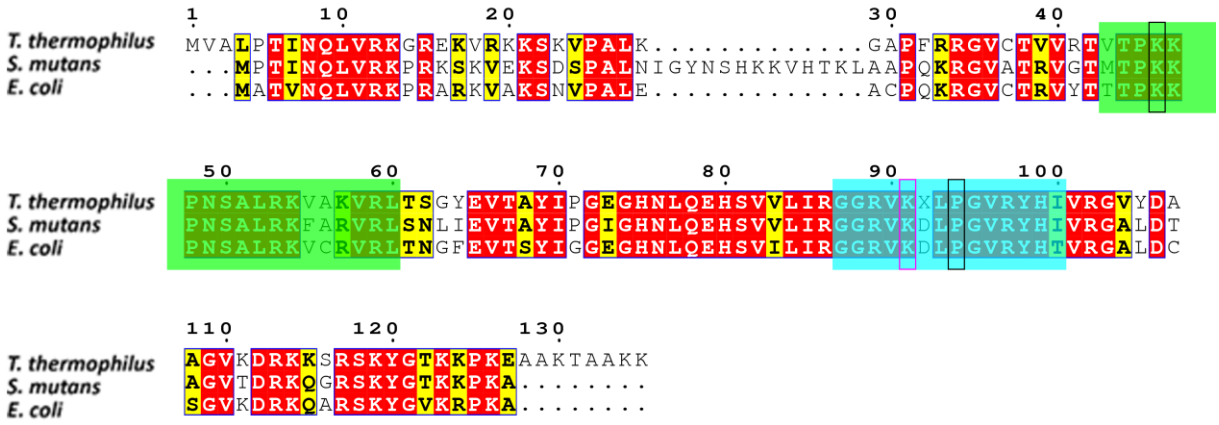

Figure 5.1: Multiple sequence alignment of 30S ribosomal protein S12 for *S. mutans*, *E. coli* strain WP$_2$ and *T. thermophilus* strain HB8. The strains were sequenced aligned with clustal omega by EMBL-EBI and visualized by ESPript with Risler coloring scheme (Risler et al., 1988). The two regions where streptomycin resistance and streptomycin dependent amino acid replacements occur are marked in green and cyan (Timms et al., 1992). The black rectangles show amino acid replacements measured in this study. The purple rectangle show the amino acid likely to form hydrogen bonds with streptomycin (Demirci et al., 2013).

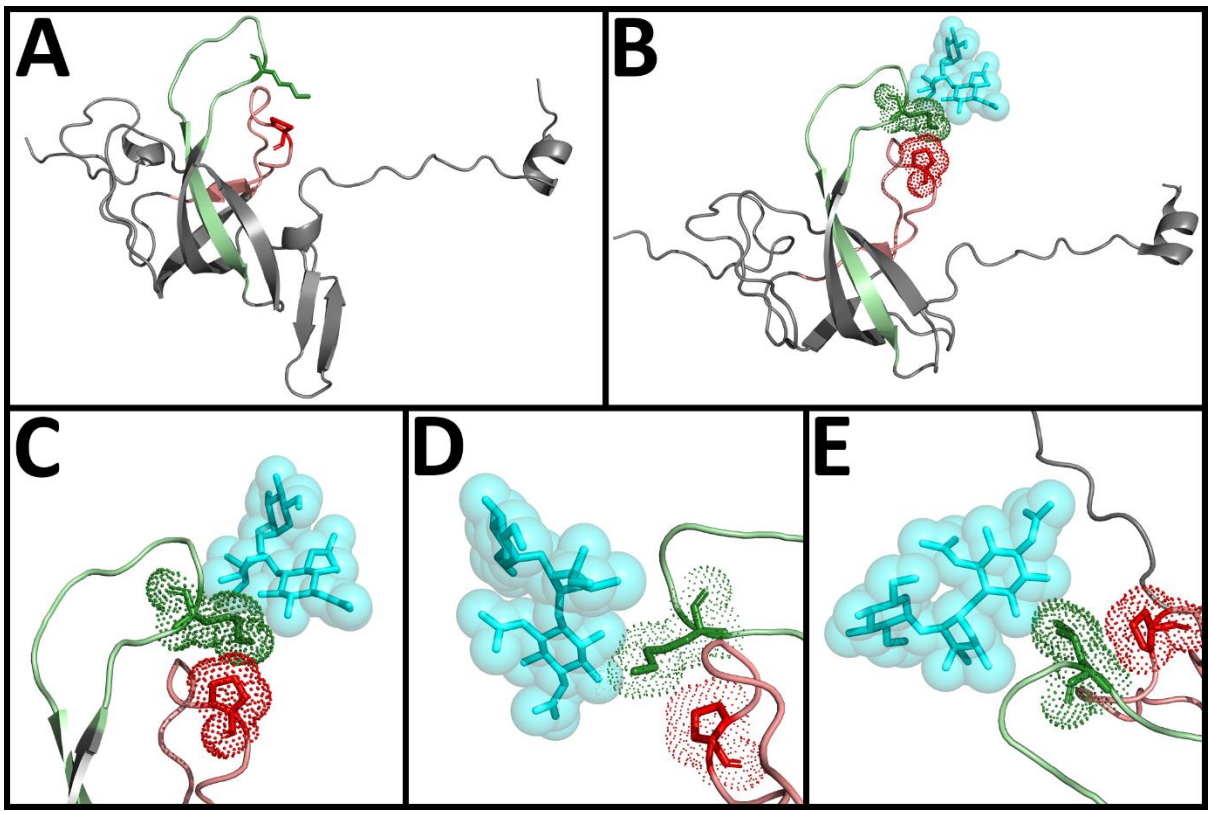

Figure 5.2: Protein structure of 30S ribosomal protein S12 and binding of streptomycin. The region of residues marked in green is the first known streptomycin dependent region while the region of residues marked in red is the second known streptomycin dependent region. The green lysine residue is the mutated 56th residue in *S. mutans* ATCC 25175. The red proline residue is the mutated 104th residue, mutated in *S. mutans* ATCC 700610. A: Predicted 12S protein structure for *S. mutans* by AlphaFold. B: X-ray crystallography data of streptomycin binding to 12S in *T. thermophilus*. C/D/E: close-up images of (B) with the interface between streptomycin and the mutated amino acids.

To generate the Janus knock-in and Janus knock-out fragments the well-established laboratory method splicing by overlap extension was used (Horton et al., 1989). The method was successfully employed to generate the Janus fragments for seven putative bacteriocin-immunity genes. The markerless gene deletions were successful for the two genes *immA* and *immB* of *S. mutans* ATCC 25175.

The success of setting up the Janus cassette system for *S. mutans* was verified by Sanger sequencing of the target genes loci. The deletions were precise and excised the intended nucleotides from the genome. In conclusion, the Janus cassette system was successfully used for *S. mutans* and could be implemented further for accumulative markerless gene deletions of this species.

5.2 Potential function of predicted immunity genes

Bacteriocin-immunity can be provided through ABC transporters often encoded by two or three genes that actively transporting the bacteriocin out of the cell, or, more commonly, by dedicated immunity proteins often encoded by one gene that inhibit bacteriocin pore formation (Pérez-Ramos et al., 2021). The putative bacteriocin-immunity genes identified through Bagel4 were all predicted to encode ABC transporters, and therefore the putative immunity function should be provided through active transport of mature bacteriocin. ABC transporter subunits are often encoded by directly adjacent genes, meaning that the putative bacteriocin-immunity genes found are likely functionally linked to some of their adjacent genes. Although the immunity function of the putative immunity genes was not shown, we decided to focus on these genes in the context of this study.

A search for information about the nine putative bacteriocin-immunity genes of this study resulted in valuable insight into the function of the encoded proteins. The most direct evidence was uncovered for the gene *immG* (SMU.1900) that has previously been found to encode the CslB subunit of the CslAB ABC transporter, a homolog of the ComAB ABC transporter of the TCS ComD/ComE in *S. pneumoniae* (Hale et al., 2005; Håvarstein & Morrison, 1999; Petersen & Scheie, 2000). The CslAB transporter is essential for competence, as deletion mutants of either *cslA* (SMU.1897 and SMU.1898) or *cslB* (SMU.1900) corresponding to *immG* has been reported to cause a severe reduction in transformability similar to that of deletion mutants of either *comA* or *comB* in *S. pneumoniae* (Hale et al., 2005; Petersen & Scheie, 2000). In addition, Bagel4 tagged *immG* (SMU.1900) as a putative bacteriocin-immunity gene due to its proximity to *cipB* (SMU.1914) encoding mutacin V however the bacteriocin-immunity gene *cipI* (SMU.925) is known to encode the bacteriocin-immunity protein CipI that provides self-immunity against mutacin V (Perry, Jones, et al., 2009). Based on the evidence from these studies, the function of *immG* (SMU.1900) is unlikely to be associated with bacteriocin-immunity but rather processing and export of a ComC homolog. Furthermore, it seems that the putative bacteriocin-immunity gene *immI* (WP_109982751) of *S. sobrinus* is a *cslB* (SMU.1900) homolog with the same function as a subunit of the CslAB ABC transporter. The amino acid sequences for *immI* and *cslB* have a 69.3% sequence similarity, in addition the amino acid sequence of the ORF (WP_032672998) directly downstream of *immI* have a 75% sequence similarity with the amino acid sequences encoded by the *cslA* (SMU.1897 and SMU.1898) genes as one unit. Based on this information, *S. sobrinus* ATCC 27352 likely produces a CslAB ABC transporter homolog encoded by *immI* (WP_109982751) and the

upstream ORF (WP_032672998). To verify the function of *immI* follow-up studies with immI mutants could be performed to test the reduction in transformability for knock-out mutants of *immI*.

The homologous genes *immA*, *immC*, and *immE* (SMU.431) along with the homologous genes *immB*, *immD*, and *immF* (SMU.413) are all in proximity to the mutacin VI gene (SMU.423) therefore these putative bacteriocin-immunity genes may be involved in self-immunity for mutacin VI (Xie et al., 2010). ComX upregulates SMU.431 whereas mutacin VI has been found to be upregulated by ComE and therefore perhaps ComX (Khan et al., 2016; Merritt & Qi, 2012; Okinaga et al., 2010). Both genes being transcriptionally activated by the same regulatory system might indicate a functional connection between the genes, potentially as immunity proteins or exporters. To check the possible involvement of these genes in immunity against mutacin VI, the sensitivity of deletion mutants *S. mutans* ATCC 25175 Δ*immA* and *S. mutans* ATCC 25175 Δ*immB* to mutacin VI could be evaluated.

The bioinformatic tool "MicrobesOnline operon predictor" give a 99.9% probability that the ORFs SMU.431 (*immA*, *immC*, *immE*) and the contiguous downstream ORF SMU.432 are in the same operon (Alm et al., 2005). The best BlastP hit of SMU.432 was the CylB subunit of the CylAB ABC transporter in *Streptococcus agalactiae* with a 44.9% sequence similarity. Additionally, the amino acid sequence of SMU.431 shares a 53.6% sequence similarity with the CylA subunit (Spellerberg et al., 1999). The CylAB transporter has been shown to act as a multidrug resistance transporter in *S. agalactiae* in addition to transport of hemolysins (Gottschalk et al., 2006), and it would be interesting to find out if the same is true for the homolog of *S. mutans*.

The best BlastP hit of SMU.413 was the EcsA subunit of the EcsAB ABC transporter in *B. subtilis* with a 56.250% sequence similarity, additionally the best BlastP hit of the downstream ORF SMU.414 was the EcsB subunit with a 34.302% sequence similarity. The EcsAB ABC transporter, also known as PptAB, has been found to be functionally important for biofilm-formation, competence development, and proteolytic cleavage in *Bacillus subtilis* (Heinrich et al., 2008). Importantly, EcsAB is known as a peptide transporter thought to be important for the export of many different peptides including ComS (Chang & Federle, 2016) as well as other pheromones and bacteriocin-like peptides. It is therefore possible that deletion of this gene influences competence as well as other traits of *S. mutans*.

No relevant information was uncovered about the putative bacteriocin-immunity gene *immH*.

The putative bacteriocin-immunity genes investigated in this study were found by the bioinformatic Bagel4, but other bioinformatic tools such as antiSMASH6 exists (Blin et al., 2021). The bioinformatic tool antiSMASH6 only identifies class I bacteriocin genes and therefore would not be effective for the putative class II bacteriocin genes identified in this study.

5.3 Strains characterization

Growth curves and crystal violet assays were performed on the individual strains to evaluate potential fitness costs derived from the gene deletions. In general, the growth curves showed that wildtype *S. mutans* ATCC 25175 strain grew slightly better than the deletion mutants of both *immA* and *immB* in addition the *immA* deletion mutant grew slightly better than the *immB* deletion mutant. This difference was not observed when measuring the CFU/mL. This disparity is likely due to a higher variability in the CFU/mL measurements.

The growth of *S. mutans* ATCC 25175 in this study compares well to previous study where there has been observed a similar time of plateauing at around 8-9 hours, marking the end of the exponential growth phase and entering the stationary phase (Filho et al., 2021; Shafiei et al., 2020; Wang et al., 2019). In conclusion, the growth curves show that it may be favourable for the fitness of the strain to carry these *immA* and *immB* genes, even if no other strains are present.

Crystal violet staining of the biofilms formed on the bottom of the 96-well microtiter plates verified that there was biofilm-formation in the standard biofilm model. The assay resulted in optical density measurements (**Section 4.6.1**) of roughly the same value. However, the data showed a slight tendency of the *immB* deletion mutants to form less biofilm than the strains without *immB* deleted. This may be due to *immB* having a role in biofilm-formation or random variation of the measurements.

Formation of biofilm on the HA discs to be used for the Guggenheim oral biofilm model was also checked by crystal violet assay to confirm the strains were able to form biofilms on this surface. Although it confirmed the formation of biofilms on the disc surfaces, the hydroxyapatite discs were stained. The staining was to a lesser degree than that of the biofilm, however it did significantly increase the measured optical density of dissolved crystal violet, causing inflated values. To successfully carry out the quantification of the biofilm, a method must be developed to separate the stained biofilm from the crystal violet coating the hydroxyapatite disc surface, either through detaching the biofilm without suspending the

crystal violet or suspending the crystal violet on the hydroxyapatite disc surface without detaching the biofilm. The former methodology might be possible through the addition of ECM-degrading enzymes such as dispersin B following the washing steps in the crystal violet protocol. The hydroxyapatite disc may then be removed from the solution after the biofilm has been suspended.

5.4 Biofilm-models

In vitro models are important tools to understand biofilms and allows standardization of experiments to a great degree (Su et al., 2022). The oral *S. mutans* strains ATCC 25175 was used in this study as a model for oral biofilms. The mono-species biofilms formed by this strain can be useful for studying the fundamental functioning of in vivo multispecies biofilms. The mono-species biofilms could also be used to research the role of specific genes and their involvement in biofilm formation (Lopez-Nguyen et al., 2020).

Two biofilm models were used in this study to evaluate bacteriocin-biofilm interactions in *Streptococcus*. The standard model in which the biofilm was formed on the bottom of the wells of 96-well plates filled with BHI and sucrose, and the Guggenheim's oral biofilm model that mimics the conditions of dental plaque formation on dental surfaces in the oral cavity (Lopez-Nguyen et al., 2020). Ex vivo models using extracted teeth and saliva may closer mimic the oral cavity than the Guggenheim's oral biofilm model and synthetic saliva, however the ex vivo models always face a greater risk of contamination and also individual factors of the donor organisms may impact the research results (Su et al., 2022). The strains within the two-strain biofilm competitions were marked with unique fluorescence and antibiotic markers to be able to differentiate between them. After a selected incubation period, the biofilms were either observed directly by confocal laser scanning microscopy or the biofilm was resuspended, and the cells were either observed by fluorescent microscopy or quantified by CFU counting. The percentagewise composition of each strain was measured through antibiotic selection. The setup of the biofilm models in *S. mutans* was successful and proved to be effective for the purpose of the study. Other methods for biofilm cell quantification could have been used such as PMA-qPCR or flow cytometry (Azeredo et al., 2017), however CFU counting is regarded as a gold standard technique and was therefore implemented. The biofilm compositions quantified by CFU counts could have been backed up with quantitative analysis of the cells observed by confocal microscopy, using software such as BiofilmQ (Hartmann et al., 2021).

The pairwise strain competitions worked well for both biofilm models. The succeeding assays of CFU count with antibiotic selection, fluorescent microscopy of suspended biofilm, and confocal laser scanning microscopy of the biofilm can be improved. The high variability of the CFU count measurements as seen in the growth assay show that more biological and technical replicates are required for increased precision. The general trends of the CFU measurements and percentagewise compositions are clear, however the high variability make the statistical analysis weak. In addition, a more rigorous statistical analysis must be developed for the percentagewise compositions where the wildtype vs. wildtype competition is used as a measurement of the variability of the system. The Guggenheim's oral biofilm model gave more significant differences than the standard biofilm model when comparing the deletion mutants vs. wildtype competitions with the wildtype vs. wildtype competition. There are several factors that may influence this result. The Guggenheim's model has 4 times longer incubation period, different medium, and a surface likely more suitable for biofilm-formation. A follow-up experiment to compare the two models where the medium and incubation period is kept the same would be interesting. The more significant result of the Guggenheim's model is likely due to the longer incubation period.

Additional fluorescence and antibiotic markers could also facilitate further multi-strain biofilm assays. To further mimic the conditions of biofilm-formation on dental surfaces with several oral species interacting and competing.

5.5 ImmA and ImmB ABC transporters affect fitness during biofilm formation

The *S. mutans* ATCC 25175 putative bacteriocin-immunity genes *immA* and *immB* both encode subunits of ABC transporters. The downstream ORF for both genes likely encode the corresponding second subunit of the ABC transporters. The growth curves, pairwise strain competitions, and microscopy all demonstrated that the ABC transporters encoded by these genes affect the fitness of the strains, especially during biofilm formation.

The pairwise strain competitions showed that the wildtype *S. mutans* ATCC 25175 outcompeted the deletion mutants of either and both *immA* and *immB*. This was the case for both the standard biofilm model and the Guggenheim's oral biofilm model. The statistical significance of the CFU counts were weak, however the trend for the three separate runs indicated the same conclusion. The confocal laser scanning microscopy of the Guggenheim's oral biofilm model showed that wildtype *S. mutans* ATCC 25175 outcompete the deletion mutant of *immA*. Microscopy images of competition between wildtype and deletion mutant of

immB were not taken due to technical difficulties, so no conclusion based on this dataset can be reached for ImmB. In conclusion, these assays show that it may be favourable for the competitiveness of the strains to carry these *immA* and *immB* genes, and therefore they could be studied further as potential therapeutic targets to control biofilm formation. The function of these two putative bacteriocin-immunity proteins ImmA and ImmB are still unknown and further studies are needed to elucidate their function.

6 Conclusion and future perspectives

In this thesis a system for studying the bacteriocin-biofilm interactions in *S. mutans* was set up. This system could be used to test the impact of putative bacteriocin genes and bacteriocin-associated genes on biofilms. First, the Janus cassette system was implemented *in S. mutans* which allows for accumulative markerless gene deletions. Both biofilm competition models, the microtiter plate, and the Guggenheim model, proved to be valid for bacteriocin-biofilm interaction studies and set the basis for future studies that can systematically analyse more putative bacteriocin genes and bacteriocin associated genes. The competition assays showed clear trends of wildtype *S. mutans* ATCC 25175 outcompeting the deletion mutants of *immA* and *immB*. Highlighting the potential role of these genes in biofilm formation. After further characterization, if these genes demonstrate a role in biofilm formation, then the genes may be potential targets for therapeutic agents to reduce biofilm formation. Further studies are needed to confirm their role with respect to bacteriocin production.

Conclusion

References

Ahn, K. B., Baik, J. E., Park, O.-J., Yun, C.-H., & Han, S. H. (2018). *Lactobacillus plantarum* lipoteichoic acid inhibits biofilm formation of *Streptococcus mutans*. *PLoS One*, *13*(2), e0192694.

Ahn, S.-J., & Burne, R. A. (2007). Effects of Oxygen on Biofilm Formation and the AtlA Autolysin of *Streptococcus mutans*. *Journal of Bacteriology*, *189*(17), 6293-6302. https://doi.org/doi:10.1128/JB.00546-07

Ahn, S.-J., Qu, M.-D., Roberts, E., Burne, R. A., & Rice, K. C. (2012). Identification of the *Streptococcus mutans* LytST two-component regulon reveals its contribution to oxidative stress tolerance. *BMC Microbiology*, *12*(1), 187. https://doi.org/10.1186/1471-2180-12-187

Ahn, S. J., Rice, K. C., Oleas, J., Bayles, K. W., & Burne, R. A. (2010). The *Streptococcus mutans* Cid and Lrg systems modulate virulence traits in response to multiple environmental signals. *Microbiology (Reading)*, *156*(Pt 10), 3136-3147. https://doi.org/10.1099/mic.0.039586-0

Alm, E. J., Huang, K. H., Price, M. N., Koche, R. P., Keller, K., Dubchak, I. L., & Arkin, A. P. (2005). The MicrobesOnline Web site for comparative genomics. *Genome Res*, *15*(7), 1015-1022. https://doi.org/10.1101/gr.3844805

Arnison, P. G., Bibb, M. J., Bierbaum, G., Bowers, A. A., Bugni, T. S., Bulaj, G., Camarero, J. A., Campopiano, D. J., Challis, G. L., Clardy, J., Cotter, P. D., Craik, D. J., Dawson, M., Dittmann, E., Donadio, S., Dorrestein, P. C., Entian, K. D., Fischbach, M. A., Garavelli, J. S., ... van der Donk, W. A. (2013). Ribosomally synthesized and post-translationally modified peptide natural products: overview and recommendations for a universal nomenclature. *Nat Prod Rep*, *30*(1), 108-160. https://doi.org/10.1039/c2np20085f

Arnott, S., Fulmer, A., Scott, W. E., Dea, I. C. M., Moorhouse, R., & Rees, D. A. (1974). The agarose double helix and its function in agarose gel structure. *Journal of Molecular Biology*, *90*(2), 269-284. https://doi.org/10.1016/0022-2836(74)90372-6

Atlagic, D., Kiliç, A. O., & Tao, L. (2006). Unmarked gene deletion mutagenesis of *gtfB* and *gtfC* in *Streptococcus mutans* using a targeted hit-and-run strategy with a thermosensitive plasmid. *Oral Microbiology and Immunology*, *21*(2), 132-135. https://doi.org/10.1111/j.1399-302X.2006.00267.x

Avilés-Reyes, A., Freires, I. A., Kajfasz, J. K., Barbieri, D., Miller, J. H., Lemos, J. A., & Abranches, J. (2018). Whole genome sequence and phenotypic characterization of a Cbm+ serotype e strain of *Streptococcus mutans*. *Molecular Oral Microbiology*, *33*(3), 257-269. https://doi.org/10.1111/omi.12222

Azeredo, J., Azevedo, N. F., Briandet, R., Cerca, N., Coenye, T., Costa, A. R., Desvaux, M., Di Bonaventura, G., Hébraud, M., Jaglic, Z., Kačániová, M., Knøchel, S., Lourenço, A., Mergulhão, F., Meyer, R. L., Nychas, G., Simões, M., Tresse, O., & Sternberg, C. (2017). Critical review on biofilm methods. *Critical Reviews in Microbiology*, *43*(3), 313-351. https://doi.org/10.1080/1040841X.2016.1208146

Banerjee, A., & Biswas, I. (2008). Markerless Multiple-Gene-Deletion System for *Streptococcus mutans*. *Applied and Environmental Microbiology*, *74*(7), 2037-2042. https://doi.org/doi:10.1128/AEM.02346-07

Barraza, D. E., Ríos Colombo, N. S., Galván, A. E., Acuña, L., Minahk, C. J., Bellomio, A., & Chalón, M. C. (2017). New insights into enterocin CRL35: mechanism of action and immunity revealed by heterologous expression in *Escherichia coli*. *Molecular microbiology*, *105*(6), 922-933. https://doi.org/10.1111/mmi.13746

References

Bayles, K. W. (2007). The biological role of death and lysis in biofilm development. *Nature Reviews Microbiology*, *5*(9), 721-726. https://doi.org/10.1038/nrmicro1743

Billroth, T. (1874). Untersuchungen über die Vegetationsformen von Coccobacteria septica und den Antheil, welchen sie an der Entstehung und Verbreitung der accidentellen Wundkrankheiten haben. G reimer. https://lib.ugent.be/catalog/rug01:002036023

Blin, K., Shaw, S., Kloosterman, A. M., Charlop-Powers, Z., van Wezel, G. P., Medema, Marnix H., & Weber, T. (2021). antiSMASH 6.0: improving cluster detection and comparison capabilities. *Nucleic Acids Research*, *49*(W1), W29-W35. https://doi.org/10.1093/nar/gkab335

Bowen, W. H., & Koo, H. (2011). Biology of *Streptococcus mutans*-derived glucosyltransferases: role in extracellular matrix formation of cariogenic biofilms. *Caries Res*, *45*(1), 69-86. https://doi.org/10.1159/000324598

Capecchi, M. R. (1989). Altering the Genome by Homologous Recombination. *Science*, *244*(4910), 1288-1292. https://doi.org/10.1126/science.2660260

Carr, F. J., Chill, D., & Maida, N. (2002). The Lactic Acid Bacteria: A Literature Survey. *Critical Reviews in Microbiology*, *28*(4), 281-370. https://doi.org/10.1080/1040-840291046759

Casino, P., Rubio, V., & Marina, A. (2010). The mechanism of signal transduction by two-component systems. *Current Opinion in Structural Biology*, *20*(6), 763-771. https://doi.org/10.1016/j.sbi.2010.09.010

Castillo Pedraza, M. C., Novais, T. F., Faustoferri, R. C., Quivey, R. G., Terekhov, A., Hamaker, B. R., & Klein, M. I. (2017). Extracellular DNA and lipoteichoic acids interact with exopolysaccharides in the extracellular matrix of *Streptococcus mutans* biofilms. *Biofouling*, *33*(9), 722-740. https://doi.org/10.1080/08927014.2017.1361412

Chang, J. C., & Federle, M. J. (2016). PptAB Exports Rgg Quorum-Sensing Peptides in *Streptococcus*. *PLoS One*, *11*(12), e0168461. https://doi.org/10.1371/journal.pone.0168461

Chawhuaveang, D. D., Yu, O. Y., Yin, I. X., Lam, W. Y.-H., Mei, M. L., & Chu, C.-H. (2021). Acquired salivary pellicle and oral diseases: A literature review. *Journal of Dental Sciences*, *16*(1), 523-529. https://doi.org/10.1016/j.jds.2020.10.007

Chien, A., Edgar, D. B., & Trela, J. M. (1976). Deoxyribonucleic acid polymerase from the extreme thermophile *Thermus aquaticus*. *Journal of Bacteriology*, *127*(3), 1550-1557. https://doi.org/doi:10.1128/jb.127.3.1550-1557.1976

Choji, A. (1956). Structure of the Agarose Constituent of Agar-agar. *Bulletin of the Chemical Society of Japan*, *29*(4), 543-544. https://doi.org/10.1246/bcsj.29.543

Christensen, G. D., Simpson, W. A., Younger, J. J., Baddour, L. M., Barrett, F. F., Melton, D. M., & Beachey, E. H. (1985). Adherence of coagulase-negative staphylococci to plastic tissue culture plates: a quantitative model for the adherence of staphylococci to medical devices. *J Clin Microbiol*, *22*(6), 996-1006. https://doi.org/10.1128/jcm.22.6.996-1006.1985

Claessen, D., Rozen, D. E., Kuipers, O. P., Søgaard-Andersen, L., & van Wezel, G. P. (2014). Bacterial solutions to multicellularity: a tale of biofilms, filaments and fruiting bodies. *Nature Reviews Microbiology*, *12*(2), 115-124. https://doi.org/10.1038/nrmicro3178

Clarke, J. K. (1924). On the Bacterial Factor in the Ætiology of Dental Caries. *British journal of experimental pathology*(5(3)), 141–147.

Costerton, J. W., Geesey, G. G., & Cheng, K. J. (1978). How bacteria stick. *Sci Am*, *238*(1), 86-95. https://doi.org/10.1038/scientificamerican0178-86

Cotter, P. D., Hill, C., & Ross, R. P. (2005). Bacteriocins: developing innate immunity for food. *Nature Reviews Microbiology*, *3*(10), 777-788. https://doi.org/10.1038/nrmicro1273

References

de Beer, D., Stoodley, P., Roe, F., & Lewandowski, Z. (1994). Effects of biofilm structures on oxygen distribution and mass transport. *Biotechnol Bioeng*, *43*(11), 1131-1138. https://doi.org/10.1002/bit.260431118

Demirci, H., Murphy, F., Murphy, E., Gregory, S. T., Dahlberg, A. E., & Jogl, G. (2013). A structural basis for streptomycin-induced misreading of the genetic code. *Nature Communications*, *4*(1), 1355. https://doi.org/10.1038/ncomms2346

Diep, D. B., Skaugen, M., Salehian, Z., Holo, H., & Nes, I. F. (2007). Common mechanisms of target cell recognition and immunity for class II bacteriocins. *Proceedings of the National Academy of Sciences*, *104*(7), 2384-2389. https://doi.org/doi:10.1073/pnas.0608775104

Dolgova, A. S., & Stukolova, O. A. (2017). High-fidelity PCR enzyme with DNA-binding domain facilitates *de novo* gene synthesis. *3 Biotech*, *7*(2), 128. https://doi.org/10.1007/s13205-017-0745-2

Donlan, R. M., & Costerton, J. W. (2002). Biofilms: survival mechanisms of clinically relevant microorganisms. *Clin Microbiol Rev*, *15*(2), 167-193. https://doi.org/10.1128/CMR.15.2.167-193.2002

Drider, D., Fimland, G., Héchard, Y., McMullen, L. M., & Prévost, H. (2006). The Continuing Story of Class IIa Bacteriocins. *Microbiology and Molecular Biology Reviews*, *70*(2), 564-582. https://doi.org/doi:10.1128/MMBR.00016-05

Elias, S., & Banin, E. (2012). Multi-species biofilms: living with friendly neighbors. *FEMS Microbiology Reviews*, *36*(5), 990-1004. https://doi.org/10.1111/j.1574-6976.2012.00325.x

Filho, J. G., Vizoto, N. L., Luiza de Aguiar Loesch, M., Dias de Sena, M., Mendes da Camara, D., Caiaffa, K. S., de Oliveira Mattos-Graner, R., & Duque, C. (2021). Genetic and physiological effects of subinhibitory concentrations of oral antimicrobial agents on *Streptococcus mutans* biofilms. *Microbial Pathogenesis*, *150*, 104669. https://doi.org/10.1016/j.micpath.2020.104669

Flemming, H.-C., & Wingender, J. (2010). The biofilm matrix. *Nature Reviews Microbiology*, *8*(9), 623-633. https://doi.org/10.1038/nrmicro2415

Fox, G. E., Magrum, L. J., Balch, W. E., Wolfe, R. S., & Woese, C. R. (1977). Classification of methanogenic bacteria by 16S ribosomal RNA characterization. *Proceedings of the National Academy of Sciences*, *74*(10), 4537-4541. https://doi.org/doi:10.1073/pnas.74.10.4537

Frey, B., & Suppmann, B. (1995). Demonstration of the Expand PCR system's greater fidelity and higher yields with a lacI-based PCR fidelity assay. *Biochemica*, *2*, 8-9.

Gibbons, R. J., & Van Houte, J. (1973). On the Formation of Dental Plaques. *Journal of Periodontology*, *44*(6), 347-360. https://doi.org/10.1902/jop.1973.44.6.347

Gibson, D. G., Young, L., Chuang, R.-Y., Venter, J. C., Hutchison, C. A., & Smith, H. O. (2009). Enzymatic assembly of DNA molecules up to several hundred kilobases. *Nature Methods*, *6*(5), 343-345. https://doi.org/10.1038/nmeth.1318

Gillespie, S. H. (1994). 2 - Gram-positive cocci. In S. H. Gillespie (Ed.), *Medical Microbiology Illustrated* (pp. 12-29). Butterworth-Heinemann. https://doi.org/10.1016/B978-0-7506-0187-0.50007-9

Gmur, R., & Guggenheim, B. (1983). Antigenic heterogeneity of *Bacteroides intermedius* as recognized by monoclonal antibodies. *Infect Immun*, *42*(2), 459-470. https://doi.org/10.1128/iai.42.2.459-470.1983

Gottschalk, B., Broker, G., Kuhn, M., Aymanns, S., Gleich-Theurer, U., & Spellerberg, B. (2006). Transport of multidrug resistance substrates by the *Streptococcus agalactiae* hemolysin transporter. *J Bacteriol*, *188*(16), 5984-5992. https://doi.org/10.1128/JB.00768-05

Grunberg-Manago, M., Ortiz, P. J., & Ochoa, S. (1955). Enzymatic Synthesis of Nucleic Acidlike Polynucleotides. *Science*, *122*(3176), 907-910. https://doi.org/doi:10.1126/science.122.3176.907

Hachler, H., Santanam, P., & Kayser, F. H. (1996). Sequence and characterization of a novel chromosomal aminoglycoside phosphotransferase gene, *aph (3')-IIb*, in *Pseudomonas aeruginosa*. *Antimicrob Agents Chemother*, *40*(5), 1254-1256. https://doi.org/10.1128/AAC.40.5.1254

Hale, J. D. F., Heng, N. C. K., Jack, R. W., & Tagg, J. R. (2005). Identification of *nlmTE*, the Locus Encoding the ABC Transport System Required for Export of Nonlantibiotic Mutacins in *Streptococcus mutans*. *Journal of Bacteriology*, *187*(14), 5036-5039. https://doi.org/doi:10.1128/JB.187.14.5036-5039.2005

Hartmann, R., Jeckel, H., Jelli, E., Singh, P. K., Vaidya, S., Bayer, M., Rode, D. K. H., Vidakovic, L., Díaz-Pascual, F., Fong, J. C. N., Dragoš, A., Lamprecht, O., Thöming, J. G., Netter, N., Häussler, S., Nadell, C. D., Sourjik, V., Kovács, Á. T., Yildiz, F. H., & Drescher, K. (2021). Quantitative image analysis of microbial communities with BiofilmQ. *Nature Microbiology*, *6*(2), 151-156. https://doi.org/10.1038/s41564-020-00817-4

Håvarstein, L. S., Diep, D. B., & Nes, I. F. (1995). A family of bacteriocin ABC transporters carry out proteolytic processing of their substrates concomitant with export. *Molecular microbiology*, *16*(2), 229-240. https://doi.org/10.1111/j.1365-2958.1995.tb02295.x

Håvarstein, L. S., & Morrison, D. A. (1999). Quorum sensing and peptide pheromones in streptococcal competence for genetic transformation. *Cell-cell signaling in bacteria. ASM Press, Washington, DC*, 9-26.

Hazlett, K. R., Michalek, S. M., & Banas, J. A. (1998). Inactivation of the *gbpA* gene of *Streptococcus mutans* increases virulence and promotes in vivo accumulation of recombinations between the glucosyltransferase B and C genes. *Infect Immun*, *66*(5), 2180-2185. https://doi.org/10.1128/IAI.66.5.2180-2185.1998

Heilbronner, S., Krismer, B., Brötz-Oesterhelt, H., & Peschel, A. (2021). The microbiome-shaping roles of bacteriocins. *Nature Reviews Microbiology*, *19*(11), 726-739. https://doi.org/10.1038/s41579-021-00569-w

Heinrich, J., Lundén, T., Kontinen, V. P., & Wiegert, T. (2008). The *Bacillus subtilis* ABC transporter EcsAB influences intramembrane proteolysis through RasP. *Microbiology*, *154*(7), 1989-1997. https://doi.org/10.1099/mic.0.2008/018648-0

Helling, R. B., Goodman, H. M., & Boyer, H. W. (1974). Analysis of endonuclease R-EcoRI fragments of DNA from lambdoid bacteriophages and other viruses by agarose-gel electrophoresis. *J Virol*, *14*(5), 1235-1244. https://doi.org/10.1128/JVI.14.5.1235-1244.1974

Hoang, T. T., Karkhoff-Schweizer, R. R., Kutchma, A. J., & Schweizer, H. P. (1998). A broad-host-range Flp-FRT recombination system for site-specific excision of chromosomally-located DNA sequences: application for isolation of unmarked *Pseudomonas aeruginosa* mutants. *Gene*, *212*(1), 77-86. https://doi.org/10.1016/S0378-1119(98)00130-9

Høiby, N., Bjarnsholt, T., Moser, C., Bassi, G. L., Coenye, T., Donelli, G., Hall-Stoodley, L., Holá, V., Imbert, C., Kirketerp-Møller, K., Lebeaux, D., Oliver, A., Ullmann, A. J., & Williams, C. (2015). ESCMID∗ guideline for the diagnosis and treatment of biofilm infections 2014. *Clinical Microbiology and Infection*, *21*, S1-S25. https://doi.org/10.1016/j.cmi.2014.10.024

Holmes, A. R., Gilbert, C., Wells, J. M., & Jenkinson, H. F. (1998). Binding Properties of *Streptococcus gordonii* SspA and SspB (Antigen I/II Family) Polypeptides Expressed on the Cell Surface of *Lactococcus lactis* MG1363. *Infection and Immunity*, *66*(10), 4633-4639. https://doi.org/doi:10.1128/IAI.66.10.4633-4639.1998

Horton, R. M., Hunt, H. D., Ho, S. N., Pullen, J. K., & Pease, L. R. (1989). Engineering hybrid genes without the use of restriction enzymes: gene splicing by overlap extension. *Gene*, *77*(1), 61-68. https://doi.org/10.1016/0378-1119(89)90359-4

Hossain, M. S., & Biswas, I. (2011). Mutacins from *Streptococcus mutans* UA159 Are Active against Multiple Streptococcal Species. *Applied and Environmental Microbiology*, *77*(7), 2428-2434. https://doi.org/doi:10.1128/AEM.02320-10

Hossain, M. S., & Biswas, I. (2012). SMU.152 Acts as an Immunity Protein for Mutacin IV. *Journal of Bacteriology*, *194*(13), 3486-3494. https://doi.org/doi:10.1128/JB.00194-12

Jakubovics, N. S., Goodman, S. D., Mashburn-Warren, L., Stafford, G. P., & Cieplik, F. (2021). The dental plaque biofilm matrix. *Periodontology 2000*, *86*(1), 32-56. https://doi.org/10.1111/prd.12361

Johnson, J. S., Spakowicz, D. J., Hong, B.-Y., Petersen, L. M., Demkowicz, P., Chen, L., Leopold, S. R., Hanson, B. M., Agresta, H. O., Gerstein, M., Sodergren, E., & Weinstock, G. M. (2019). Evaluation of 16S rRNA gene sequencing for species and strain-level microbiome analysis. *Nature Communications*, *10*(1), 5029. https://doi.org/10.1038/s41467-019-13036-1

Jumper, J., Evans, R., Pritzel, A., Green, T., Figurnov, M., Ronneberger, O., Tunyasuvunakool, K., Bates, R., Žídek, A., Potapenko, A., Bridgland, A., Meyer, C., Kohl, S. A. A., Ballard, A. J., Cowie, A., Romera-Paredes, B., Nikolov, S., Jain, R., Adler, J., . . . Hassabis, D. (2021). Highly accurate protein structure prediction with AlphaFold. *Nature*, *596*(7873), 583-589. https://doi.org/10.1038/s41586-021-03819-2

Jung, G. (1991). *Lantibiotics: a survey. In: Nisin and Novel Lantibiotics*. ESCOM, Leiden.

Junges, R., Khan, R., Tovpeko, Y., Åmdal, H. A., Petersen, F. C., & Morrison, D. A. (2017). Markerless Genome Editing in Competent Streptococci. In G. J. Seymour, M. P. Cullinan, & N. C. K. Heng (Eds.), *Oral Biology: Molecular Techniques and Applications* (pp. 233-247). Springer New York. https://doi.org/10.1007/978-1-4939-6685-1_14

Junges, R., Salvadori, G., Chen, T., Morrison, D. A., & Petersen, F. C. (2019). Hidden Gems in the Transcriptome Maps of Competent Streptococci [Perspective]. *Frontiers in Molecular Biosciences*, *5*. https://doi.org/10.3389/fmolb.2018.00116

Kaplan, J. á. (2010). Biofilm dispersal: mechanisms, clinical implications, and potential therapeutic uses. *Journal of Dental Research*, *89*(3), 205-218.

Kawada-Matsuo, M., & Komatsuzawa, H. (2017). Role of *Streptococcus mutans* two-component systems in antimicrobial peptide resistance in the oral cavity. *Japanese Dental Science Review*, *53*(3), 86-94. https://doi.org/10.1016/j.jdsr.2016.12.002

Khan, R., Rukke, H. V., Høvik, H., Åmdal, H. A., Chen, T., Morrison, D. A., & Petersen, F. C. (2016). Comprehensive Transcriptome Profiles of *Streptococcus mutans* UA159 Map Core Streptococcal Competence Genes. *mSystems*, *1*(2), e00038-00015. https://doi.org/doi:10.1128/mSystems.00038-15

Klaenhammer, T. R. (1993). Genetics of bacteriocins produced by lactic acid bacteria. *FEMS Microbiology Reviews*, *12*(1-3), 39-85. https://doi.org/10.1111/j.1574-6976.1993.tb00012.x

Kleppe, K., Ohtsuka, E., Kleppe, R., Molineux, I., & Khorana, H. G. (1971). Studies on polynucleotides: XCVI. Repair replication of short synthetic DNA's as catalyzed by DNA polymerases. *Journal of Molecular Biology*, *56*(2), 341-361. https://doi.org/10.1016/0022-2836(71)90469-4

Kolenbrander, P. E., & London, J. (1993). Adhere today, here tomorrow: oral bacterial adherence. *J Bacteriol*, *175*(11), 3247-3252. https://doi.org/10.1128/jb.175.11.3247-3252.1993

Kuramitsu, H. K., Smorawinska, M., Nakano, Y. J., Shimamura, A., & Lis, M. (1995). Analysis of glucan synthesis by *Streptococcus mutans*. *Dev Biol Stand*, *85*, 303-307. https://www.ncbi.nlm.nih.gov/pubmed/8586194

References

Kurland, C. G. (1960). Molecular characterization of ribonucleic acid from *Escherichia coli* ribosomes: I. Isolation and molecular weights. *Journal of Molecular Biology*, *2*(2), 83-91. https://doi.org/10.1016/S0022-2836(60)80029-0

Lagedroste, M., Reiners, J., Smits, S. H. J., & Schmitt, L. (2020). Impact of the nisin modification machinery on the transport kinetics of NisT. *Scientific Reports*, *10*(1), 12295. https://doi.org/10.1038/s41598-020-69225-2

Lee, P. Y., Costumbrado, J., Hsu, C. Y., & Kim, Y. H. (2012). Agarose gel electrophoresis for the separation of DNA fragments. *J Vis Exp*(62). https://doi.org/10.3791/3923

Lévesque, C. M., Mair, R. W., Perry, J. A., Lau, P. C. Y., Li, Y. H., & Cvitkovitch, D. G. (2007). Systemic inactivation and phenotypic characterization of two-component systems in expression of *Streptococcus mutans* virulence properties. *Letters in Applied Microbiology*, *45*(4), 398-404. https://doi.org/10.1111/j.1472-765X.2007.02203.x

Li, W., Wyllie, R. M., & Jensen, P. A. (2020). A ComRS competence pathway in the oral pathogen *Streptococcus sobrinus*. *bioRxiv*, 2020.2003.2015.992891. https://doi.org/10.1101/2020.03.15.992891

Li, Y.-H., & Tian, X. (2012). Quorum Sensing and Bacterial Social Interactions in Biofilms. *Sensors*, *12*(3), 2519-2538. https://www.mdpi.com/1424-8220/12/3/2519

López-Cuellar, M. d. R., Rodríguez-Hernández, A.-I., & Chavarría-Hernández, N. (2016). LAB bacteriocin applications in the last decade. *Biotechnology & Biotechnological Equipment*, *30*(6), 1039-1050. https://doi.org/10.1080/13102818.2016.1232605

Lopez-Nguyen, D., Chonsui, H., Payet, S., Chane Kam Ho, J., Claisse, O., Samot, J., & Badet, C. (2020). Improvement of an experimental model of oral biofilm. *Microbiota in Health and Disease*(Microb Health Dis 2020; 2: e308). https://doi.org/10.26355/mhd_20207_308

Lundberg, K. S., Shoemaker, D. D., Adams, M. W. W., Short, J. M., Sorge, J. A., & Mathur, E. J. (1991). High-fidelity amplification using a thermostable DNA polymerase isolated from *Pyrococcus furiosus*. *Gene*, *108*(1), 1-6. https://doi.org/10.1016/0378-1119(91)90480-Y

Ma, J. K., Hunjan, M., Smith, R., Kelly, C., & Lehner, T. (1990). An investigation into the mechanism of protection by local passive immunization with monoclonal antibodies against *Streptococcus mutans*. *Infect Immun*, *58*(10), 3407-3414. https://doi.org/10.1128/iai.58.10.3407-3414.1990

Mah, T.-F. C., & O'Toole, G. A. (2001). Mechanisms of biofilm resistance to antimicrobial agents. *Trends in Microbiology*, *9*(1), 34-39. https://doi.org/10.1016/S0966-842X(00)01913-2

Markham, J. L., Knox, K. W., Wicken, A. J., & Hewett, M. J. (1975). Formation of extracellular lipoteichoic acid by oral streptococci and lactobacilli. *Infect Immun*, *12*(2), 378-386. https://doi.org/10.1128/iai.12.2.378-386.1975

Marsh, P. D., & Bradshaw, D. J. (1995). Dental plaque as a biofilm. *Journal of industrial microbiology and biotechnology*, *15*(3), 169-175.

Medema, M. H., Kottmann, R., Yilmaz, P., Cummings, M., Biggins, J. B., Blin, K., de Bruijn, I., Chooi, Y. H., Claesen, J., Coates, R. C., Cruz-Morales, P., Duddela, S., Düsterhus, S., Edwards, D. J., Fewer, D. P., Garg, N., Geiger, C., Gomez-Escribano, J. P., Greule, A., ... Glöckner, F. O. (2015). Minimum Information about a Biosynthetic Gene cluster. *Nature Chemical Biology*, *11*(9), 625-631. https://doi.org/10.1038/nchembio.1890

Merritt, J., & Qi, F. (2012). The mutacins of *Streptococcus mutans*: regulation and ecology. *Molecular Oral Microbiology*, *27*(2), 57-69. https://doi.org/10.1111/j.2041-1014.2011.00634.x

Miller, M. B., & Bassler, B. L. (2001). Quorum Sensing in Bacteria. *Annual Review of Microbiology*, *55*(1), 165-199. https://doi.org/10.1146/annurev.micro.55.1.165

Montelongo-Jauregui, D., Srinivasan, A., Ramasubramanian, A. K., & Lopez-Ribot, J. L. (2016). An In Vitro Model for Oral Mixed Biofilms of *Candida albicans* and *Streptococcus gordonii* in Synthetic Saliva. *Front Microbiol*, *7*, 686. https://doi.org/10.3389/fmicb.2016.00686

Muhammad, M. H., Idris, A. L., Fan, X., Guo, Y., Yu, Y., Jin, X., Qiu, J., Guan, X., & Huang, T. (2020). Beyond risk: bacterial biofilms and their regulating approaches. *Frontiers in microbiology*, *11*, 928.

Mullis, K. B. (1990). The Unusual Origin of the Polymerase Chain Reaction. *Scientific American*, *262*(4), 56-65. http://www.jstor.org/stable/24996713

Nes, I. F., Diep, D. B., & Holo, H. (2007). Bacteriocin Diversity in *Streptococcus* and *Enterococcus*. *Journal of Bacteriology*, *189*(4), 1189-1198. https://doi.org/10.1128/JB.01254-06

Nes, I. F., Holo, H., Fimland, G., Hauge, H. H., & Nissen-Meyer, J. (2001). Unmodified peptide-bacteriocins (class II) produced by lactic acid bacteria. *Peptide antibiotics: discovery, modes of action and application, section B. Distribution of antimicrobial peptides. Marcel Dekker, Inc., New York, NY*, 81-115.

O'Connor, P. M., Kuniyoshi, T. M., Oliveira, R. P. S., Hill, C., Ross, R. P., & Cotter, P. D. (2020). Antimicrobials for food and feed; a bacteriocin perspective. *Current Opinion in Biotechnology*, *61*, 160-167. https://doi.org/10.1016/j.copbio.2019.12.023

Okinaga, T., Xie, Z., Niu, G., Qi, F., & Merritt, J. (2010). Examination of the hdrRM regulon yields insight into the competence system of *Streptococcus mutans*. *Molecular Oral Microbiology*, *25*(3), 165-177. https://doi.org/10.1111/j.2041-1014.2010.00574.x

Oman, T. J., & van der Donk, W. A. (2010). Follow the leader: the use of leader peptides to guide natural product biosynthesis. *Nature Chemical Biology*, *6*(1), 9-18. https://doi.org/10.1038/nchembio.286

Pérez-Ramos, A., Madi-Moussa, D., Coucheney, F., & Drider, D. (2021). Current Knowledge of the Mode of Action and Immunity Mechanisms of LAB-Bacteriocins. *Microorganisms*, *9*(10), 2107. https://www.mdpi.com/2076-2607/9/10/2107

Perry, J. A., Cvitkovitch, D. G., & Lévesque, C. M. (2009). Cell death in *Streptococcus mutans* biofilms: a link between CSP and extracellular DNA. *FEMS Microbiology Letters*, *299*(2), 261-266. https://doi.org/10.1111/j.1574-6968.2009.01758.x

Perry, J. A., Jones, M. B., Peterson, S. N., Cvitkovitch, D. G., & Lévesque, C. M. (2009). Peptide alarmone signalling triggers an auto-active bacteriocin necessary for genetic competence. *Molecular microbiology*, *72*(4), 905-917. https://doi.org/10.1111/j.1365-2958.2009.06693.x

Petersen, F. C., Fimland, G., & Scheie, A. A. (2006). Purification and functional studies of a potent modified quorum-sensing peptide and a two-peptide bacteriocin in *Streptococcus mutans*. *Molecular microbiology*, *61*(5), 1322-1334. https://doi.org/10.1111/j.1365-2958.2006.05312.x

Petersen, F. C., & Scheie, A. A. (2000). Genetic transformation in *Streptococcus mutans* requires a peptide secretion–like apparatus. *Oral Microbiology and Immunology*, *15*(5), 329-334. https://doi.org/10.1034/j.1399-302x.2000.150511.x

Pitts, N. B., Zero, D. T., Marsh, P. D., Ekstrand, K., Weintraub, J. A., Ramos-Gomez, F., Tagami, J., Twetman, S., Tsakos, G., & Ismail, A. (2017). Dental caries. *Nature Reviews Disease Primers*, *3*(1), 17030. https://doi.org/10.1038/nrdp.2017.30

Ricomini Filho, A. P., Khan, R., Amdal, H. A., & Petersen, F. C. (2019). Conserved Pheromone Production, Response and Degradation by *Streptococcus mutans*. *Front Microbiol*, *10*, 2140. https://doi.org/10.3389/fmicb.2019.02140

Risler, J. L., Delorme, M. O., Delacroix, H., & Henaut, A. (1988). Amino acid substitutions in structurally related proteins. A pattern recognition approach. Determination of a new and

efficient scoring matrix. *J Mol Biol*, *204*(4), 1019-1029. https://doi.org/10.1016/0022-2836(88)90058-7

Ritz, H. L. (1967). Microbial population shifts in developing human dental plaque. *Arch Oral Biol*, *12*(12), 1561-1568. https://doi.org/10.1016/0003-9969(67)90190-2

Robson, C. L., Wescombe, P. A., Klesse, N. A., & Tagg, J. R. (2007). Isolation and partial characterization of the *Streptococcus mutans* type AII lantibiotic mutacin K8. *Microbiology*, *153*(5), 1631-1641. https://doi.org/10.1099/mic.0.2006/003756-0

Rogers, L. A. (1928). The inhibiting effect of *Streptococcus lactis* on *Lactobacillus bulgaricus*. *Journal of Bacteriology*, *16*(5), 321-325. https://doi.org/doi:10.1128/jb.16.5.321-325.1928

Römling, U., & Balsalobre, C. (2012). Biofilm infections, their resilience to therapy and innovative treatment strategies. *Journal of Internal Medicine*, *272*(6), 541-561. https://doi.org/10.1111/joim.12004

Rosan, B., & Lamont, R. J. (2000). Dental plaque formation. *Microbes and Infection*, *2*(13), 1599-1607. https://doi.org/10.1016/S1286-4579(00)01316-2

Rozen, R., Bachrach, G., Bronshteyn, M., Gedalia, I., & Steinberg, D. (2001). The role of fructans on dental biofilm formation by *Streptococcus sobrinus*, *Streptococcus mutans*, *Streptococcus gordonii* and *Actinomyces viscosus*. *FEMS Microbiology Letters*, *195*(2), 205-210. https://doi.org/10.1016/S0378-1097(01)00009-X

Salvadori, G., Junges, R., Khan, R., Åmdal, H. A., Morrison, D. A., & Petersen, F. C. (2017). Natural Transformation of Oral Streptococci by Use of Synthetic Pheromones. In G. J. Seymour, M. P. Cullinan, & N. C. K. Heng (Eds.), *Oral Biology: Molecular Techniques and Applications* (pp. 219-232). Springer New York. https://doi.org/10.1007/978-1-4939-6685-1_13

Sauer, K., Stoodley, P., Goeres, D. M., Hall-Stoodley, L., Burmølle, M., Stewart, P. S., & Bjarnsholt, T. (2022). The biofilm life cycle: expanding the conceptual model of biofilm formation. *Nature Reviews Microbiology*, *20*(10), 608-620. https://doi.org/10.1038/s41579-022-00767-0

Seal, S. E., Jackson, L. A., & Daniels, M. J. (1992). Use of tRNA consensus primers to indicate subgroups of *Pseudomonas solanacearum* by polymerase chain reaction amplification. *Applied and Environmental Microbiology*, *58*(11), 3759-3761. https://doi.org/doi:10.1128/aem.58.11.3759-3761.1992

Senadheera, M. D., Guggenheim, B., Spatafora, G. A., Huang, Y.-C. C., Choi, J., Hung, D. C. I., Treglown, J. S., Goodman, S. D., Ellen, R. P., & Cvitkovitch, D. G. (2005). A VicRK Signal Transduction System in *Streptococcus mutans* Affects *gtfBCD*, *gbpB*, and *ftf* Expression, Biofilm Formation, and Genetic Competence Development. *Journal of Bacteriology*, *187*(12), 4064-4076. https://doi.org/doi:10.1128/JB.187.12.4064-4076.2005

Shafiei, Z., Rahim, Z. H. A., Philip, K., Thurairajah, N., & Yaacob, H. (2020). Potential effects of *Psidium* sp., *Mangifera* sp., *Mentha* sp. and its mixture (PEM) in reducing bacterial populations in biofilms, adherence and acid production of *S. sanguinis* and *S. mutans*. *Archives of Oral Biology*, *109*, 104554. https://doi.org/10.1016/j.archoralbio.2019.104554

Shields, R. C., Kaspar, J. R., Lee, K., Underhill, S. A. M., & Burne, R. A. (2019). Fluorescence Tools Adapted for Real-Time Monitoring of the Behaviors of *Streptococcus* Species. *Applied and Environmental Microbiology*, *85*(15), e00620-00619. https://doi.org/doi:10.1128/AEM.00620-19

Siegrist, H., & Gujer, W. (1985). Mass transfer mechanisms in a heterotrophic biofilm. *Water Research*, *19*(11), 1369-1378. https://doi.org/10.1016/0043-1354(85)90303-3

Simons, A., Alhanout, K., & Duval, R. E. (2020). Bacteriocins, antimicrobial peptides from bacterial origin: overview of their biology and their impact against multidrug-resistant bacteria. *Microorganisms*, *8*(5), 639.

References

Socransky, S. S., & Haffajee, A. D. (2002). Dental biofilms: difficult therapeutic targets. *Periodontology 2000*, *28*(1), 12-55.

Son, M., Shields, R. C., Ahn, S.-J., Burne, R. A., & Hagen, S. J. (2015). Bidirectional signaling in the competence regulatory pathway of *Streptococcus mutans*. *FEMS Microbiology Letters*, *362*(19). https://doi.org/10.1093/femsle/fnv159

Spellerberg, B., Pohl, B., Haase, G., Martin, S., Weber-Heynemann, J., & Lütticken, R. (1999). Identification of Genetic Determinants for the Hemolytic Activity of *Streptococcus agalactiae* by IS *S1* Transposition. *Journal of Bacteriology*, *181*(10), 3212-3219. https://doi.org/doi:10.1128/JB.181.10.3212-3219.1999

Stephan, R. M. (1944). Intra-Oral Hydrogen-Ion Concentrations Associated With Dental Caries Activity. *Journal of Dental Research*, *23*(4), 257-266. https://doi.org/10.1177/00220345440230040401

Sternberg, N., & Hamilton, D. (1981). Bacteriophage P1 site-specific recombination: I. Recombination between loxP sites. *Journal of Molecular Biology*, *150*(4), 467-486. https://doi.org/10.1016/0022-2836(81)90375-2

Su, Y., Yrastorza, J. T., Matis, M., Cusick, J., Zhao, S., Wang, G., & Xie, J. (2022). Biofilms: Formation, Research Models, Potential Targets, and Methods for Prevention and Treatment. *Advanced Science*, *9*(29), 2203291. https://doi.org/https://doi.org/10.1002/advs.202203291

Sung, C. K., Li, H., Claverys, J. P., & Morrison, D. A. (2001). An rpsL Cassette, Janus, for Gene Replacement through Negative Selection in *Streptococcus pneumoniae*. *Applied and Environmental Microbiology*, *67*(11), 5190-5196. https://doi.org/doi:10.1128/AEM.67.11.5190-5196.2001

Thomas, P., Sekhar, A. C., Upreti, R., Mujawar, M. M., & Pasha, S. S. (2015). Optimization of single plate-serial dilution spotting (SP-SDS) with sample anchoring as an assured method for bacterial and yeast cfu enumeration and single colony isolation from diverse samples. *Biotechnol Rep (Amst)*, *8*, 45-55. https://doi.org/10.1016/j.btre.2015.08.003

Tian, X. L., Dong, G., Liu, T., Gomez, Z. A., Wahl, A., Hols, P., & Li, Y. H. (2013). MecA protein acts as a negative regulator of genetic competence in *Streptococcus mutans*. *J Bacteriol*, *195*(22), 5196-5206. https://doi.org/10.1128/JB.00821-13

Timms, A. R., Steingrimsdottir, H., Lehmann, A. R., & Bridges, B. A. (1992). Mutant sequences in the rpsL gene of *Escherichia coli* B/r: Mechanistic implications for spontaneous and ultraviolet light mutagenesis. *Molecular and General Genetics MGG*, *232*(1), 89-96. https://doi.org/10.1007/BF00299141

Vacca-Smith, A. M., Venkitaraman, A. R., Schilling, K. M., & Bowen, W. H. (1996). Characterization of glucosyltransferase of human saliva adsorbed onto hydroxyapatite surfaces. *Caries Res*, *30*(5), 354-360. https://doi.org/10.1159/000262342

van Heel, A. J., de Jong, A., Song, C., Viel, J. H., Kok, J., & Kuipers, O. P. (2018). BAGEL4: a user-friendly web server to thoroughly mine RiPPs and bacteriocins. *Nucleic Acids Research*, *46*(W1), W278-W281. https://doi.org/10.1093/nar/gky383

Veerachamy, S., Yarlagadda, T., Manivasagam, G., & Yarlagadda, P. K. (2014). Bacterial adherence and biofilm formation on medical implants: A review. *Proceedings of the Institution of Mechanical Engineers, Part H: Journal of Engineering in Medicine*, *228*(10), 1083-1099. https://doi.org/10.1177/0954411914556137

Venema, K., Abee, T., Haandrikman, A. J., Leenhouts, K. J., Kok, J., Konings, W. N., & Venema, G. (1993). Mode of Action of Lactococcin B, a Thiol-Activated Bacteriocin from *Lactococcus lactis*. *Appl Environ Microbiol*, *59*(4), 1041-1048. https://doi.org/10.1128/aem.59.4.1041-1048.1993

References

Vianna, J. F., S. Bezerra, K., I. N. Oliveira, J., Albuquerque, E. L., & Fulco, U. L. (2019). Binding energies of the drugs capreomycin and streptomycin in complex with tuberculosis bacterial ribosome subunits. *Physical Chemistry Chemical Physics*, *21*(35), 19192-19200. https://doi.org/10.1039/C9CP03631H

Wang, J., Shi, Y., Jing, S., Dong, H., Wang, D., & Wang, T. (2019). Astilbin Inhibits the Activity of Sortase A from *Streptococcus mutans*. *Molecules*, *24*(3), 465. https://www.mdpi.com/1420-3049/24/3/465

Wang, Y., Prosen, D. E., Mei, L., Sullivan, J. C., Finney, M., & Vander Horn, P. B. (2004). A novel strategy to engineer DNA polymerases for enhanced processivity and improved performance in vitro. *Nucleic Acids Res*, *32*(3), 1197-1207. https://doi.org/10.1093/nar/gkh271

Welch, m., Jessica, L., Rossetti, B. J., Rieken, C. W., Dewhirst, F. E., & Borisy, G. G. (2016). Biogeography of a human oral microbiome at the micron scale. *Proceedings of the National Academy of Sciences*, *113*(6), E791-E800. https://doi.org/doi:10.1073/pnas.1522149113

Willey, J. M., Sherwood, L., & Woolverton, C. J. (2011). *Prescott's microbiology* (Vol. 7). McGraw-Hill New York.

Wingender, J., Neu, T. R., & Flemming, H.-C. (1999). What are bacterial extracellular polymeric substances? Microbial extracellular polymeric substances. In: Springer Berlin.

Woese, C. R., Fox, G. E., Zablen, L., Uchida, T., Bonen, L., Pechman, K., Lewis, B. J., & Stahl, D. (1975). Conservation of primary structure in 16S ribosomal RNA. *Nature*, *254*(5495), 83-86. https://doi.org/10.1038/254083a0

Wu, D. Y., Ugozzoli, L., Pal, B. K., Qian, J., & Wallace, R. B. (1991). The Effect of Temperature and Oligonucleotide Primer Length on the Specificity and Efficiency of Amplification by the Polymerase Chain Reaction. *DNA and Cell Biology*, *10*(3), 233-238. https://doi.org/10.1089/dna.1991.10.233

Xie, Z., Okinaga, T., Niu, G., Qi, F., & Merritt, J. (2010). Identification of a novel bacteriocin regulatory system in *Streptococcus mutans*. *Mol Microbiol*, *78*(6), 1431-1447. https://doi.org/10.1111/j.1365-2958.2010.07417.x

Yang, S. C., Lin, C. H., Sung, C. T., & Fang, J. Y. (2014). Antibacterial activities of bacteriocins: application in foods and pharmaceuticals. *Front Microbiol*, *5*, 241. https://doi.org/10.3389/fmicb.2014.00241

Zimina, M., Babich, O., Prosekov, A., Sukhikh, S., Ivanova, S., Shevchenko, M., & Noskova, S. (2020). Overview of Global Trends in Classification, Methods of Preparation and Application of Bacteriocins. *Antibiotics*, *9*(9), 553. https://www.mdpi.com/2079-6382/9/9/553

References

Appendix

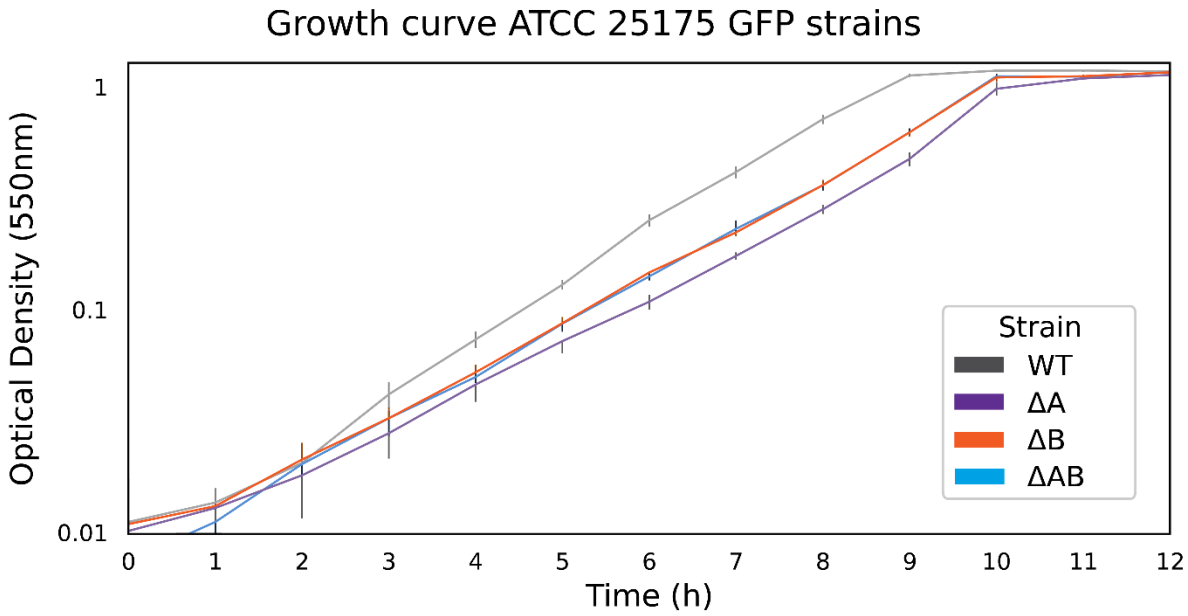

Figure A.1: Growth curve of *S. mutans* ATCC 25175 knock-out strains labelled with P_{veg}::GFP::spec. The optical density at 550 nm was measured every hour by a spectrophotometer. The error bars show the standard deviation of the measurements. 'WT GFP-spec' in grey. 'ΔA GFP-spec' in purple. 'ΔB GFP-spec' in orange. 'ΔAB GFP-spec' in cyan.

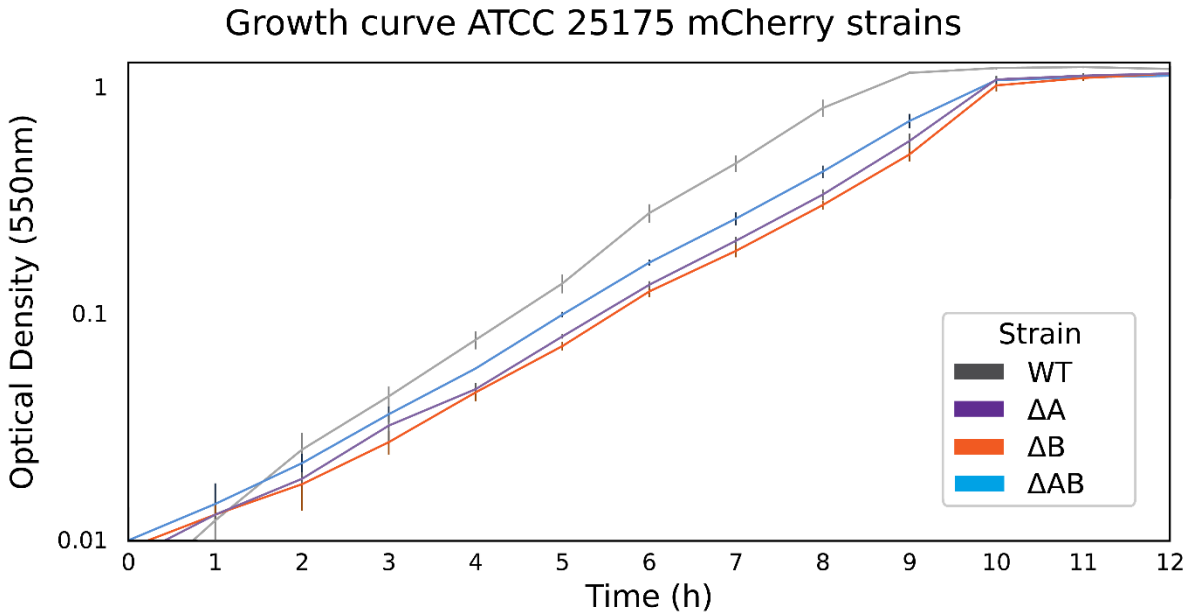

Figure A.2: Growth curve of *S. mutans* ATCC 25175 knock-out strains labelled with P_{veg}::mCherry::cam. The optical density at 550 nm was measured every 1 hour by a spectrophotometer. The error bars show the standard deviation of the measurements. 'WT mCherry-cam' in grey. 'ΔA mCherry-cam' in purple. 'ΔB mCherry-cam' in orange. 'ΔAB mCherry-cam' in cyan.

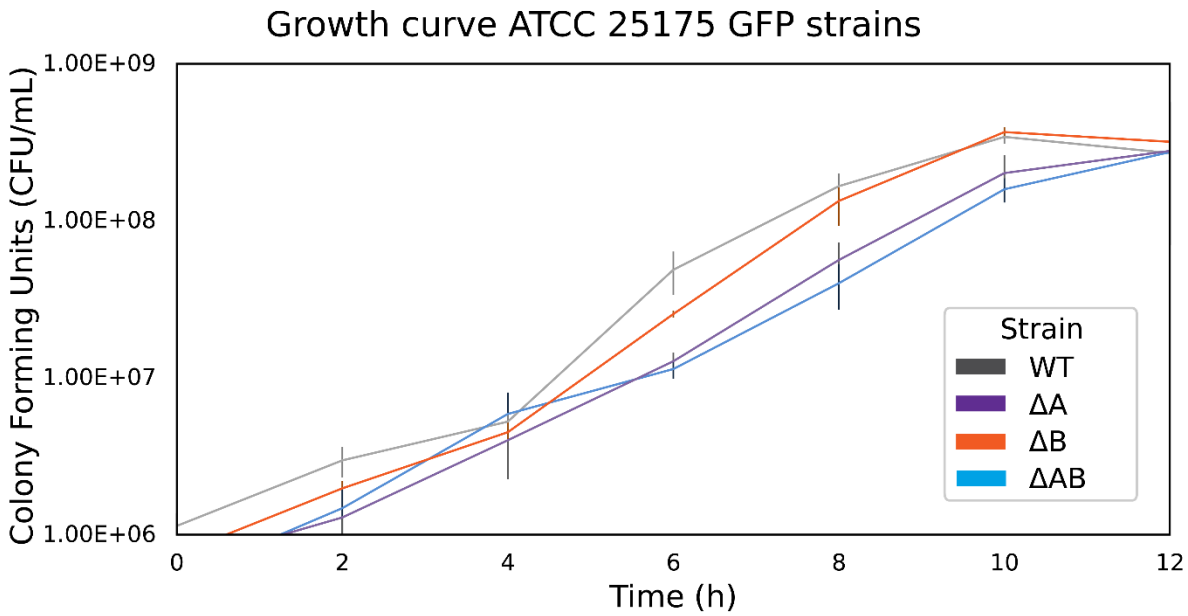

Figure A.3: Growth curve of *S. mutans* ATCC 25175 knock-out strains labelled with P_{veg}::GFP::spec. The colony forming units (CFU/mL) were measured every 2 hours. The error bars show the standard deviation of the measurements. 'WT GFP-spec' in grey. 'ΔA GFP-spec' in purple. 'ΔB GFP-spec' in orange. 'ΔAB GFP-spec' in cyan.

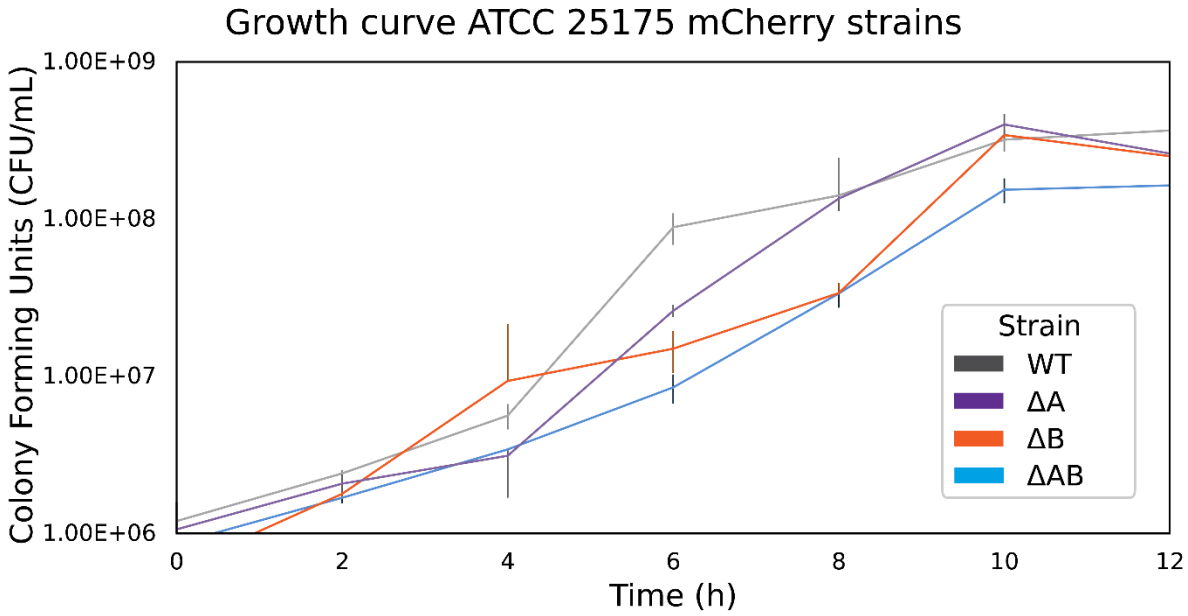

Figure A.4: Growth curve of *S. mutans* ATCC 25175 knock-out strains labelled with P_{veg}::mCherry::cam. The colony forming units (CFU/mL) were measured every 2 hours. The error bars show the standard deviation of the measurements. 'WT mCherry-cam' in grey. 'ΔA mCherry-cam' in purple. 'ΔB mCherry-cam' in orange. 'ΔAB mCherry-cam' in cyan.

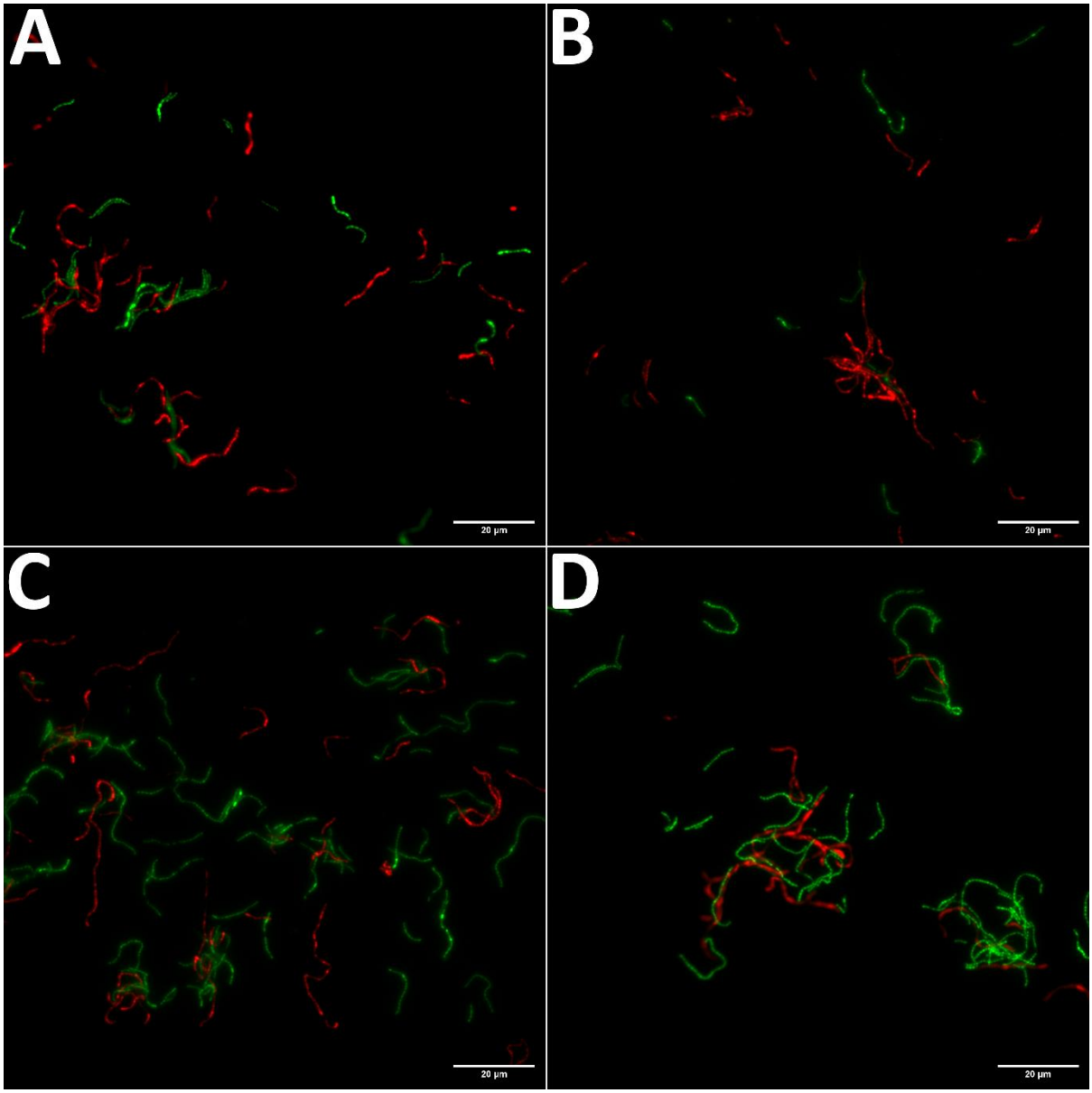

Figure A.5: Fluorescence microscopy images of pairwise strain competition in the standard biofilm model. A: 'WT GFP-spec' in green and 'WT mCherry-cam' in red, B: 'ΔA GFP-spec' in green and 'WT mCherry-cam' in red, C: 'WT GFP-spec' in green and 'ΔB mCherry-cam' in red, D: 'WT GFP-spec' in green and 'ΔAB mCherry-cam' in red.

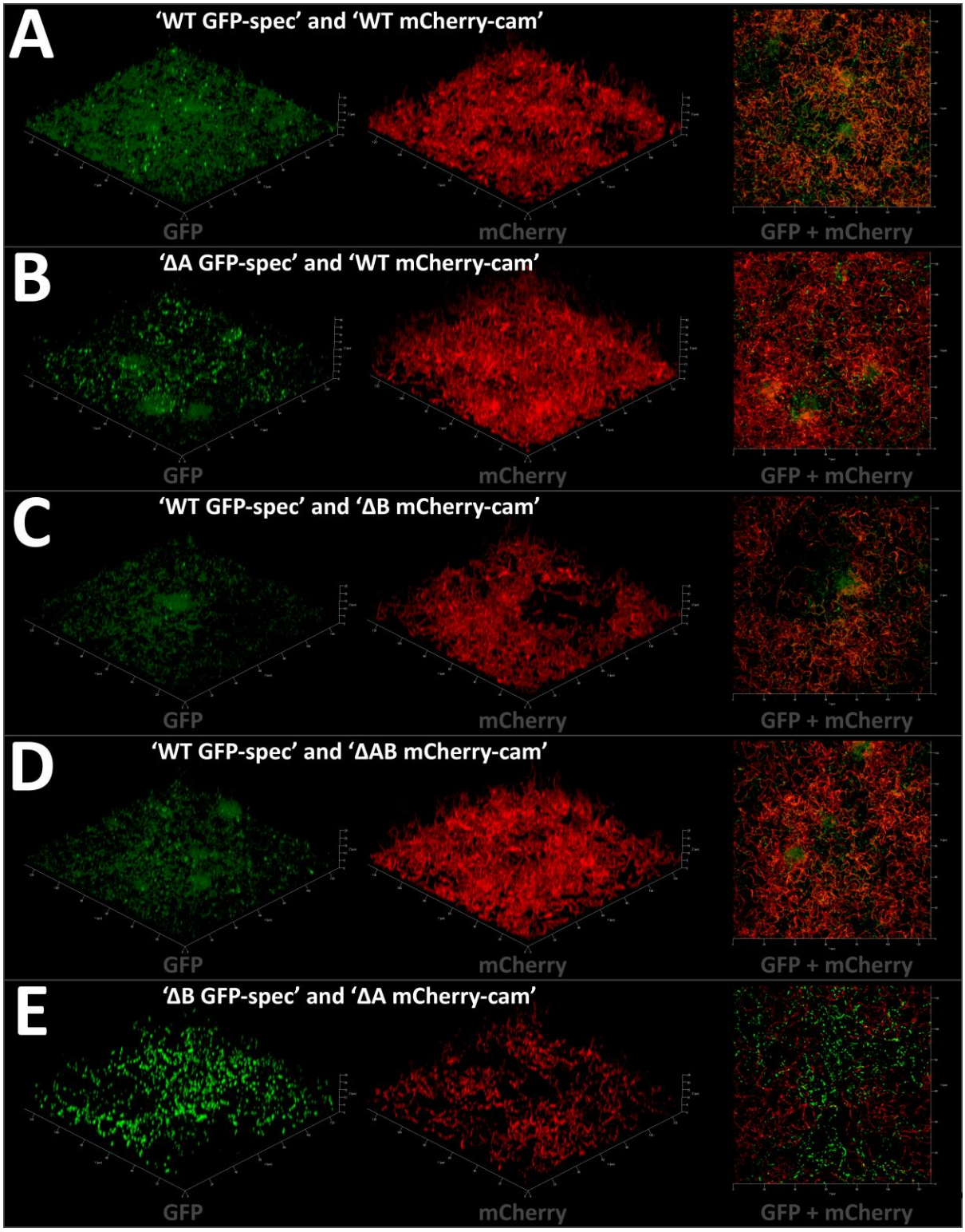

Figure A.6: Confocal microscopy images of pairwise strain combinations in the standard biofilm model. A: 'WT GFP-spec' and 'WT mCherry-cam'. B: 'ΔA GFP-spec' and 'WT mCherry-cam'. C: 'WT GFP-spec' and 'ΔB mCherry-cam'. D: 'WT GFP-spec' and 'ΔAB mCherry-cam'. E: 'ΔB GFP-spec' and 'ΔA mCherry-cam'.

Appendix

Norges miljø- og biovitenskapelige universitet
Noregs miljø- og biovitskapelege universitet
Norwegian University of Life Sciences

Postboks 5003
NO-1432 Ås
Norway